LHC: Detectors and Upgrades

XXXII INTERNATIONAL SEMINAR of NUCLEAR and SUBNUCLEAR PHYSICS "Francesco Romano"

7 June 2021

Attilio Andreazza

Università di Milano e INFN Sezione di Milano)

INFN Sezione di Milano

Istituto Nazionale di Fisica Nucleare

UNIVERSITÀ DEGLI STUDI DI MILANO

DIPARTIMENTO DI FISICA

LHC AND HL-LHC

Istituto Nazionale di Fisica Nucleare Sezione di Milano

UNIVERSITÀ DEGLI STUDI DI MILANO
DIPARTIMENTO DI FISICA

The CERN Large Hadron Collider

(*) Main topics of these lectures

- **p-p(*)**, p-A and A-A collider
  - 2009-2012: Run1 $\sqrt{s}$ = 7-8 TeV
  - 2015-2019: Run2 $\sqrt{s}$ = 13 TeV
- Seven experiments: ALICE, **ATLAS, CMS(*)**, LHCb, LHCf, TOTEM and MoEDAL
- 40 MHz (25 ns) collision rate

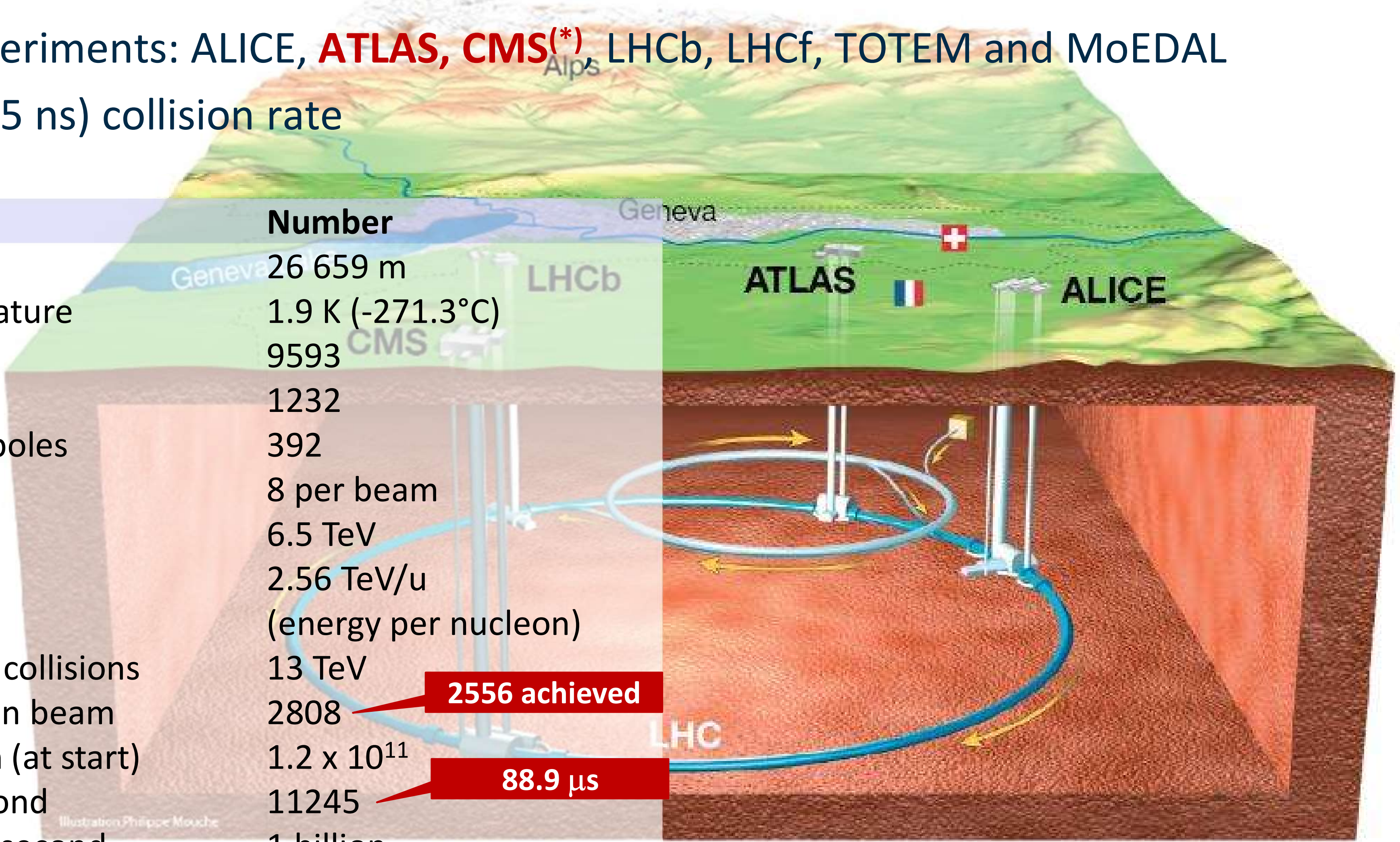

Quantity	**Number**	
Circumference	26 659 m	
Dipole operating temperature	1.9 K (-271.3°C)	
Number of magnets	9593	
Number of main dipoles	1232	
Number of main quadrupoles	392	
Number of RF cavities	8 per beam	
Nominal energy, protons	6.5 TeV	
Nominal energy, ions	2.56 TeV/u (energy per nucleon)	
Nominal energy, protons collisions	13 TeV	
No. of bunches per proton beam	2808	2556 achieved
No. of protons per bunch (at start)	1.2 x 10^{11}	
Number of turns per second	11245	88.9 μs
Number of collisions per second	1 billion	

Luminosity

Luminosity $\mathcal{L}$

$$\frac{dN}{dt} = \sigma\mathcal{L}$$

- rate of interactions

$$\mathcal{L} = \frac{n_b f_{rev} N^2}{4\pi\sigma_x\sigma_y}$$

- n_b number of bunches
- f_{rev} revolution frequency
- N particles per bunch
- $\sigma_{x,y}$ beam size at interaction point

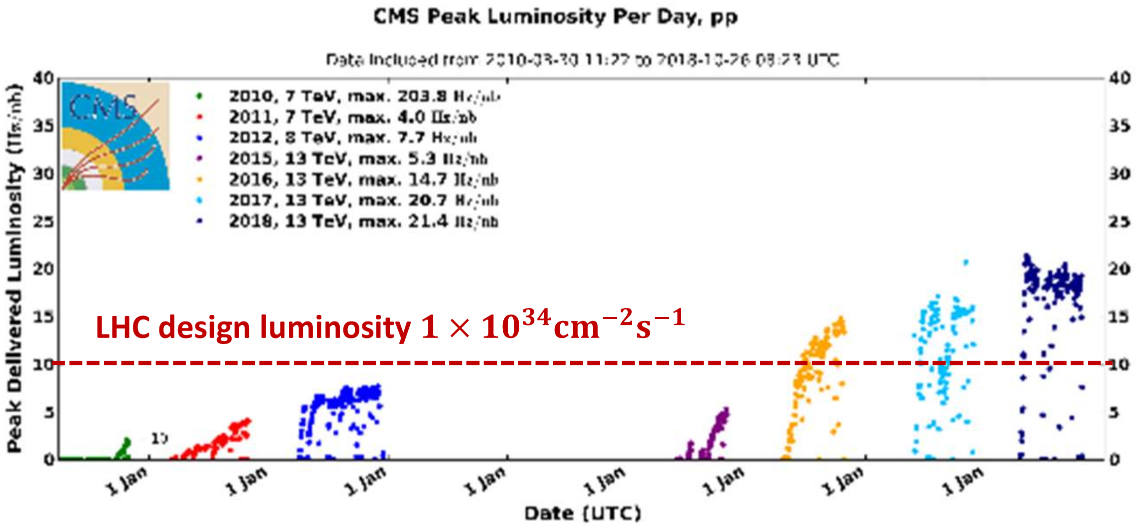

Integrated luminosity

$$N = \sigma\int\mathcal{L}dt$$

- total number of produced events
- determines the physics reach of the experiment

At the end of Run2 ~150 pb^{-1}/experiment

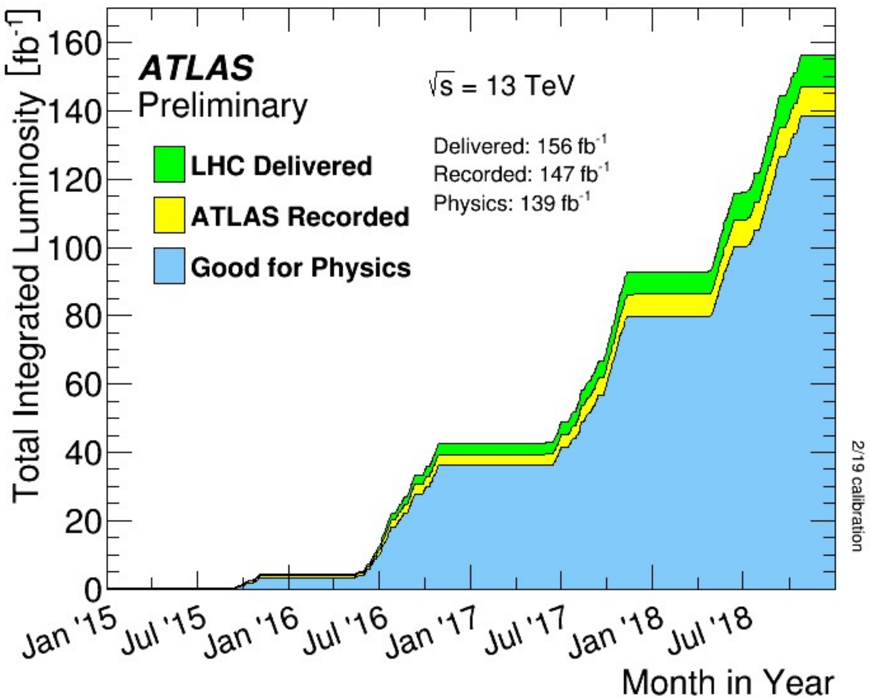

Standard Model Physics Output

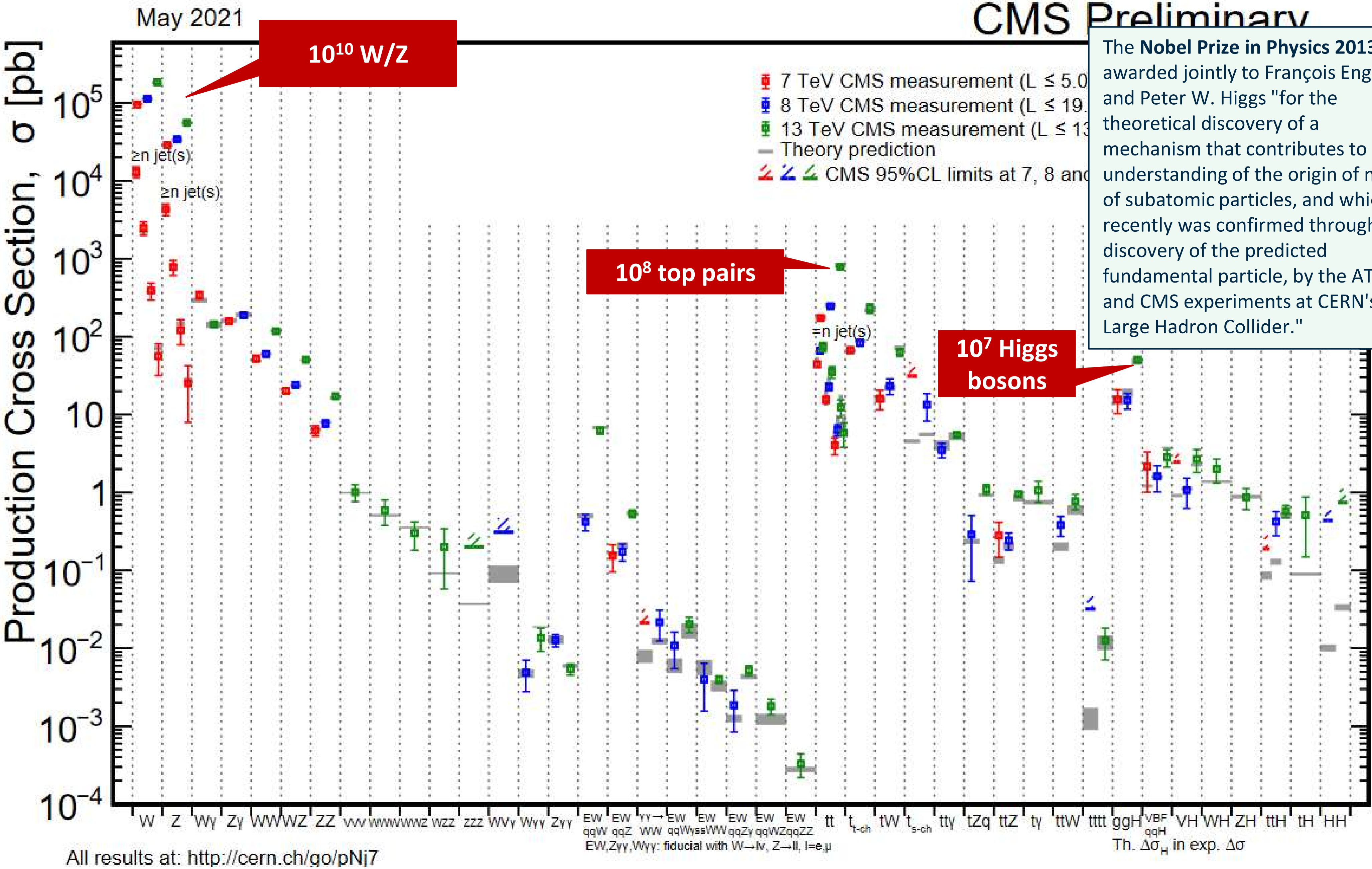

The **Nobel Prize in Physics 2013** was awarded jointly to François Englert and Peter W. Higgs "for the theoretical discovery of a mechanism that contributes to our understanding of the origin of mass of subatomic particles, and which recently was confirmed through the discovery of the predicted fundamental particle, by the ATLAS and CMS experiments at CERN's Large Hadron Collider."

Beyond the Standard Model

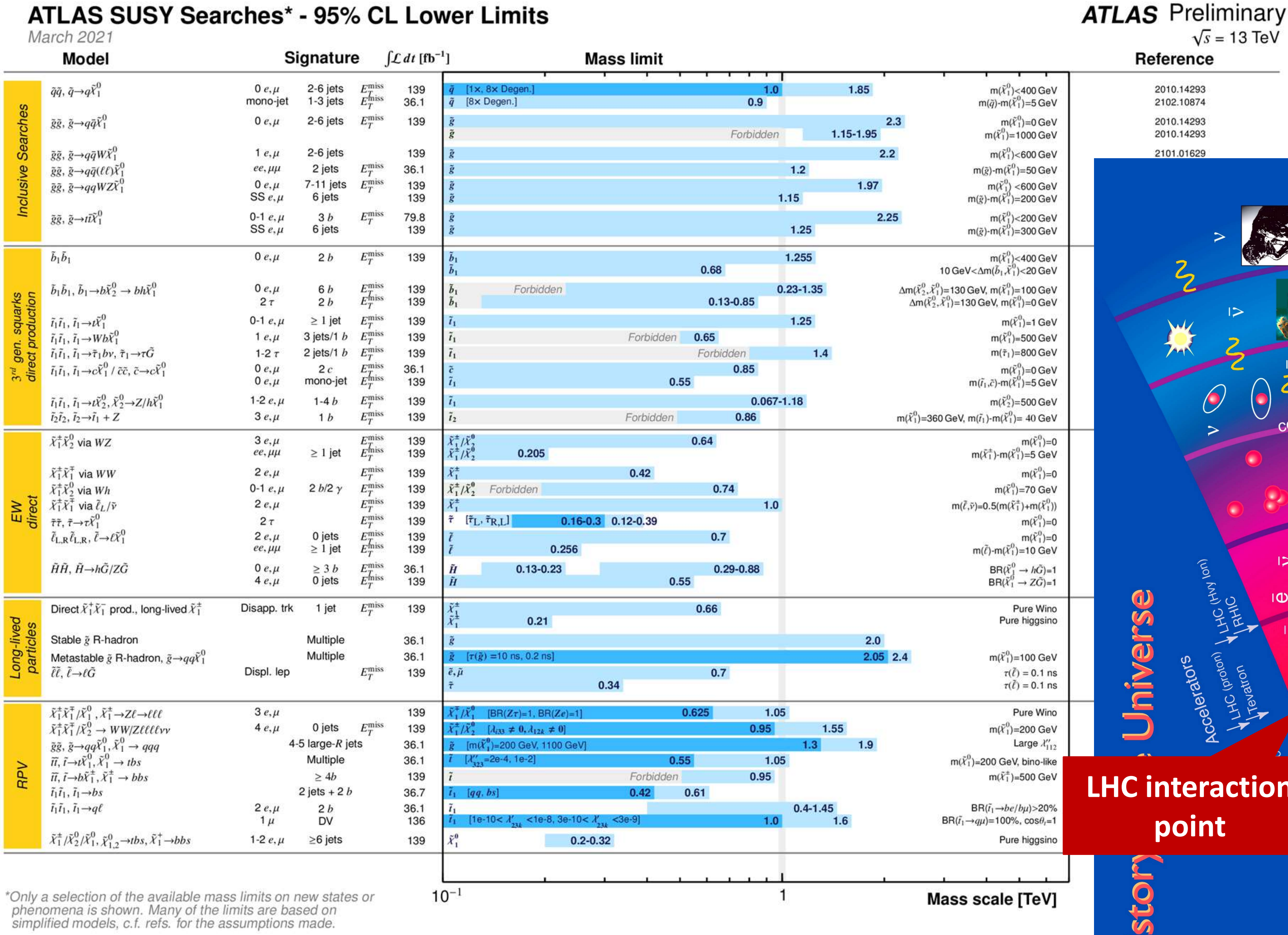

LHC dipoles

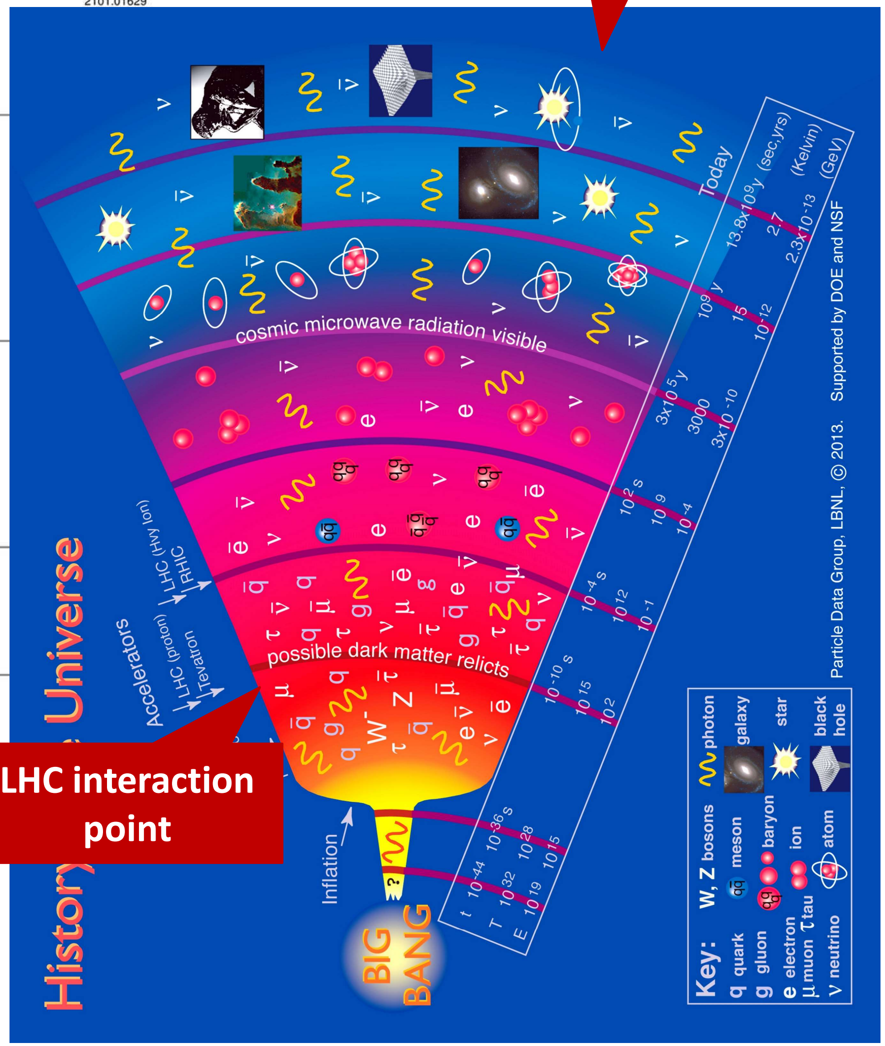

LHC interaction point

High-Luminosity LHC

Coordinate system

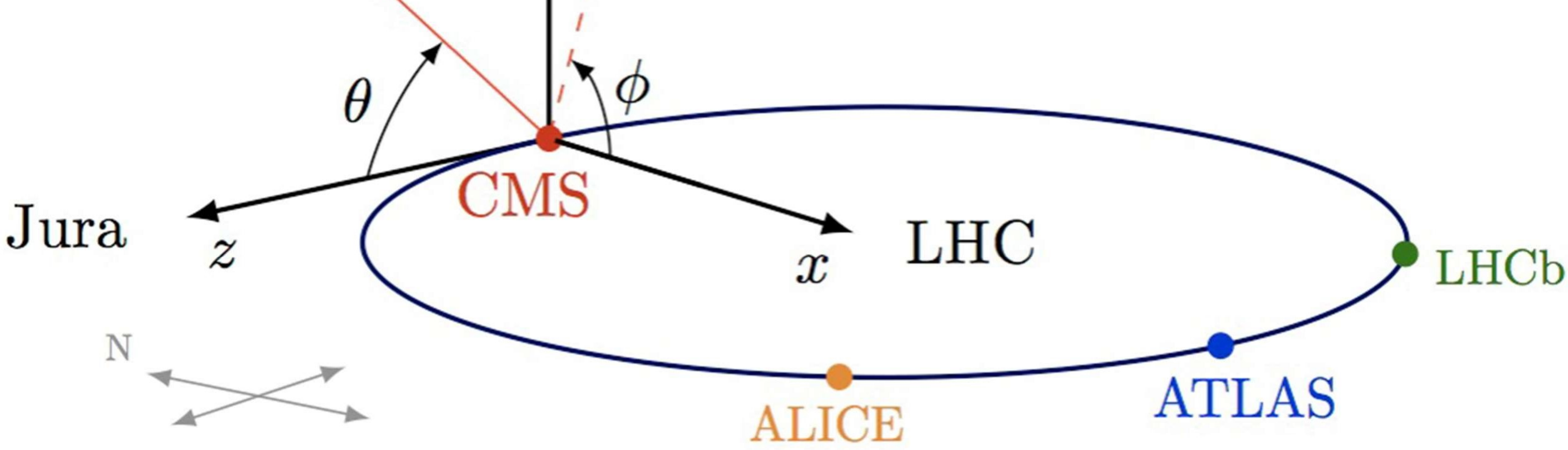

Pseudorapidity

$$\eta = -\ln \tan \frac{\theta}{2}$$

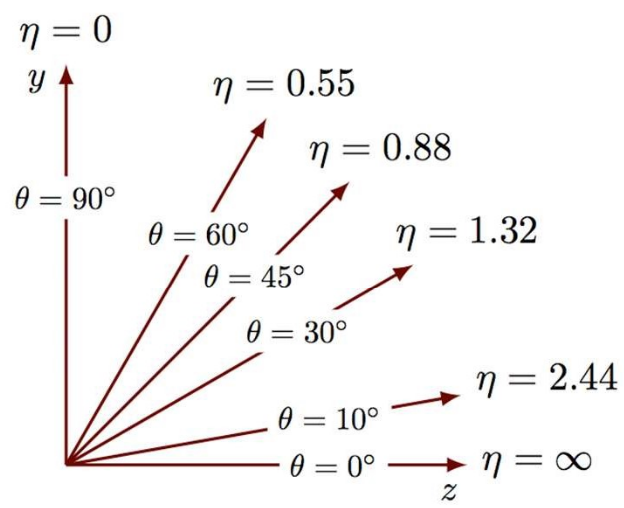

HL-LHC properties and operation

Parameter	Nominal LHC (design report)	HL-LHC 25 ns (standard)
Number of bunches	2808	2760
Beam current (A)	0.58	1.1
Minimum β^* (m)	0.55	0.15
Peak luminosity with crab cavities $L_{\text{peak}} \times R_1/R_0$ (10^{34} cm^{-2} s^{-1})	(1.18)	17
Levelled luminosity for μ = 140 (10^{34} cm^{-2} s^{-1})	-	5.0
Events/crossing μ (with levelling and crab cavities)	27	131
Maximum line density of pile-up events during fill (events/mm)	0.21	1.28

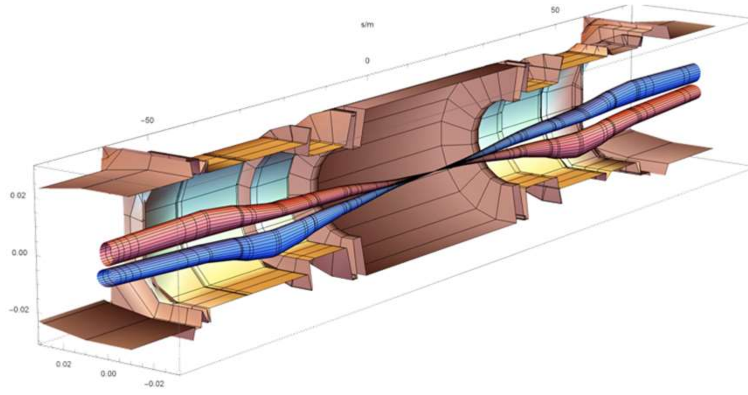

$$\mathcal{L} = \frac{n_b f_{rev} N^2}{4\pi\sigma_x\sigma_y} \Leftrightarrow \frac{n_b f_{rev} N^2}{4\pi\varepsilon_n\beta^*/\gamma} R, \qquad R = \left(1 + \frac{\theta_c\sigma_z}{\sigma_{x,y}}\right)^{-\frac{1}{2}}$$

- γ relativistic factor
- ε_n normalized emittance
- β^* beta function at the collision point
- θ_c crossing angle
- σ_z longitudinal bunch length

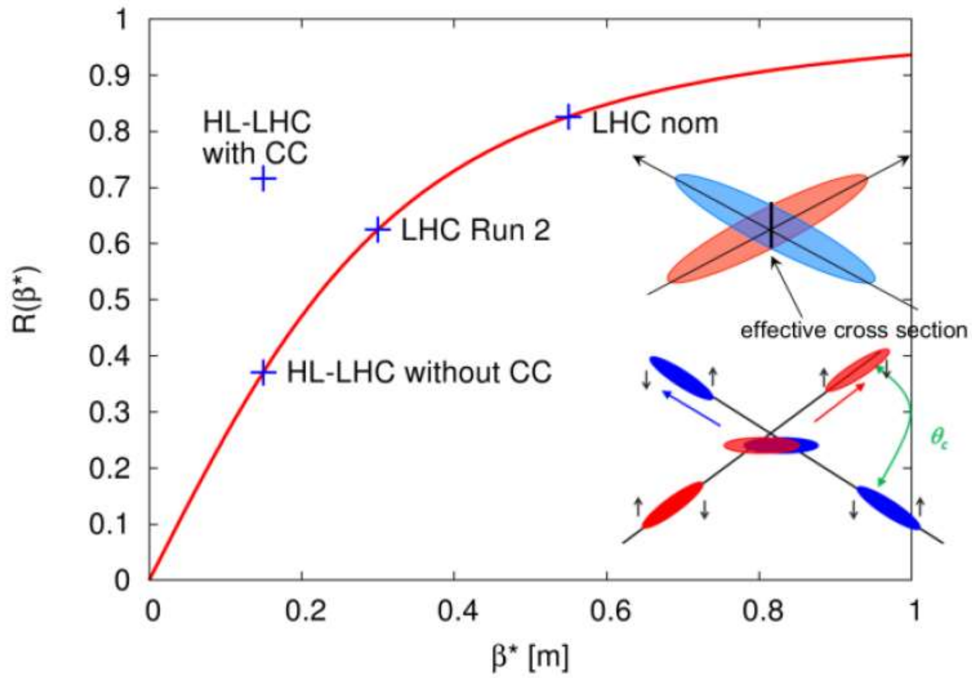

Luminosity: pile-up

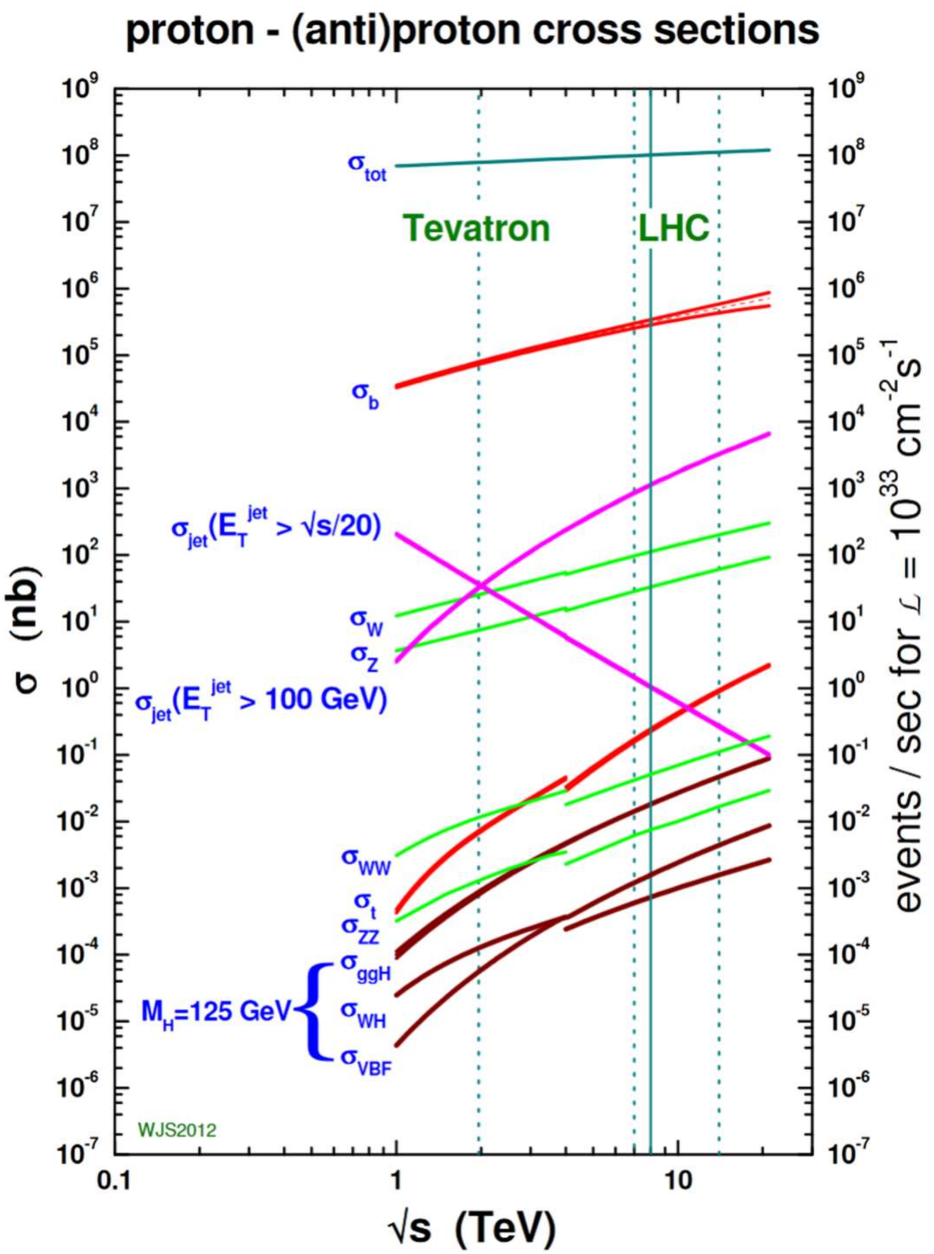

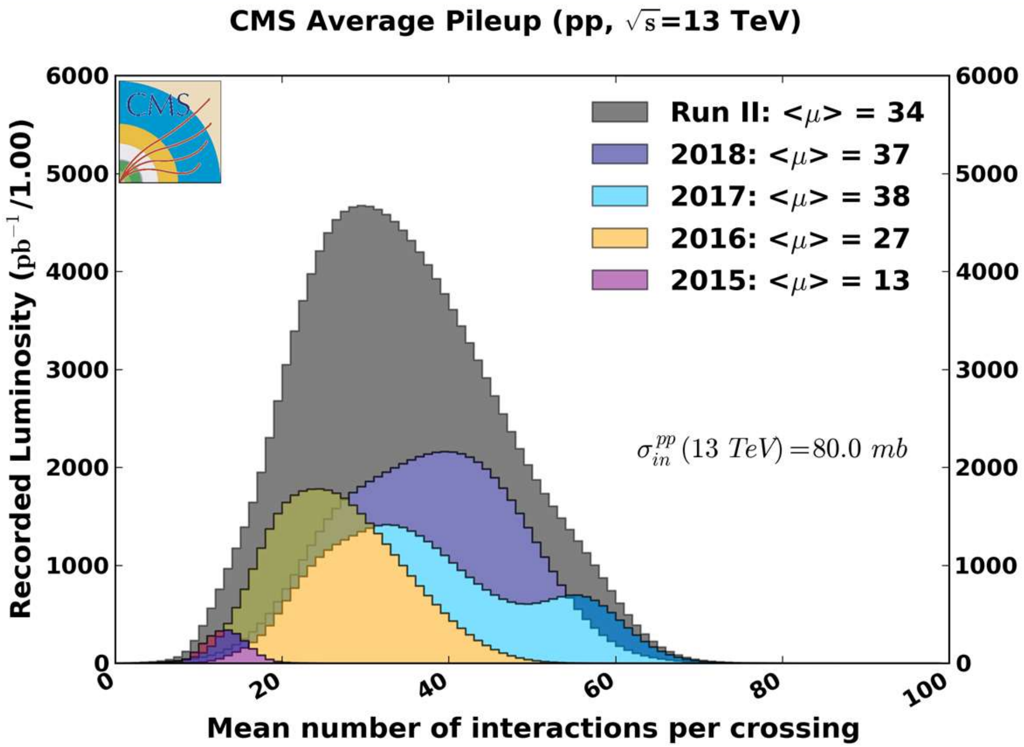

- Total pp cross section: 80 mb
  - For $1 \times 10^{34}\mathrm{cm}^{-2}\mathrm{s}^{-1}$, 10^9 events/s
  - With 25 ns collision rate: 25 events/collision

Luminosity: pile-up

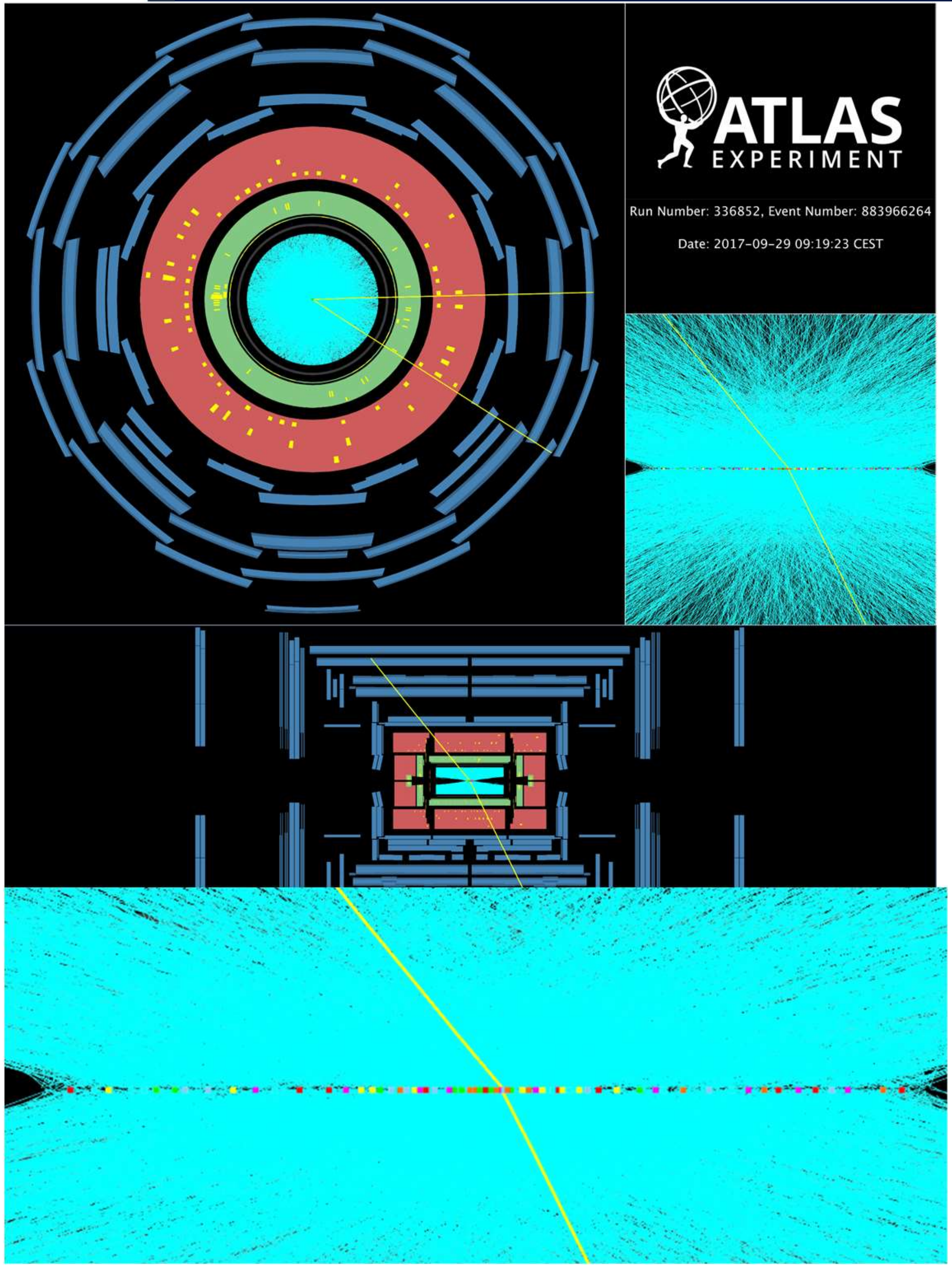

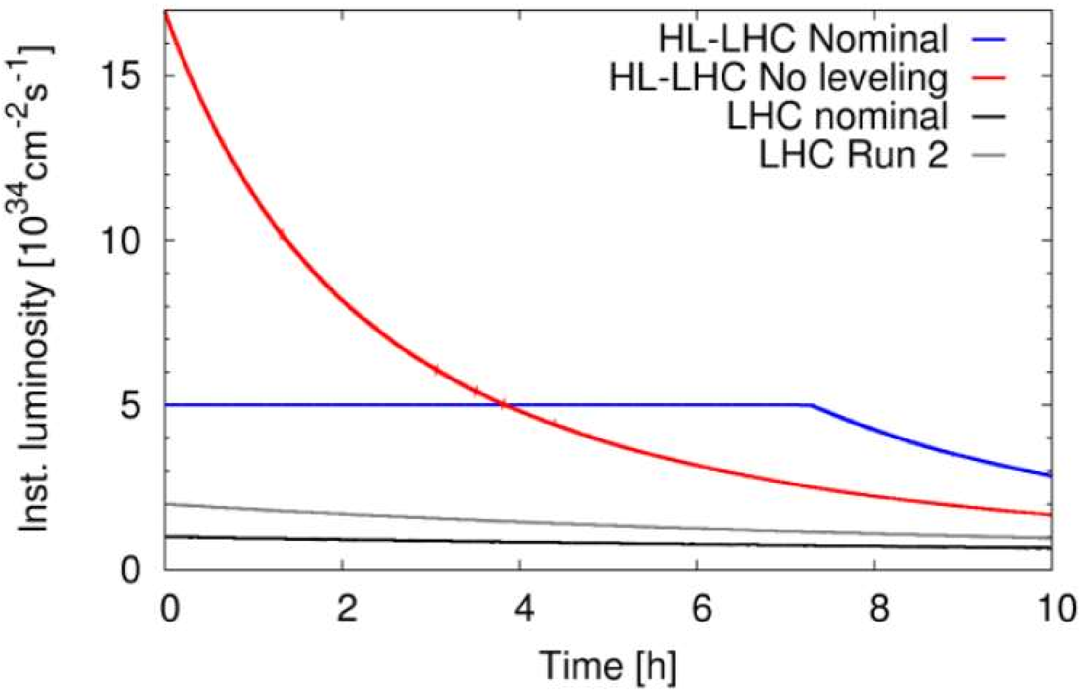

- Total pp cross section: 80 mb
  - For $1 \times 10^{34} \mathrm{cm}^{-2}\mathrm{s}^{-1}$, 10^9 events/s
  - With 25 ns collision rate: 25 events/collision
- Can be mitigated by Luminosity Levelling (already used at ALICE and LHCb IP)

Luminosity: radiation effect

- Radiation effects from the high interaction rate:
  - high particle flux:
    - requirements on detector granularity
    - background rates and space charge effects
  - permanent damage on detector and electronics
  - detector activation

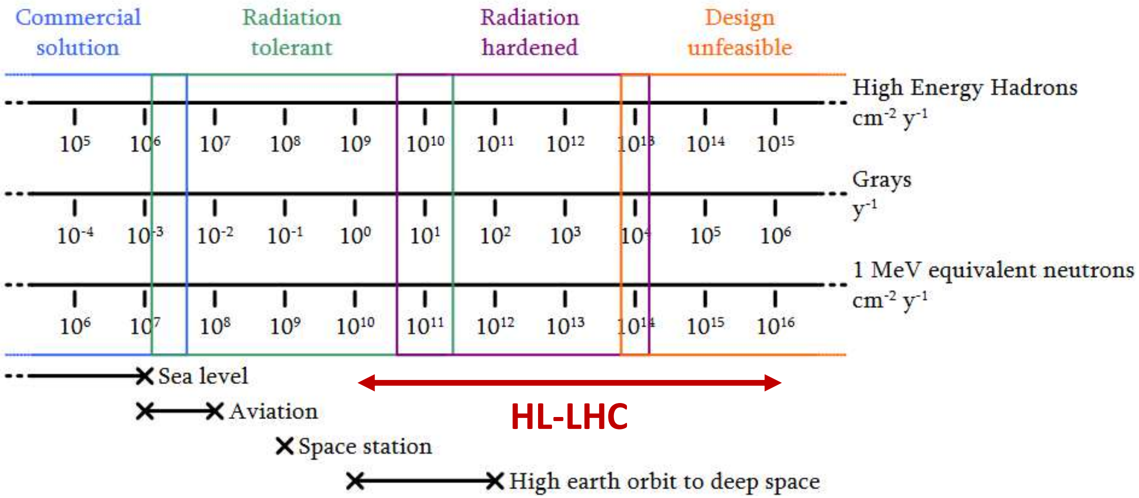

reproduced from B. Todd and S. Uznanski, *Radiation Risks and Mitigation in Electronics System,* in CERN-2015-003

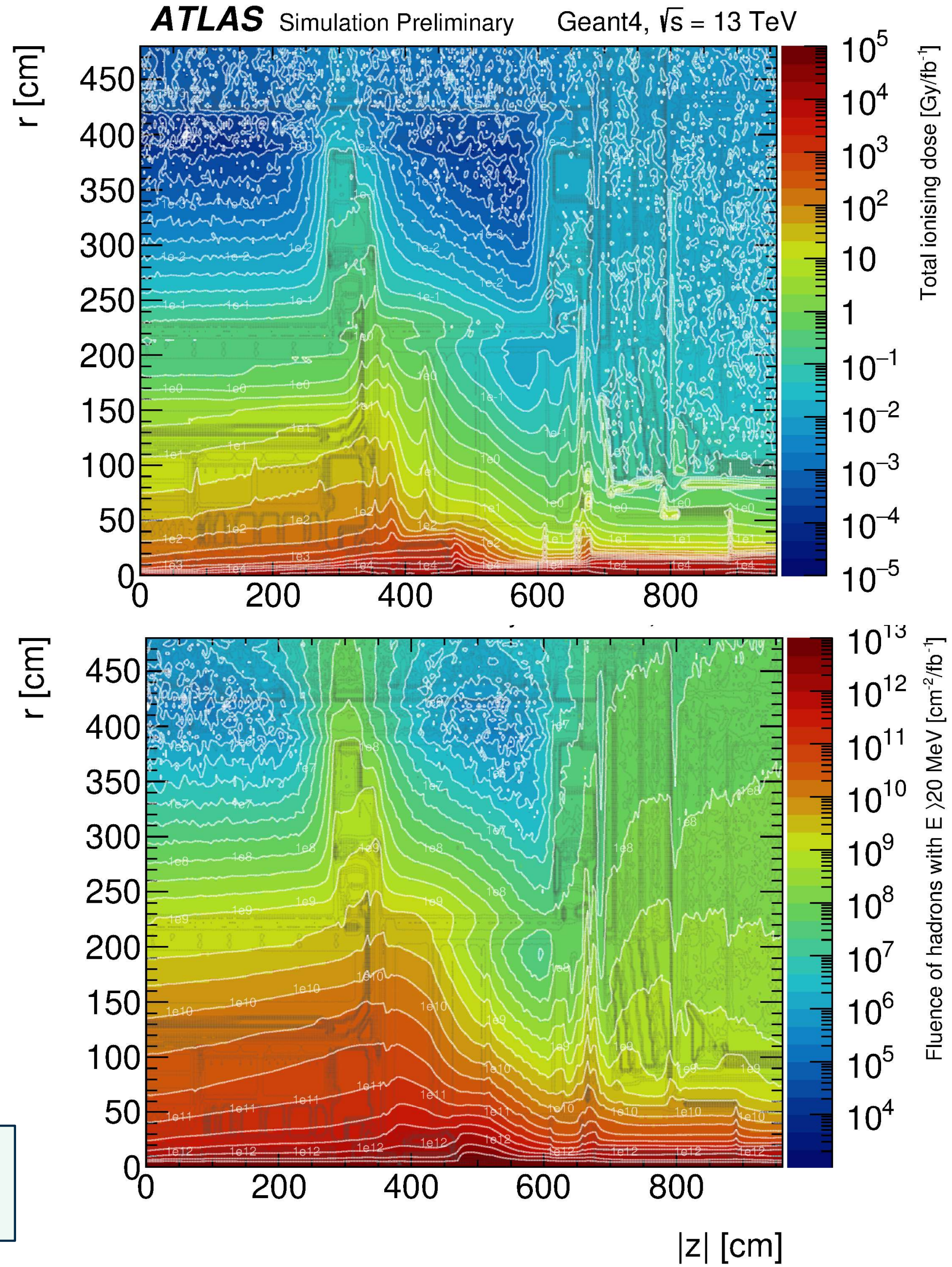

Layout of the lectures

- In the following I'll try to review:
  - general detector concepts in high-energy particle physics
  - which technologies have been chosen for the ATLAS and CMS detectors to cope with the LHC harsh environment
  - how they have been evolved to match the 10 more challenging environment at the LHC
- **Layout**
  - **ATLAS and CMS detector concepts**
  - **The detectors inside-out:**
    - **Inner tracking**
    - **Calorimetry**
    - **Muon systems**
  - **DAQ and trigger** (if time allows)
- Most material is from the experiment Phase II upgrade TDRs
  - sometimes not up-to-date, but it present the projects in an organic way
  - but I'll try to throw in some basic principles for non-experts

I am not an expert on everything, my apologies for any incomplete/erroneous information reported

ATLAS AND CMS DETECTOR CONCEPTS

Istituto Nazionale di Fisica Nucleare
Sezione di Milano
UNIVERSITÀ DEGLI STUDI DI MILANO
DIPARTIMENTO DI FISICA

The "All-purpose" HEP Detector

CMS Slice

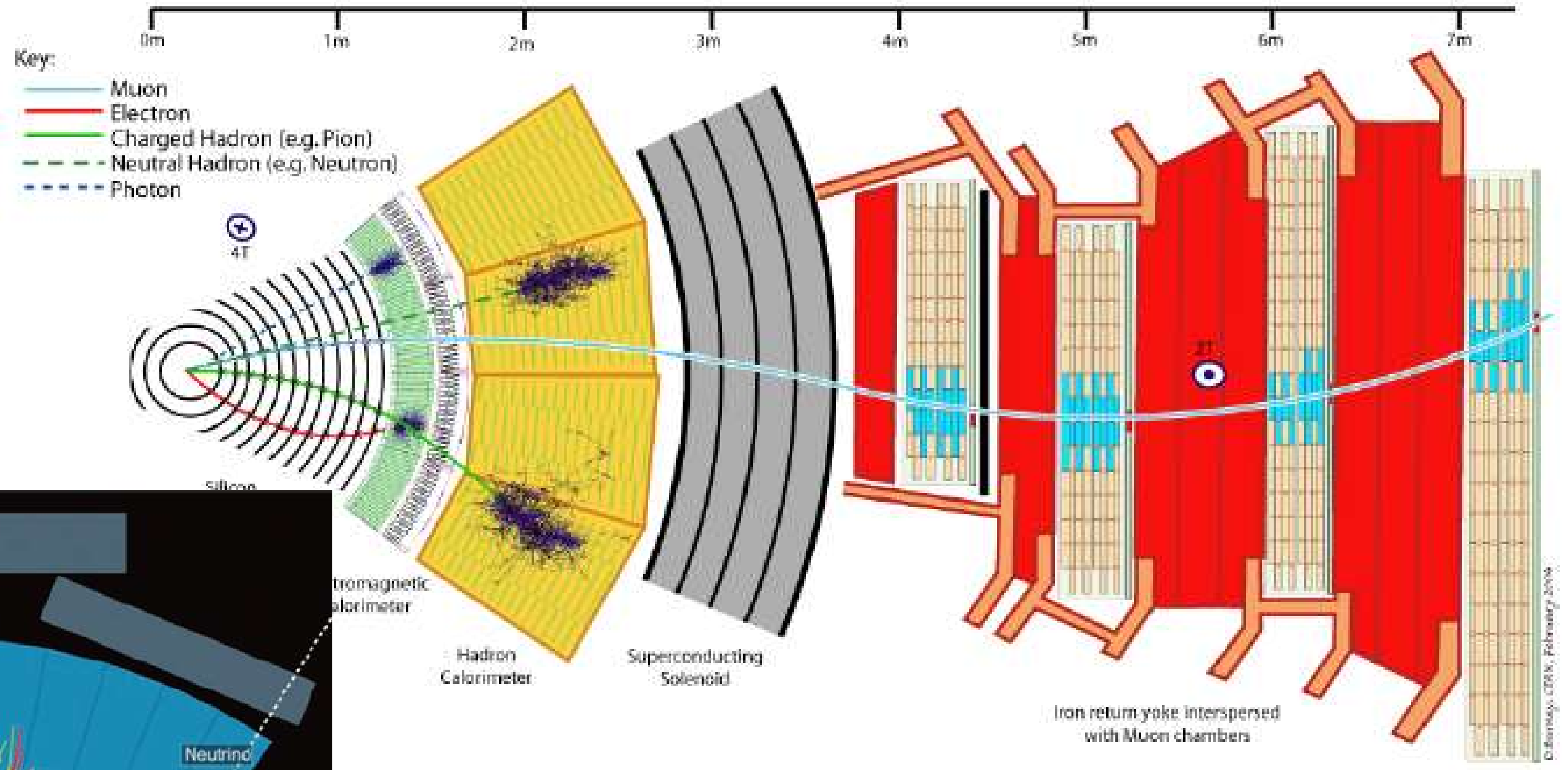

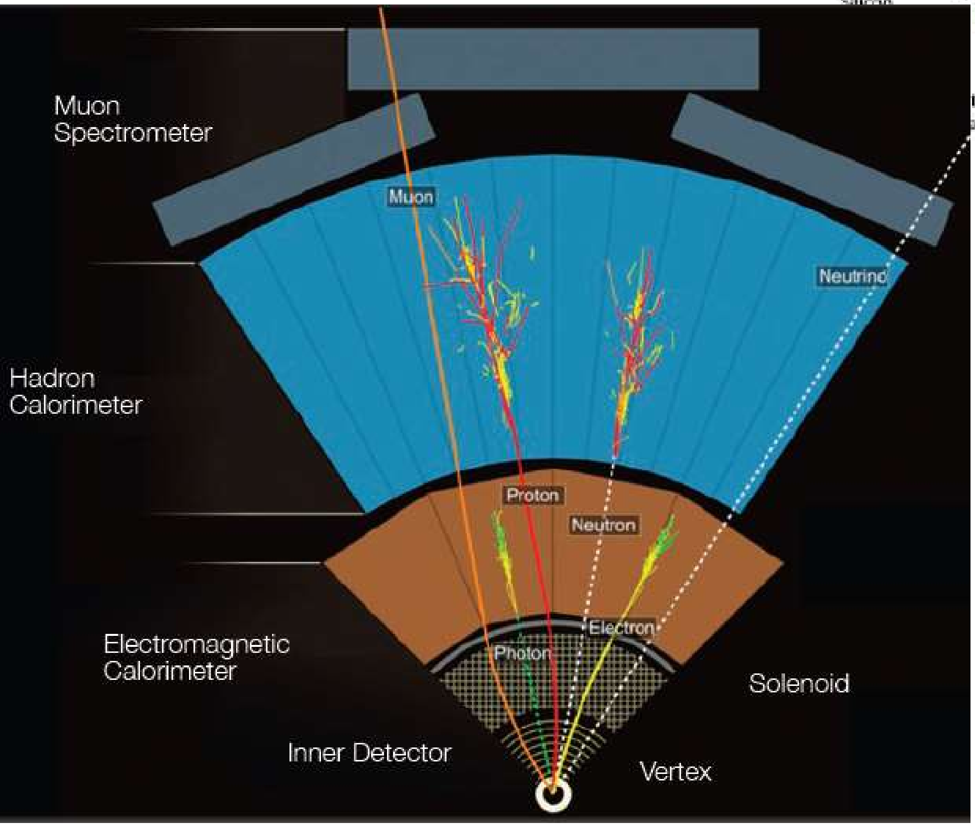

What's the difference?

ATLAS Slice

The "All-purpose" HEP Detector

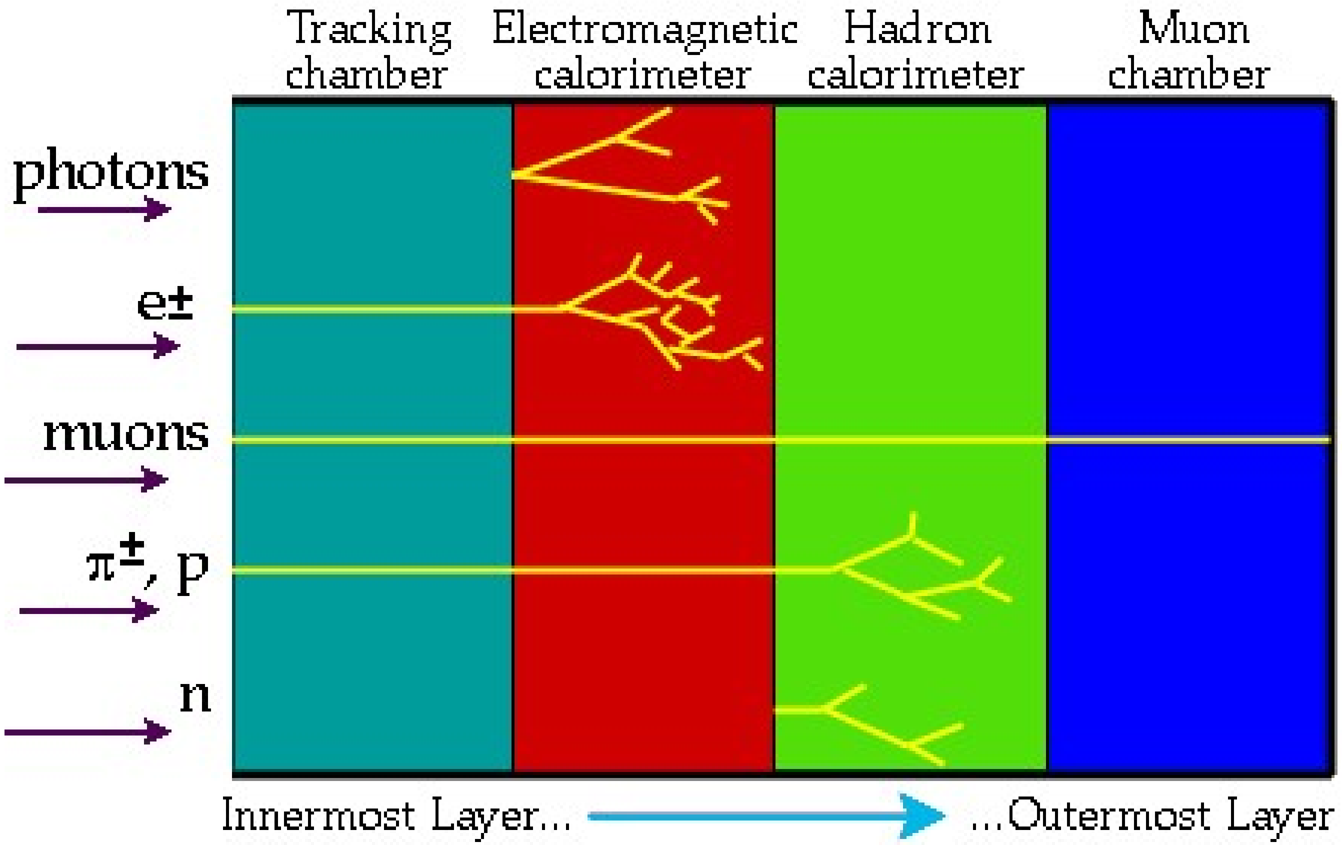

Momentum measurement
decay vertex reconstruction,
hadron identification
Low material (~1X_0)

Electron idenfication,
photon detection
~20X_0, 1-2λ_I

Charged hadron absorption,
neutral hadron detectionr
5-6λ_I

Identification of muons with enough energy to cross the calorimeters (>2-3 GeV)

The magnetic systems

ATLAS

A **Toroidal** LHC ApparatuS

- Large air-core **toroids** integrated with the muon system
- Thin solenoid around the central tracker
  - **2 T** magnetic field
  - **inside** the calorimeters

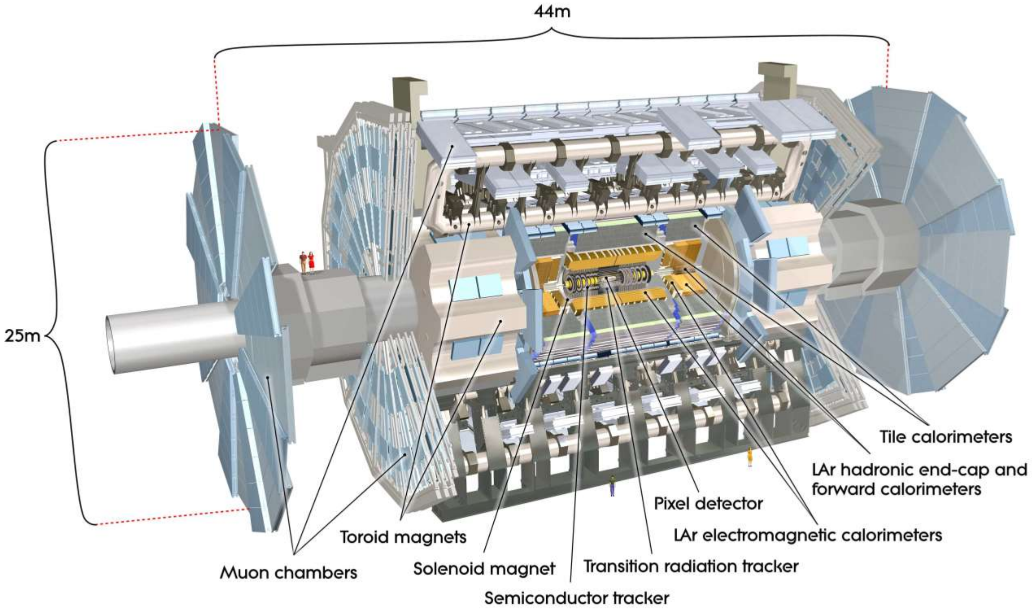

CMS

Compact Muon **Solenoid**

- Powerful solenoid
  - **4 T** magnetic field
  - **outside** of the calorimeter
- Muon system integrated in the solenoid **yoke**

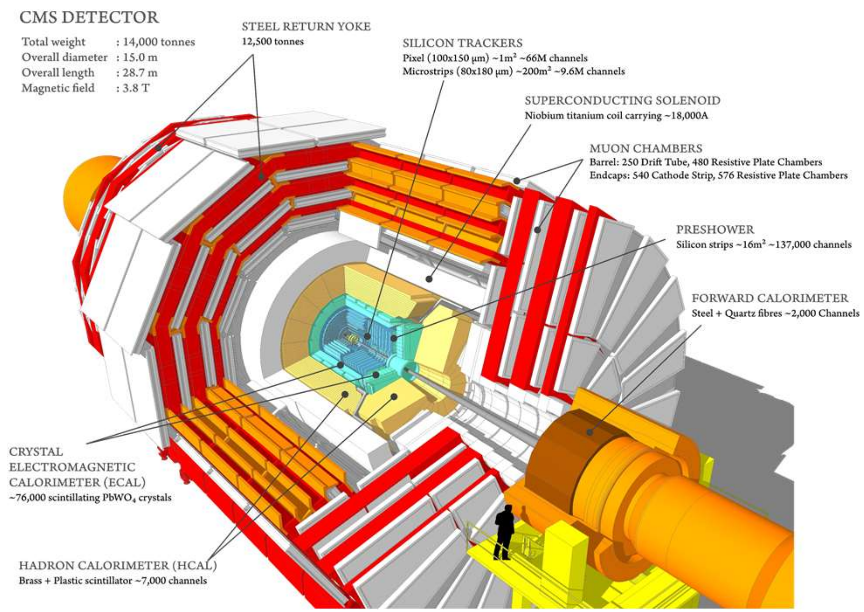

The magnetic systems

ATLAS

A **Toroidal** LHC ApparatuS

- Large air-core **toroids** integrated with the muon system
- Thin solenoid around the central tracker
  - **2 T** magnetic field
  - **inside** the calorimeters

CMS

Compact Muon **Solenoid**

- Powerful solenoid
  - **4 T** magnetic field
  - **outside** of the calorimeter
- Muon system integrated in the solenoid **yoke**

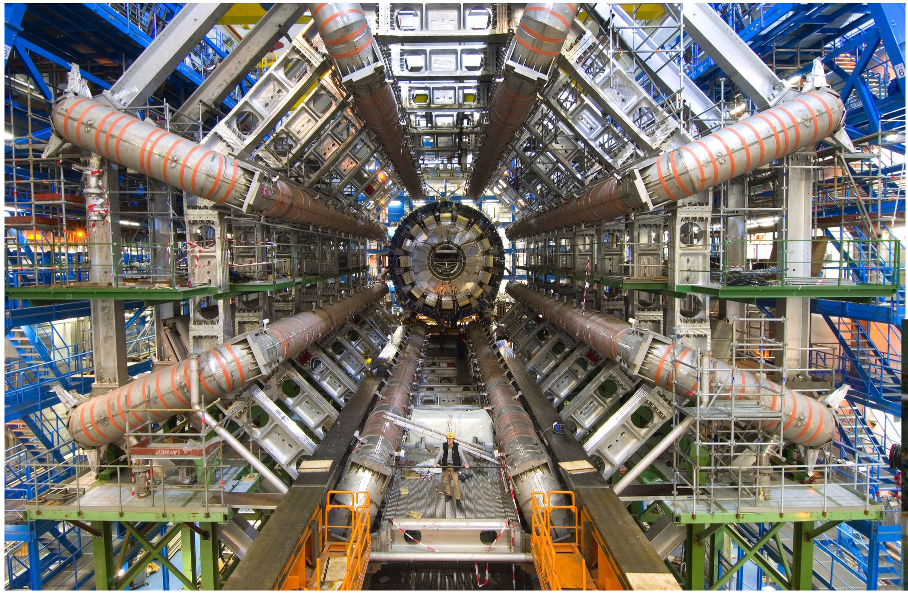

Momentum measurement concepts

- A charged particle bending radius in magnetic field:
$$p[\mathrm{GeV/c}] = 0.3\, q\, B[\mathrm{T}]\, R[\mathrm{m}]$$
- Deflection due to the Lorenz force on a length L:
$$\theta = \frac{L}{R} = \frac{0.3\, qBL}{p}$$
  - in case of non-uniform magnetic field, use the bending power
$$\int B dl$$

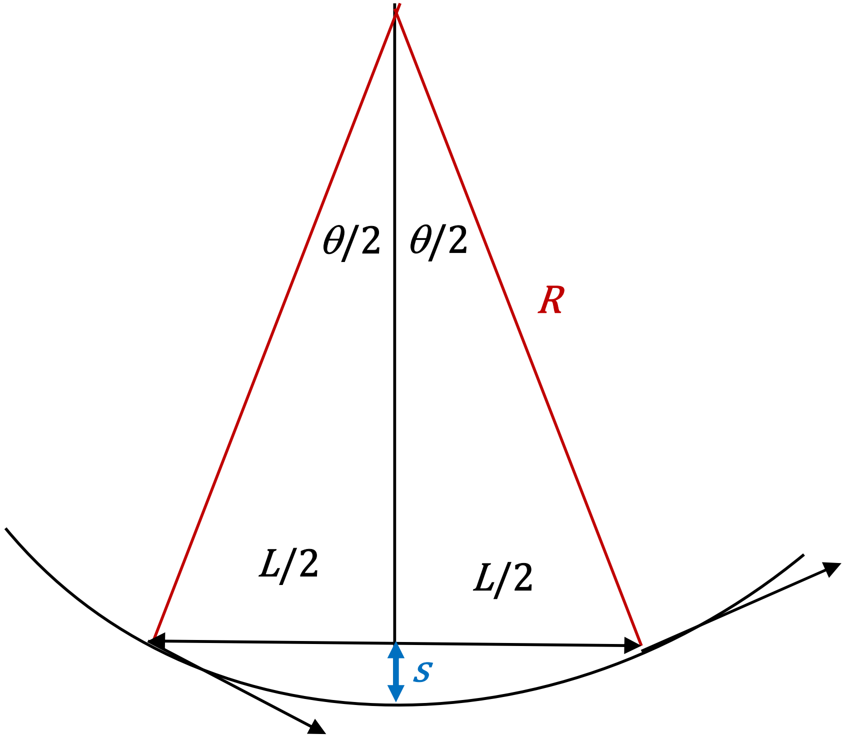

- **Deflection measurement**
  - direction before and after the bending field
$$\frac{\sigma_p}{p} = \frac{\sigma_\theta}{\theta} = \frac{p\sigma_\theta}{0.3\, qBL}$$

Detector resolution:
$$\frac{\sigma_p}{p} \propto p$$

- **Sagitta measurement**
  - deviation from a "straight line" inside the magnetic field:
$$s = R(1 - \cos\theta) \approx \frac{L^2}{8R} = \frac{0.3\, qBL^2}{8p}$$
$$\frac{\sigma_p}{p} = \frac{\sigma_s}{s} = \frac{8p\sigma_s}{0.3\, qBL^2}$$

Multiple scattering

- Deflection of a charged particle trajectory due to soft interactions with the material
  - on average $\langle \varepsilon_p \rangle = 0,\ \langle \theta_p \rangle = 0$
  - but the standard deviation is finite:

$$\theta_{p,\mathrm{rms}} = \frac{13.6\ \mathrm{MeV}}{\beta c p} z \sqrt{\frac{X}{X_0}} \left(1 + 0.038 \ln \frac{X}{X_0}\right)$$

Relevant for small thickenesss

- βc particle velocity
- p particle momentum
- z particle charge (in units of e)
- X_0 is the radiation length of the material

$$X_0 \approx \frac{716.4\ \mathrm{g\,cm^{-2}} A}{Z(Z+1)\ln\left(287/\sqrt{Z}\right)} \times \frac{1}{\rho}$$

- A, Z mass and atomic number of the element
- ρ density

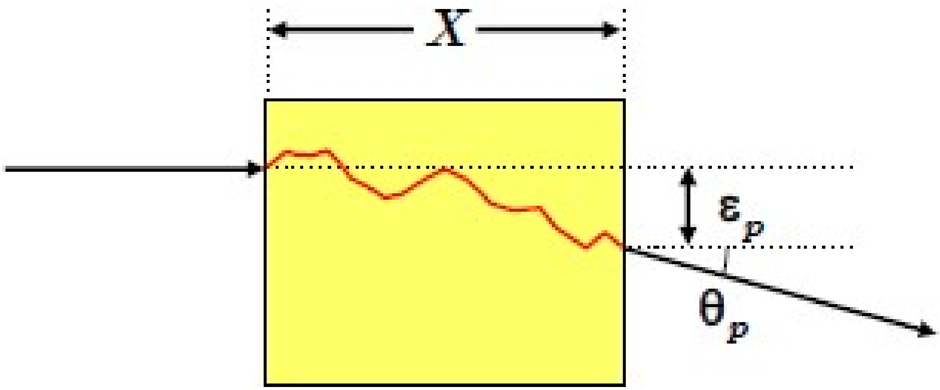

- Full covariance matrix is given by

$$\varepsilon_{p,\mathrm{rms}} = \frac{1}{\sqrt{3}} \theta_{p,\mathrm{rms}} X$$

$$\langle \varepsilon_p \theta_p \rangle = \frac{1}{2} \theta_{p,\mathrm{rms}}^2 X$$

Resolution term due to multiple scattering:

$$\frac{\sigma_p}{p} = \frac{\theta_{p,\mathrm{rms}}}{\theta} \propto \frac{1/p}{1/p} \propto \mathrm{const.}$$

ATLAS Muon Spectrometer

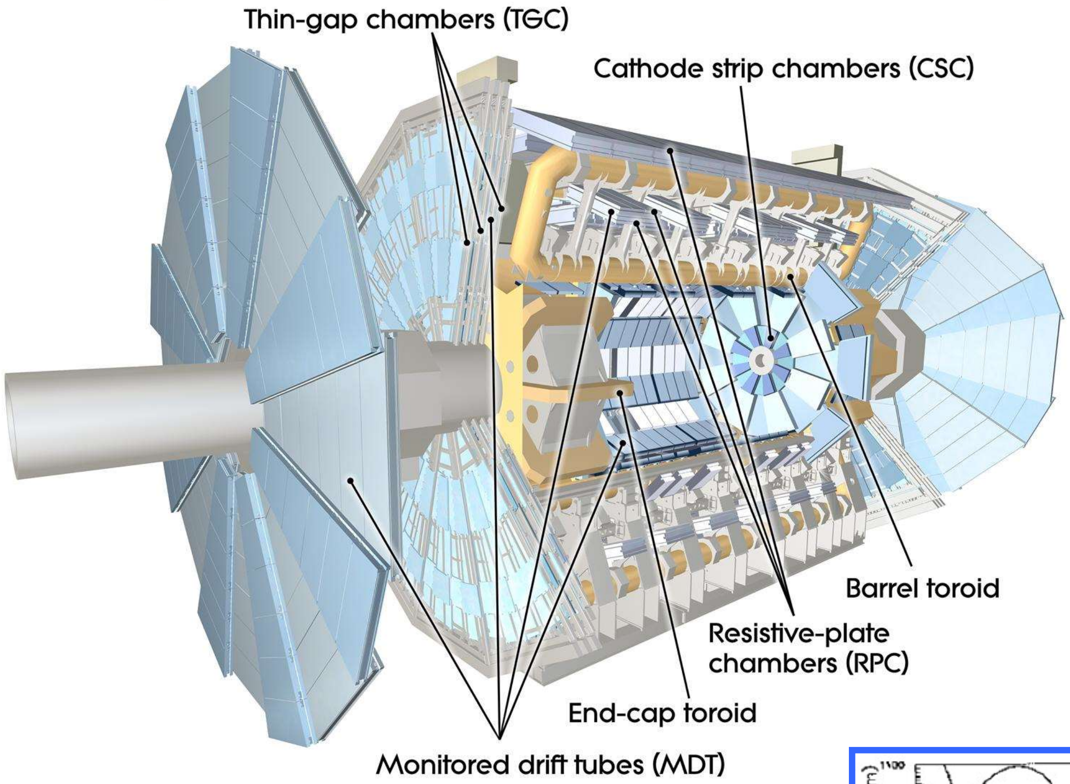

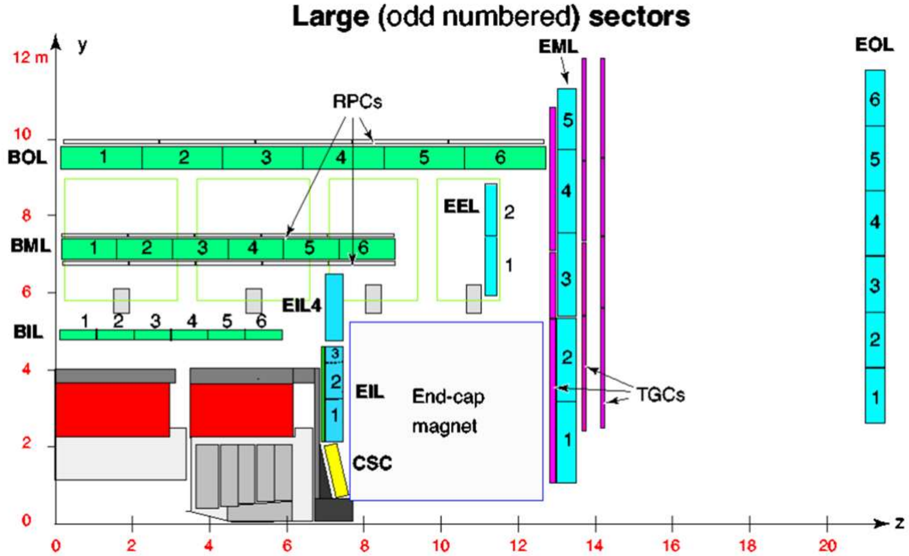

Instrumented air-core toroid system:

- bending power 1–7.5 Tm
- standalone momentum reconstruction capability σ_{p_T}/p_T = 10% at p_T=1 TeV

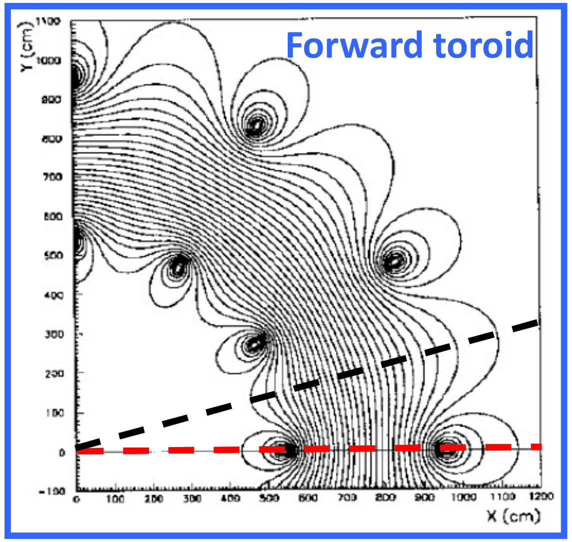

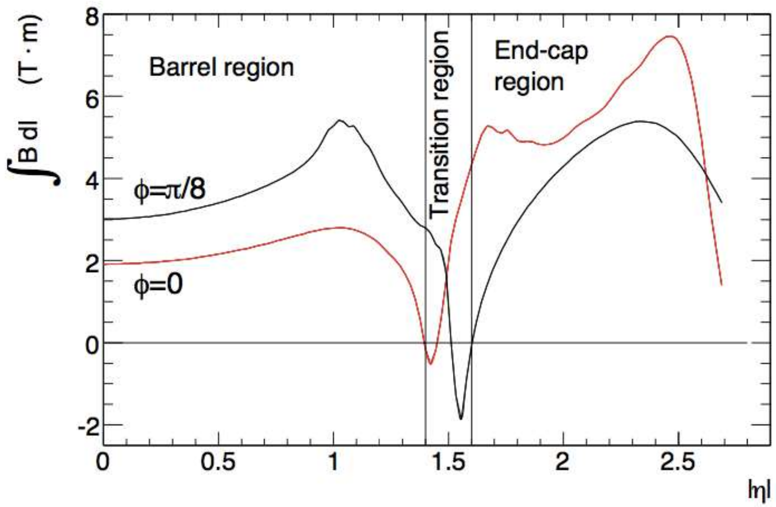

CMS Muon System

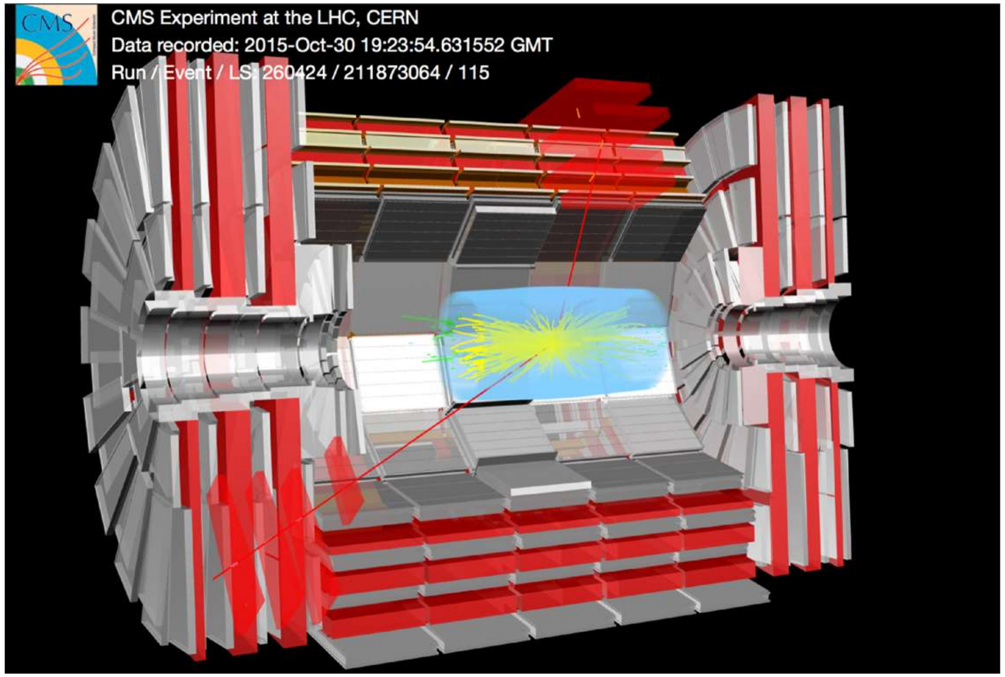

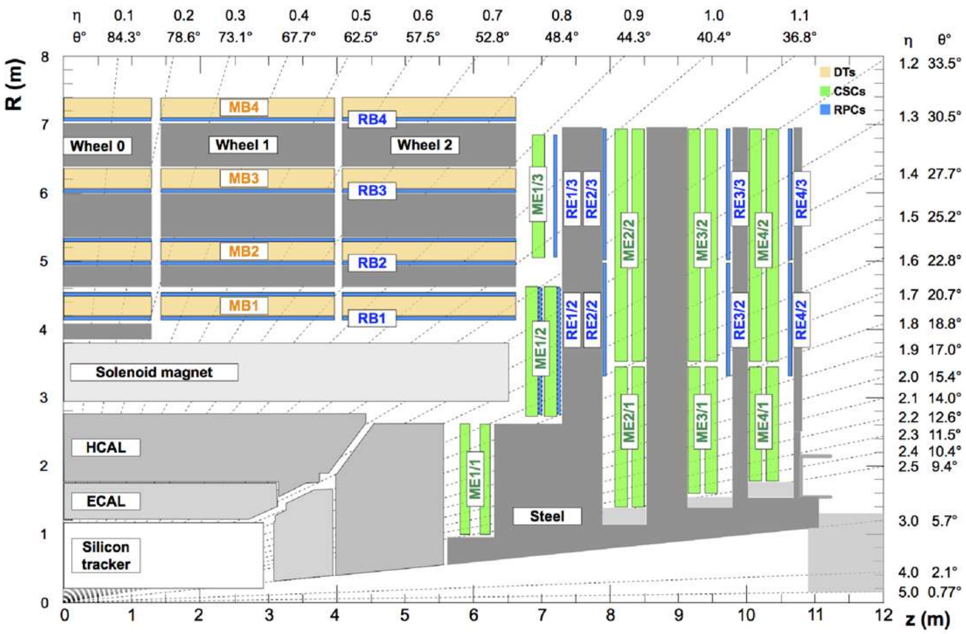

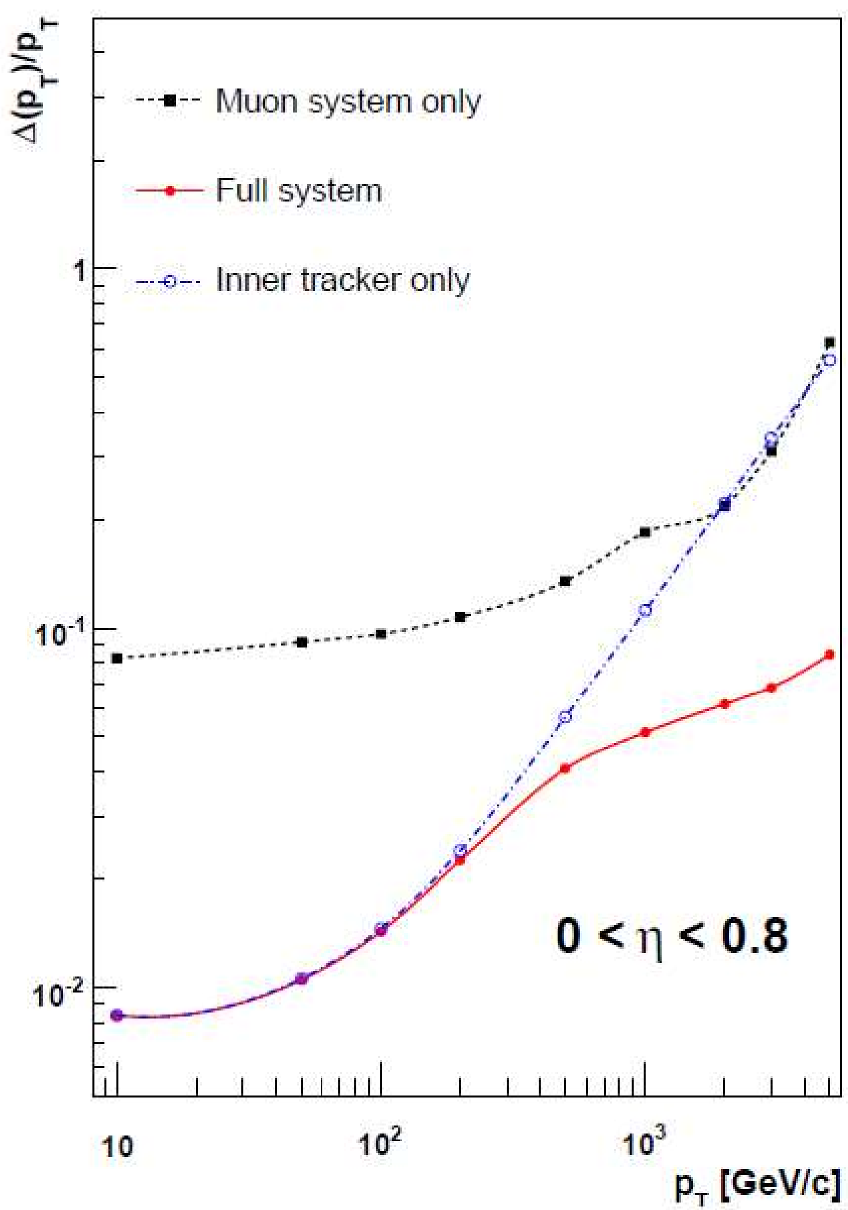

ATLAS Inner Detector

- **Pixel Detector**
  - 4 barrel layers, 3+3 disks, **10^8 pixels**
  - barrel radii: 33, 50, 85, 122 mm
  - pixel size 50×400 μm^2 (50×250 IBL)
  - **$\sigma_{R\Phi}$=6-10 μm, σ_z~66 μm**
- **SemiConductor Tracker**
  - 4 barrel layers, 7+7 disks, **6×10^6 strips**
  - barrel radii: 30, 37, 44, 51 cm
  - strip pitch 80 μm (40 mrad stereo)
  - **$\sigma_{R\Phi=}$16 μm, σ_z=580 μm**
- **Transition Radiation Tracker**
  - barrel 55<R<102 cm
  - 36 layers, **4×10^5 drift tubes**
  - 4 mm diameter
  - **$\sigma_{R\Phi=}$170 μm**
  - Also contributes to electron identification

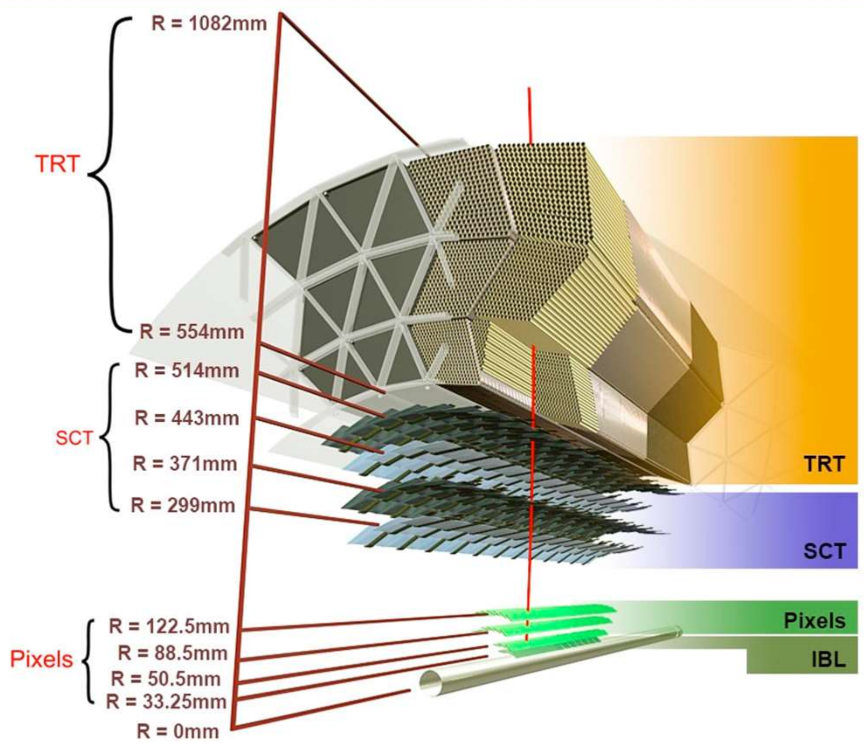

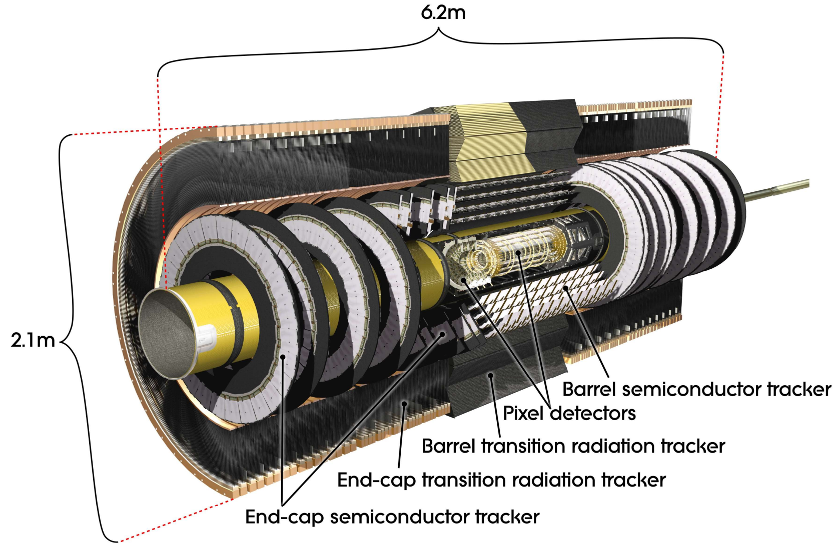

CMS Silicon Tracker

- **Pixel Detector**
  - 3 barrel layers, 2+2 disks, **10^7 pixels**
  - barrel radii: 44, 73, 102 mm
  - upgraded to 4 barrel layers, 3+3 disks, **10^8 pixels**
  - pixel size 100×150 μm²
  - **$\sigma_{R\Phi}$~10 μm, σ_z~10 μm**
- **Internal Silicon Strip Tracker (TIB, TID)**
  - 4 barrel layers, 3+3 disks, **2×10^6 strips**
  - barrel radii: 20-55 cm
  - strip pitch 80-120 μm
  - **$\sigma_{R\Phi}$~23-35 μm**
- **External Silicon Strip Tracker (TOB, TEC)**
  - 6 barrel layers, 9+9 disks, **7×10^6 strips**
  - barrel radii: max 116 cm
  - strip pitch 120-180 μm
  - **$\sigma_{R\Phi}$~35-53 μm**

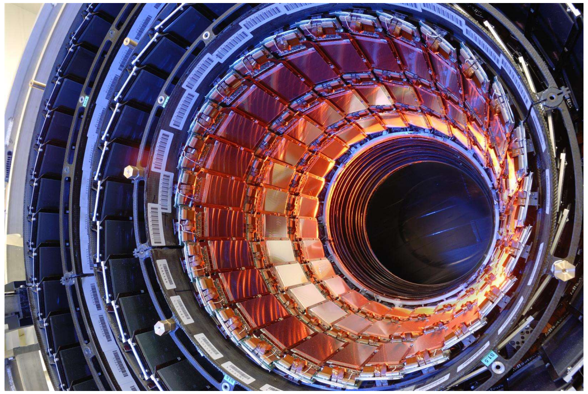

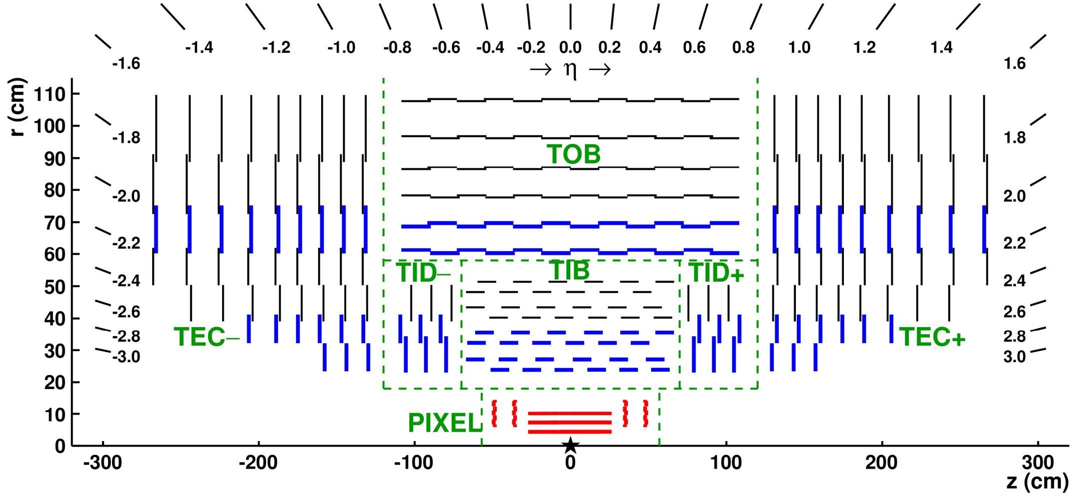

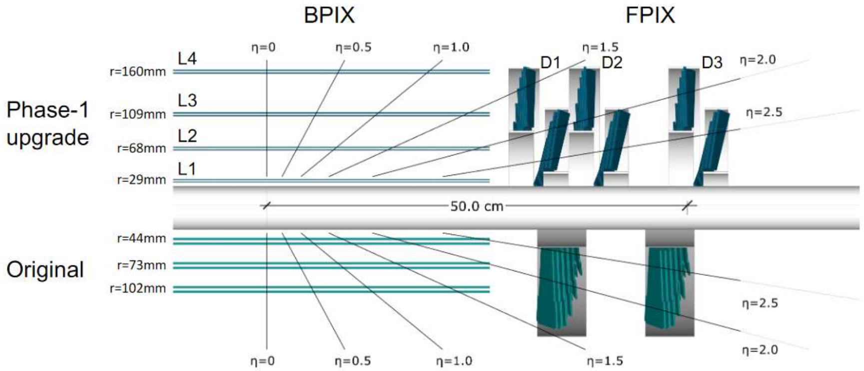

Technology choice

- The inner tracking system purpose is to:
  - measure particle momentum
  - identify and separate the pileup interactions
  - detect decay of particles with a flight length from 1 mm (*b*-, *c*-hadrons, τ) to several cm (*s*-hadrons, new physics)
- and has to cope with:
  - particle rate: 100 MHz/cm^2 at 1×10^{34} cm^{-2}s^{-1}
  - doses up to 10^7 Gy and NIEL 10^{16} (1 MeV n_{eq}/cm^{-2})

few μm resolution

several particles/cm^2/bunch crossing

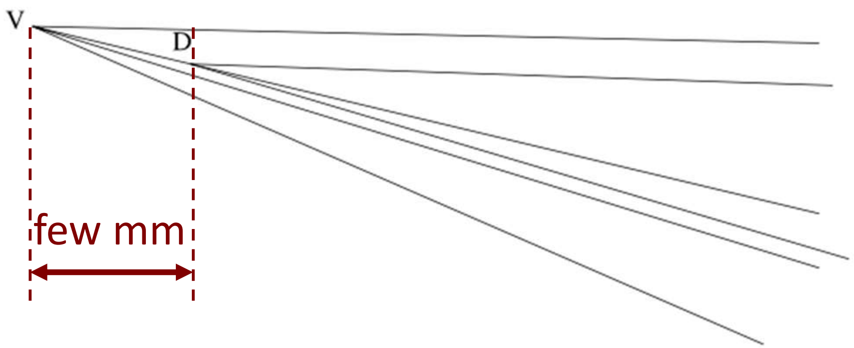

opening angle ~0.1 rad
transverse vertex resolution ~10 μm
decay length resolution ~100 μm

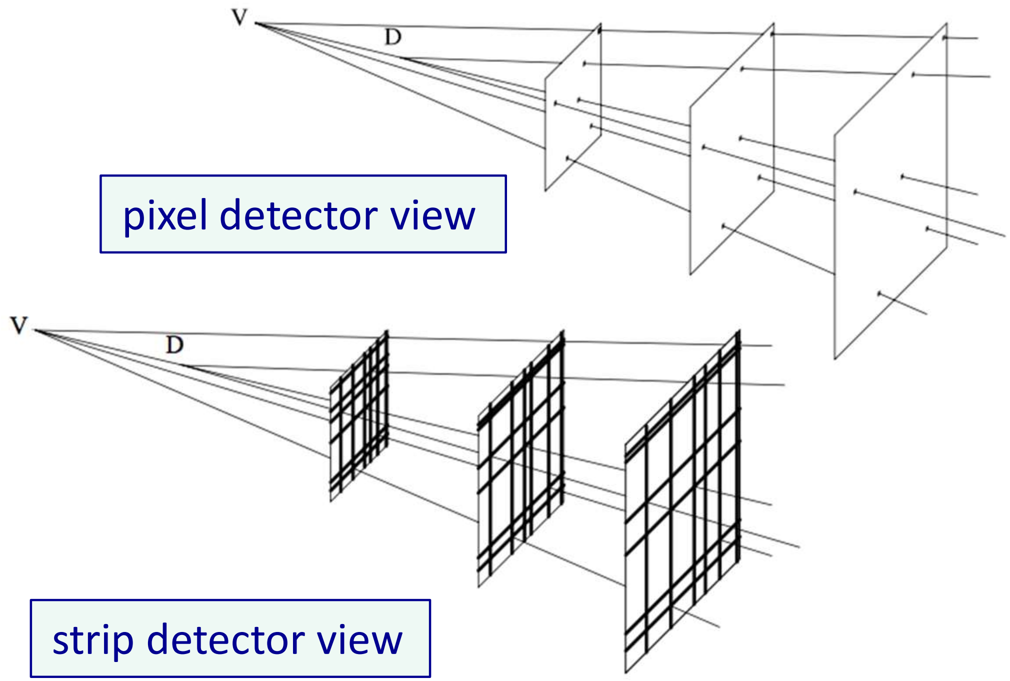

Technology choice

- The inner tracking system purpose is to:
  - measure particle momentum
  - identify and separate the pileup interactions
  - detect decay of particles with a flight length from 1 mm (*b*-, *c*-hadrons, τ) to several cm (*s*-hadrons, new physics)
- and has to cope with:
  - particle rate: 100 MHz/cm^2 at 1×10^{34} cm^{-2}s^{-1}
  - doses up to 10^7 Gy and NIEL 10^{16} (1 MeV n_{eq}/cm^{-2})

few μm resolution

several particles/cm^2/bunch crossing

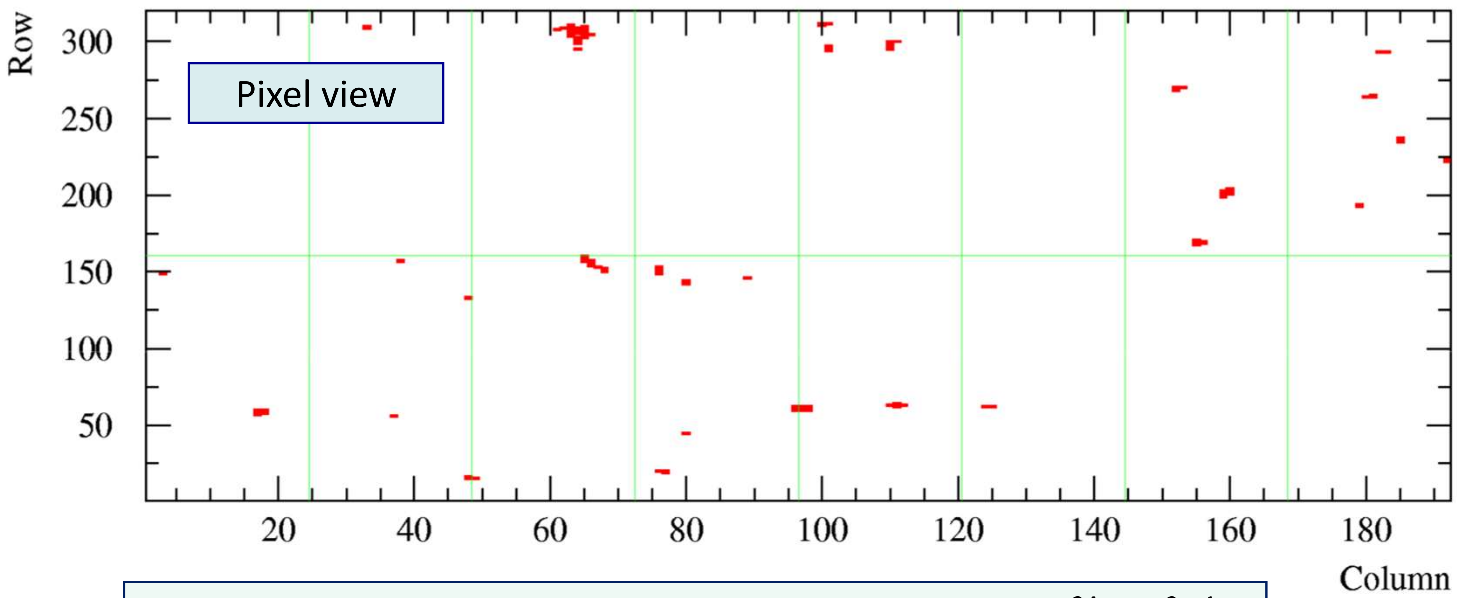

Simulated event in the ATLAS pixel at *R*=50 mm and 10^{34} cm^{-2}s^{-1}

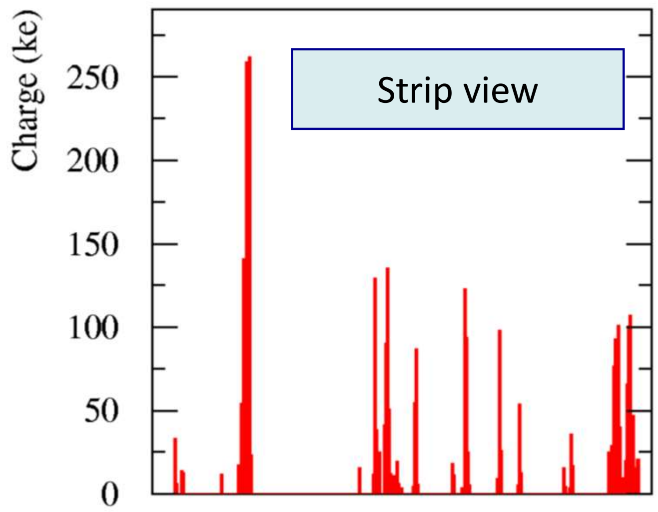

Impact parameter(s) resolution

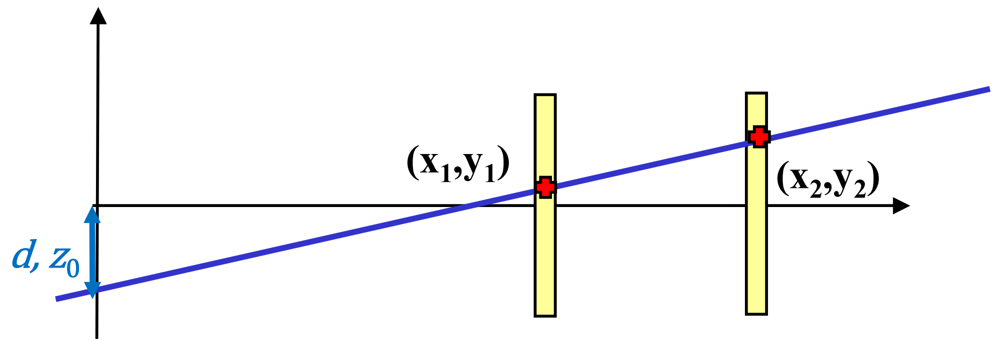

- d transverse distance with of trajectory from the interaction region
  - ~0 for primary particles
  - ~$c\tau$ for decay products (independent of boost)
- z_0 position along the beam axis
- Resolution is dominated by the first measurement points
  - rest of trajectory determine the curvature/momentum
- **Detector resolution**

$$\sigma_d = \sqrt{\frac{n^2+1}{(n-1)^2}}\sigma_y$$

  - $n = x_2/x_1$ often referred as lever arm
- Multiple scattering

$$\sigma_d = \sqrt{\sum_i x_i^2 \theta_{p,\mathrm{rms},i}^2}$$

  - where the index i runs over all material crossed by the particle up to and including the first measured point

Impact parameter(s) resolution

- d transverse distance with of trajectory from the interaction region
  - ~0 for primary particles
  - ~$c\tau$ for decay products (independent of boost)
- z_0 position along the beam axis
- Resolution is dominated by the first measurement points
  - rest of trajectory determine the curvature/momentum

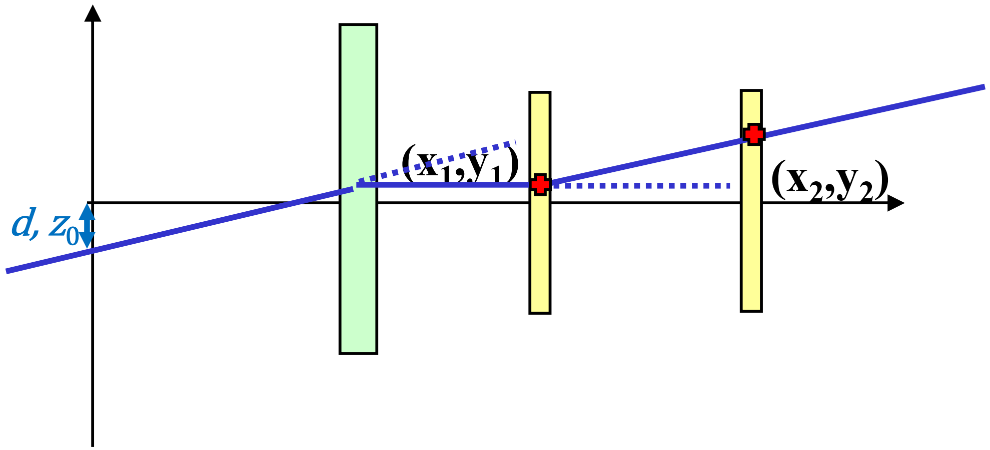

- **Detector resolution** $$\sigma_d = \sqrt{\frac{n^2+1}{(n-1)^2}}\sigma_y \quad \propto \text{cost.}$$
  - $n = x_2/x_1$ often referred as lever arm
- Multiple scattering $$\sigma_d = \sqrt{\sum_i x_i^2 \theta_{p,\mathrm{rms},i}^2} \quad \propto \frac{1}{p}$$
  - where the index i runs over all material crossed by the particle up to and including the first measured point

Example: ATLAS IBL insertion in LS1

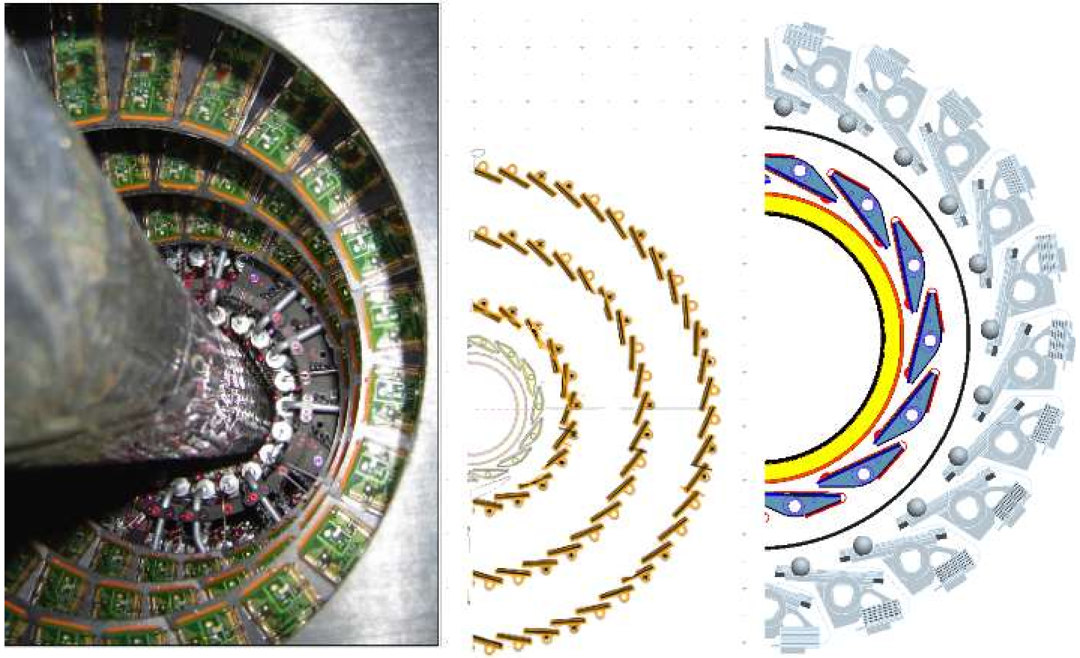

- During Run1 (up to 2012), innermost barrel layer:
  - radius at 50 mm
  - pixel size 50×400 μm²
- In Run2, inserted a new layer
  - radius at 33 mm
  - pixel size 50×250 μm²

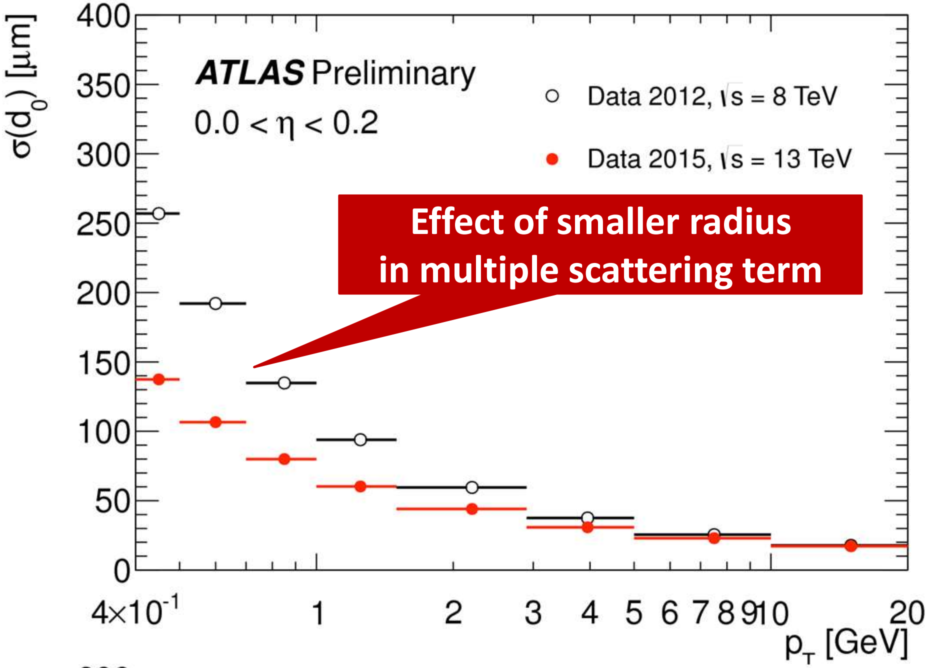

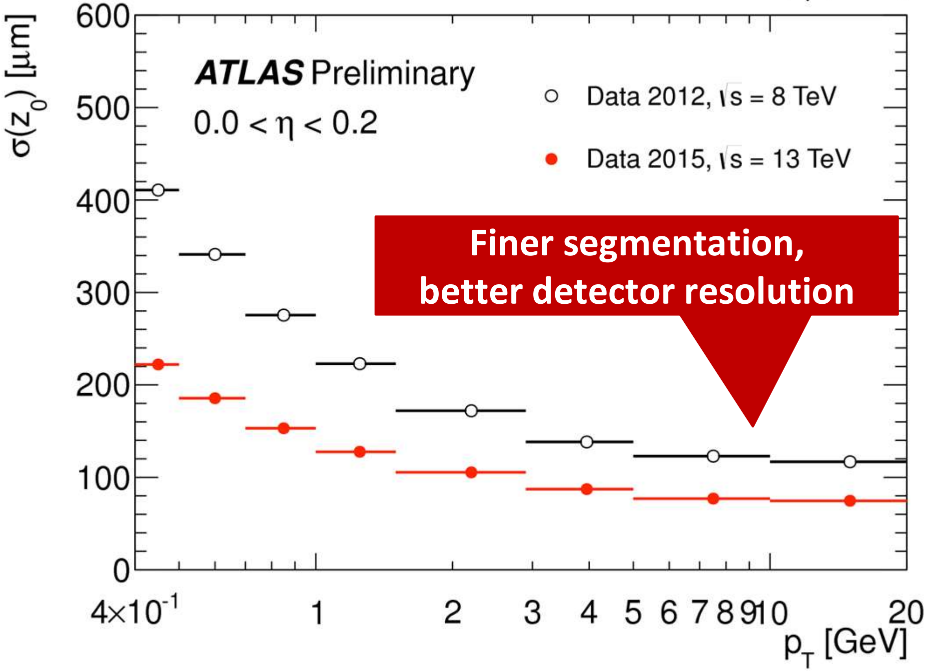

Back to history: most famous $t\bar{t}$

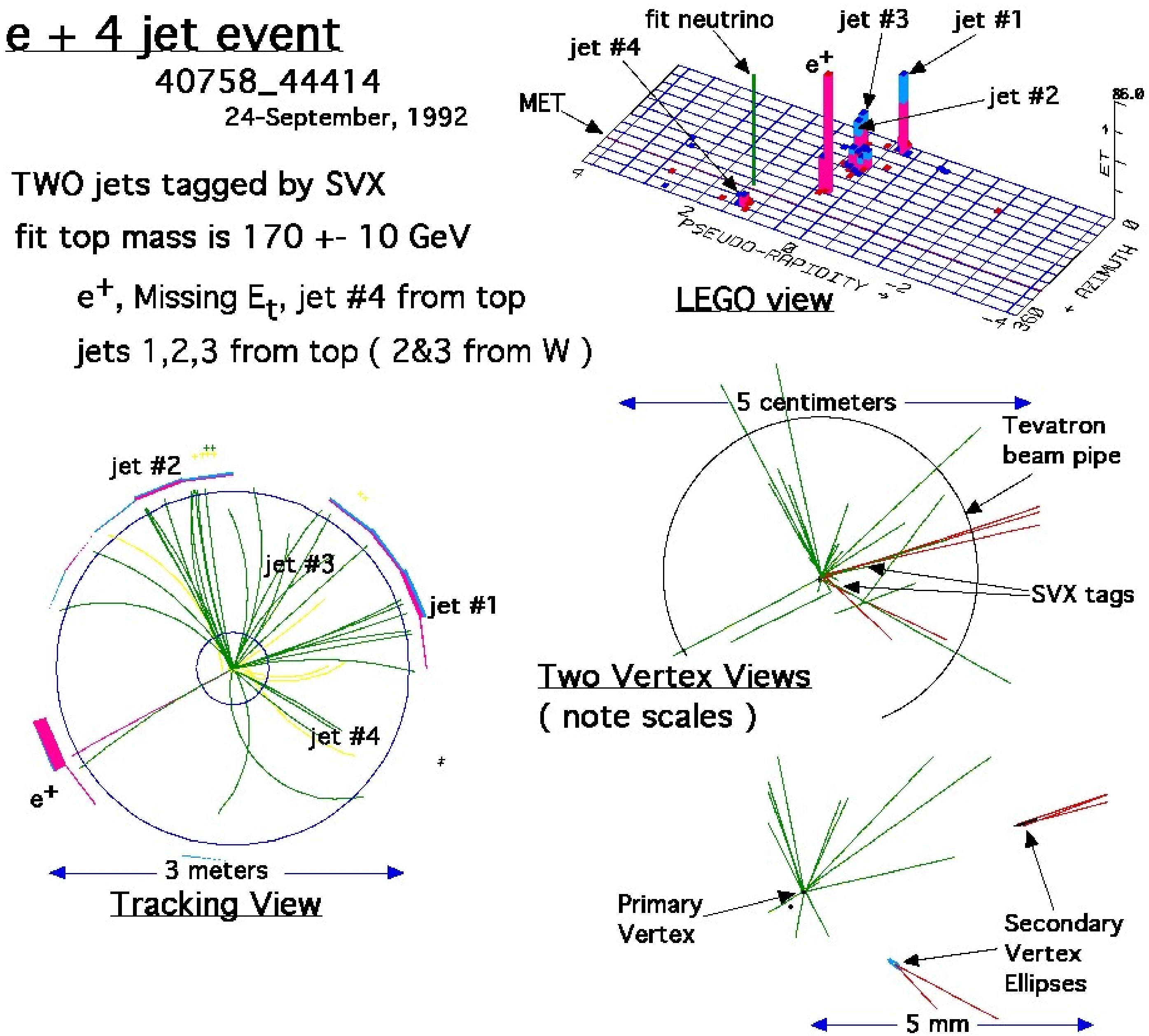

$$p\bar{p} \to t\bar{t} + X$$
$$\hookrightarrow \bar{b}W^- \to \bar{b}q\bar{q}$$
$$\hookrightarrow bW^+ \to be^+\nu_e$$

- Lorentz boost increases decay length L
- it decreases opening angle of decay products to build the vertex, increasing σ_L
- The two effects compensate

$$\frac{\sigma_L}{L} = O\left(\frac{\sigma_d}{c\tau}\right)$$

  - τ average lifetime of decaying particle

Calorimetric systems

- Detection of neutral particles
  - interaction and conversion to charged particle
  - energy deposited by ionization
- Lepton identification
- Energy measurement (improving with increasing energy)
- Neutrino/Dark particle detection (missing energy/momentum)

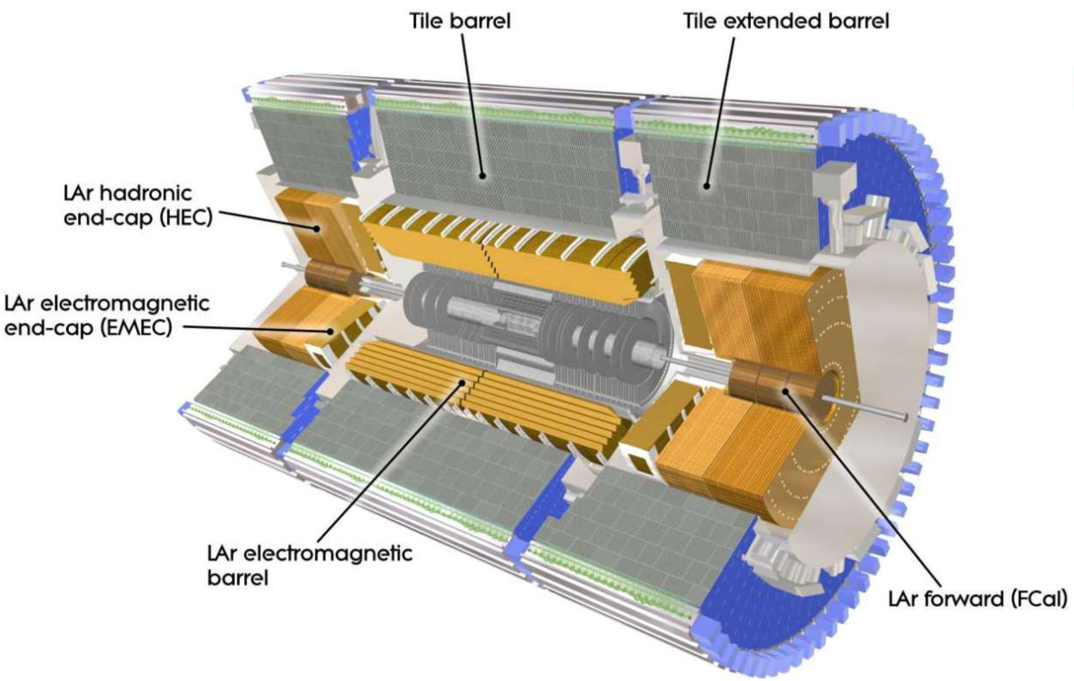

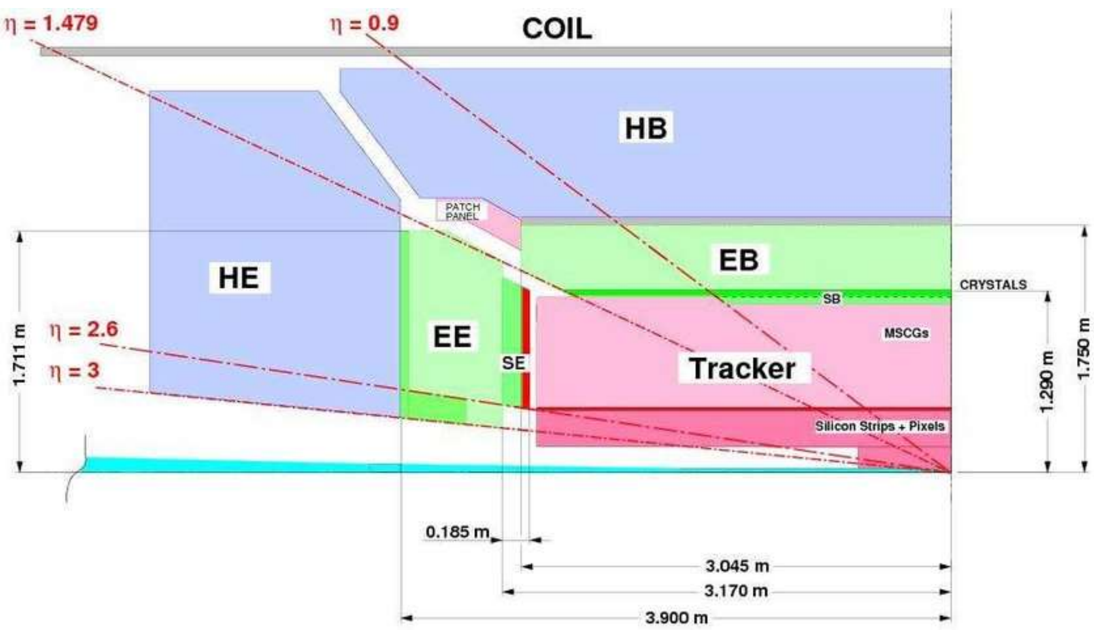

Calorimetry basics: interactions

High energy particles have different interactions with matter:

- **electrons and photons** degrade their energy by bremsstrahlung and pair production; the length scale is given by the *radiation length* X_0:

$$X_o \approx \frac{716.4\mathrm{g\,cm}^{-2} A}{Z(Z+1)\ln\left(287/\sqrt{Z}\right)}$$

- **hadrons** undergo nuclear interactions, with mean free path given by the *interaction length* λ_I;

$$\lambda_I \approx 35\ \mathrm{g\,cm}^{-2} A^{1/3}$$

- as to **muons**, and **low evergy charged particles**, usually the dominant energy loss process is by soft collisions following the Bethe-Bloch law:

$$\frac{dE}{dx} = \frac{N_A}{\varepsilon_0} z^2 e^2 \frac{Z}{A} \frac{1}{\beta^2}\left[\frac{1}{2}\ln\frac{2m_e c^2 \beta^2 \gamma^2 T_{\max}}{I^2} - \beta^2 - \frac{\delta}{2}\right]$$

which is in the inteval 1-2 MeV/ g cm^{-2} for most materials.

Calorimetry basics: *Heitler* model

Despite electrons and hadrons having different behavior, it is possible to grasp the more relevant features through a simplified model:

- a particle fly a fixed lenght λ between two interactions;
- at each interaction m particles are produced, with typical transverse momentum p_T;
- the secondary particles interact again, originating a particle shower, until they fall below a critical energy E_c;
- after that they are absorbed in a typical length given by $E_c/(-dE/dx)$.

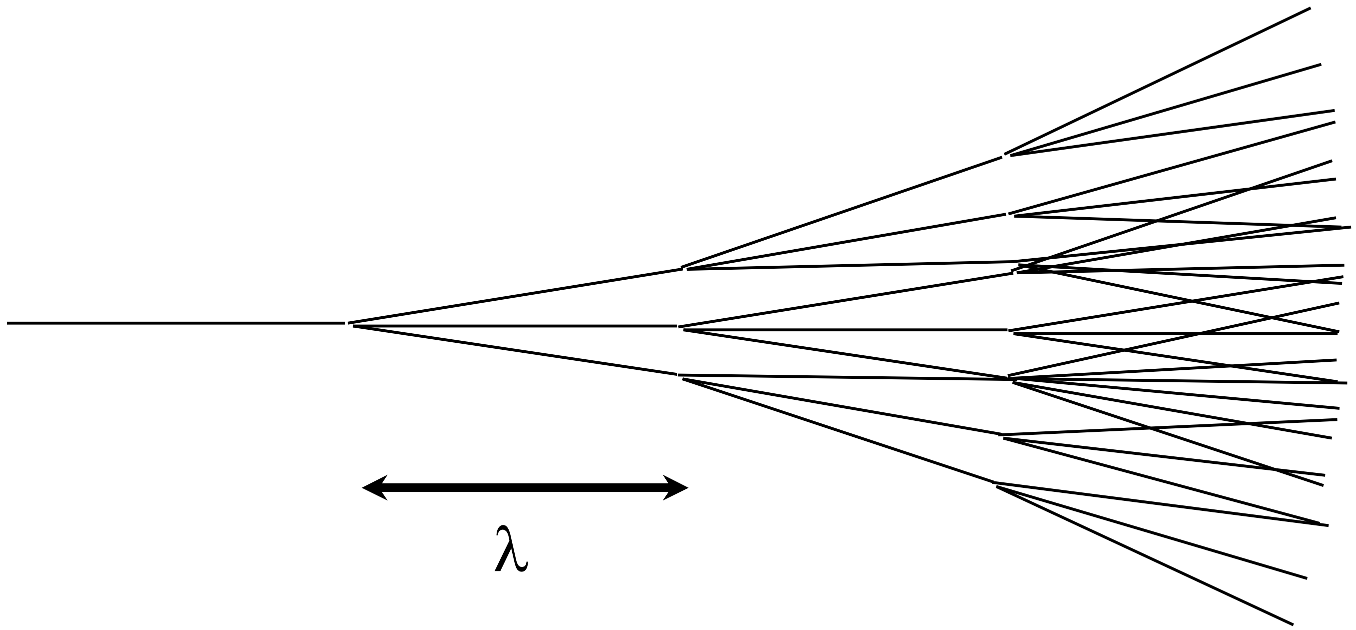

Calorimetry basics: *Heitler* model

Starting with a primary particle of energy *E*:

- the total number ***N*** of secondary particles is

$$N = E / E_c$$

- this number is reached at a length $n\lambda$, where n is given by:

$$N = m^n \Rightarrow n = \ln \frac{E}{E_c} / \ln m$$

resulting in shower length ***L***: $L = \frac{\lambda}{\ln m} \ln \frac{E}{E_c} + \frac{E_c}{-dE/dx}$

Longitudinal dimension scales logarithmically on E

- between the i^{th} and the $(i+1)^{\text{th}}$ interactions, the secondaries expand by $R_i = \lambda \frac{p_T}{E_i} = \frac{\lambda p_T}{E} m^i$ resulting in a transverse shower size at maximum, $R_{\max}$:

$$R_{\max} = \sum_{i=1}^{n-1} \frac{\lambda p_T}{E} m^i = \frac{\lambda p_T}{E} \frac{m^n - m}{m-1} \approx \frac{1}{m-1} \frac{\lambda p_T}{E_c}$$

- finally shower fluctuations will be driven by the number of interactions:

$$\sigma \propto \sqrt{\frac{N}{m}} = \sqrt{\frac{E}{mE_c}}$$

$\sigma_E / E \propto 1/\sqrt{E}$

Calorimetry basics: em and had

Electromagnetic showers

- $m = 2$
- $\lambda = X_0$
- $p_T = \sqrt{\frac{4\pi}{\alpha}} m_e c$
- $E_c = \frac{800 \text{ MeV}}{Z+1.2}$

- Shower dimension
  - longitudinal: $L = \ln \frac{E}{E_c} + 14$
  - trasversal: $R = 2\rho_M, \rho_M = X_0 \frac{E_S}{E_c}$ (Moliere radius)
- Energy resolution
  - clearly technology dependent

$$\frac{\sigma_E}{E} = \frac{1-20\%}{\sqrt{E[\text{GeV}]}}$$

Compact ~ 10 cm
High energy resolution

Hadronic showers

- $m \sim 6$
- $\lambda = \lambda_I$
- $p_T = p_F \approx 340 \text{ MeV}/c$
- $E_c \approx 2m_\pi$

- Shower dimension
  - longitudinal: $L = 0.2 \ln E[\text{GeV}] + 3.2$
  - trasversal: $R = \lambda_I$
- Energy resolution
  - clearly technology dependent

$$\frac{\sigma_E}{E} = \frac{50-100\%}{\sqrt{E[\text{GeV}]}}$$

Some interaction lengths ~ 1 m
Lesser energy resolution

ATLAS and CMS

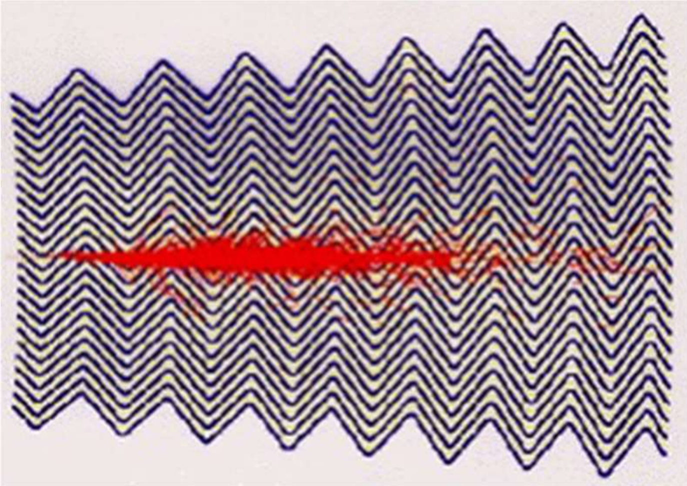

Technology	
Pb (passive) / LAr (active)	$PbWO_4$ crystals
Depth	
25 X_0	25 X_0
Resolution	
10%/√E	3%/√E

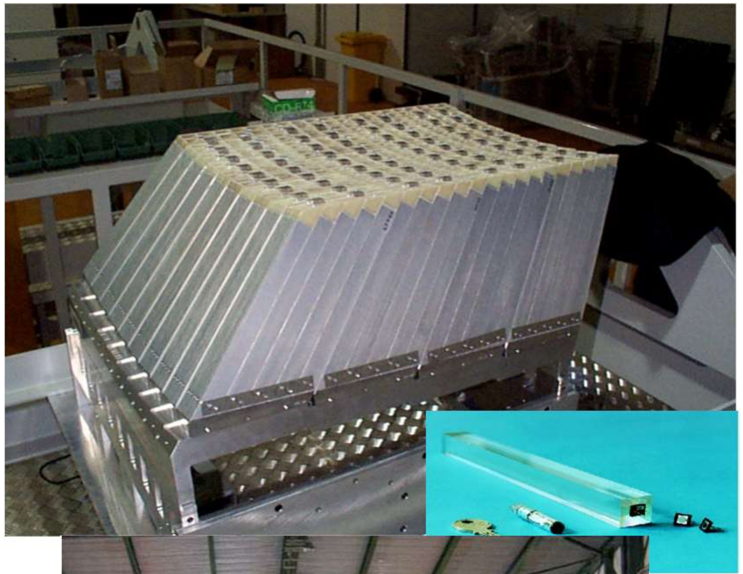

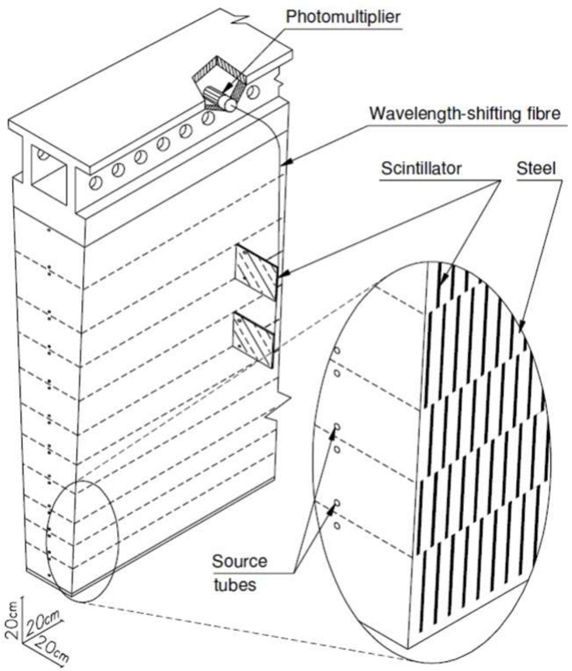

Technology	
Steel / Scintillator Cu+W / LAr	Brass / Scintillator
Depth	
8-10 λ_I	6-10 λ_I
Resolution	
50%/√E	100%/√E

Energy resolution

Comparison of the LHC calorimeters' energy resolution

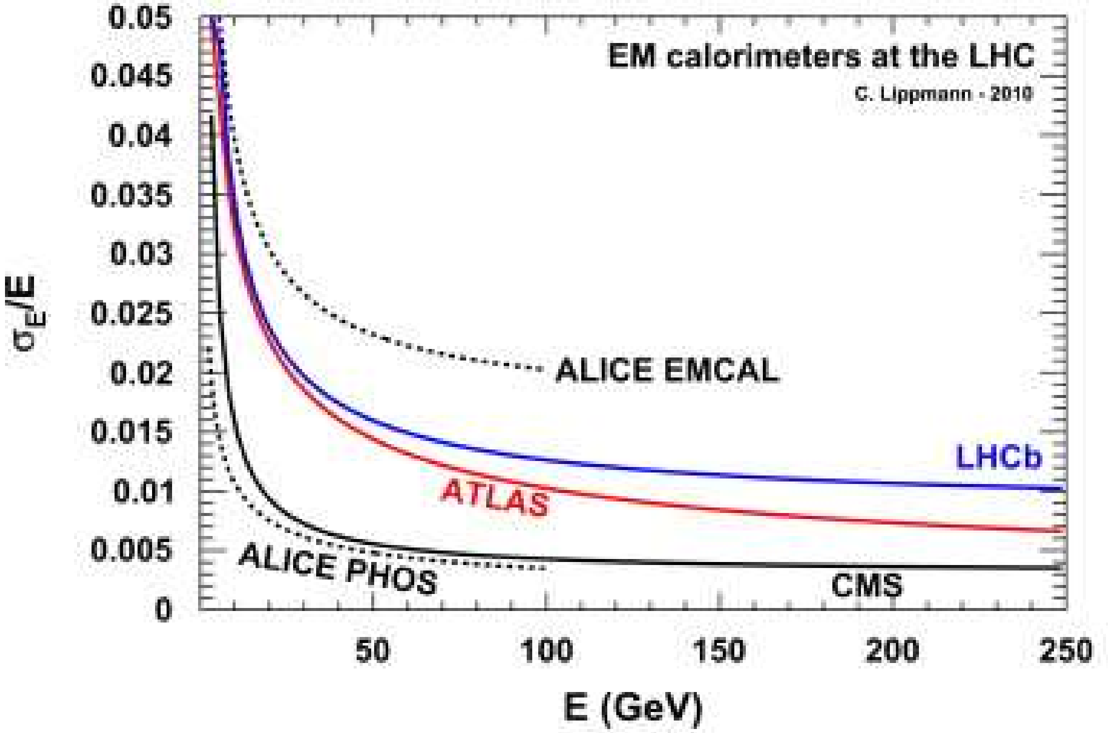

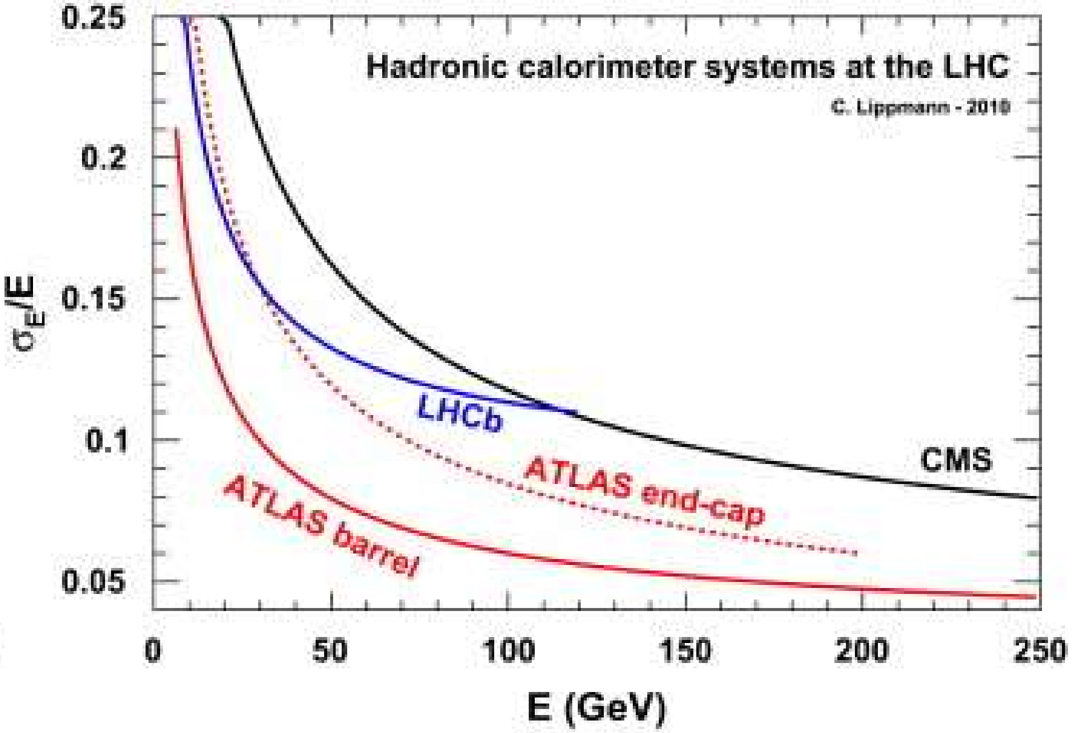

$$\frac{\sigma_E}{E} = \frac{a}{\sqrt{E}} \oplus \frac{b}{E} \oplus c$$

Sampling

Noise

Calibration / leakage

DAQ and Trigger

- Data reduction:
  - from 40 MHz bunch crossing rate
  - to ~1 kHz storage for offline analysis
- 1st level hardware trigger:
  - calorimeters
  - muon systems
  - only trigger components
  - initiate full detector readout within a predefined latency
  - ~100 kHz rate
- High Level Trigger:
  - in principle full detector information available
  - streamlined offline-analysis algorithms
  - partial (regional) reconstruction

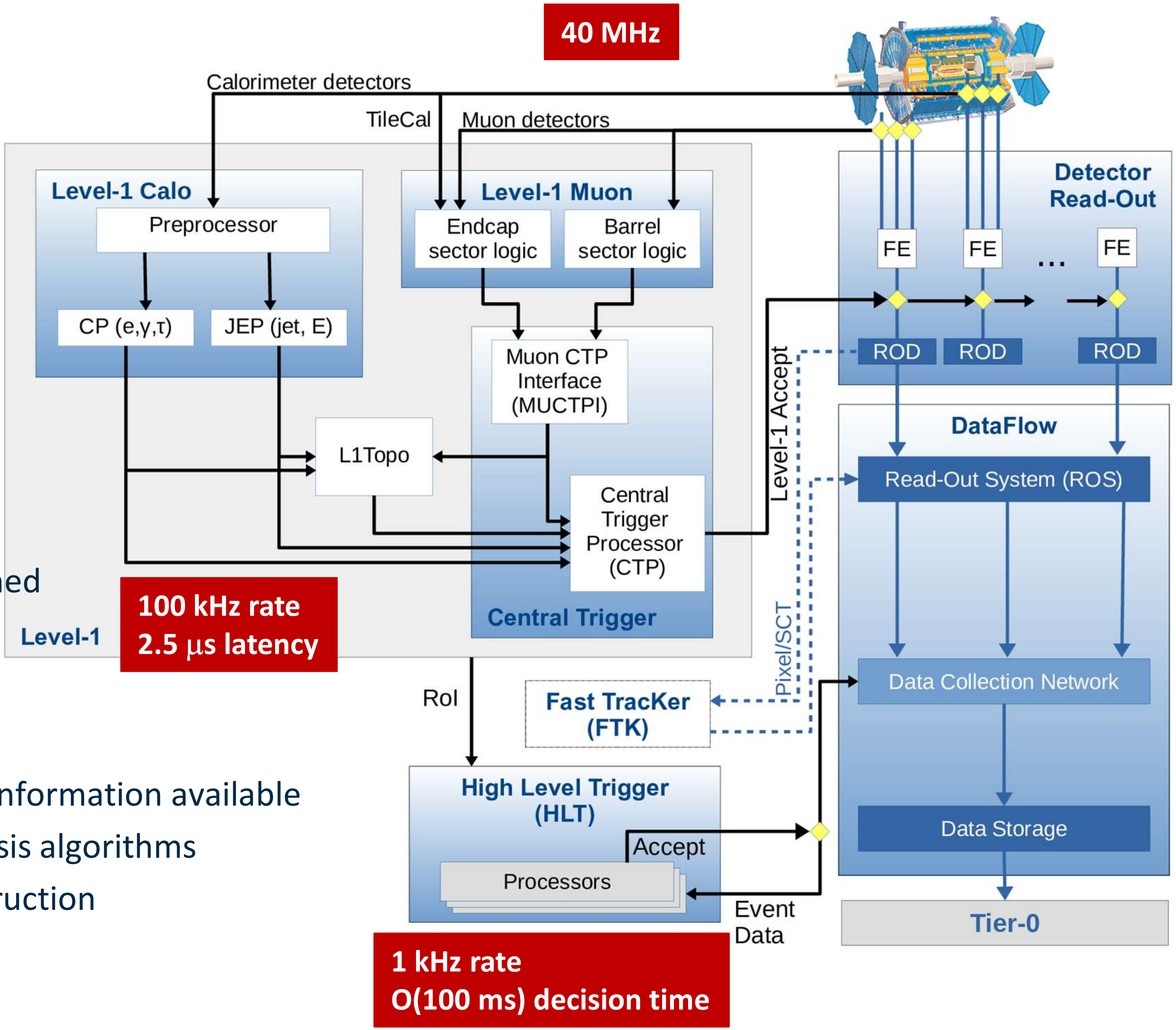

The upgrades for HL-LHC

- **Trigger/DAQ**
  - Add tracking at first level trigger, exploit higher granularity
  - Improve bandwidth and processing for triggering, increase in latency
- **Tracking detectors**
  - New all silicon tracking detectors for ATLAS and CMS with extended coverage to $|\eta| < 4$
- **Timing detectors** New at LHC
  - **ATLAS**: High granularity timing detector in front of forward calorimeter ATLAS
  - **CMS**: MIP timing layer around trackers
- **Calorimetry**
  - **ATLAS**: New FE electronics for Tile and LAr calorimeter (increase granularity)
  - **CMS**: New High Granularity Calorimeter (HGCAL) in the endcaps and replace electronics in electromagnetic calorimeter
- **Muon system**
  - **ATLAS**: New FE electronics and additional units in muon spectrometer
  - **CMS**: Extend forward chambers and replace electronics

For selected items: LHC technology → Upgrades for HL-LHC

DAQ and Trigger Upgrades

- Trigger selection defines the acceptance of phsycis measurements
  - compromise between **efficiency** (on interesting events) and **rate** (dominated by backgrounds)
- At HL-LHC:
  - **signal** proportional to luminosity increase
  - **background** increase due to higher pileup
  - even if improving the recording capability to 10 kHz, it is necessary to be **improve the background rejection**
  - more complex trigger algorithms require **longer latency**, ~2.5 μs → ~12.5 μs : more memory needed to store data waiting for L1 decision
- **This will be a major driver on some detector upgrades:**
  - Improved trigger readout granularity
  - Fake reduction
  - Addition of tracking information at L1

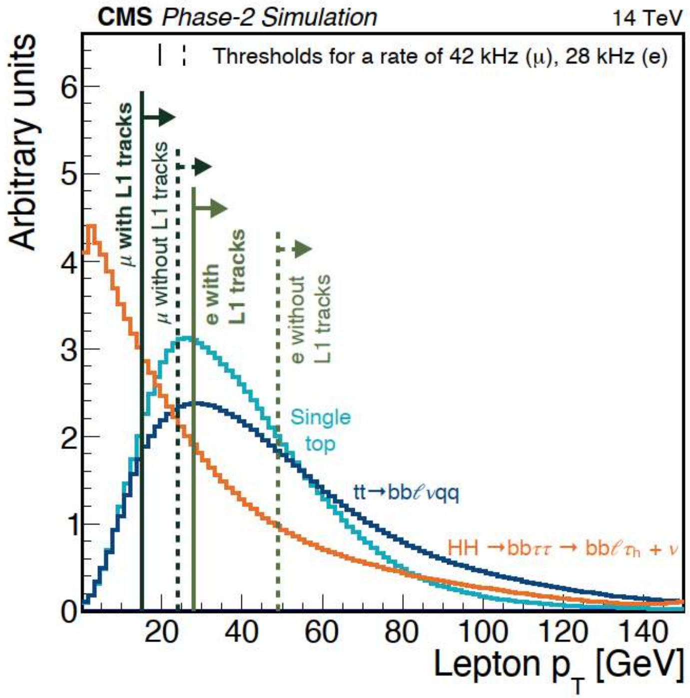

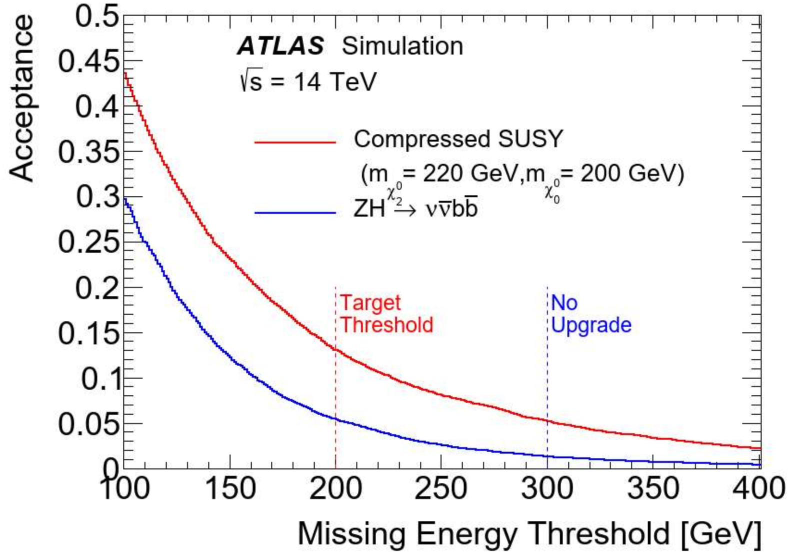

CMS L1 Trigger for HL-LHC

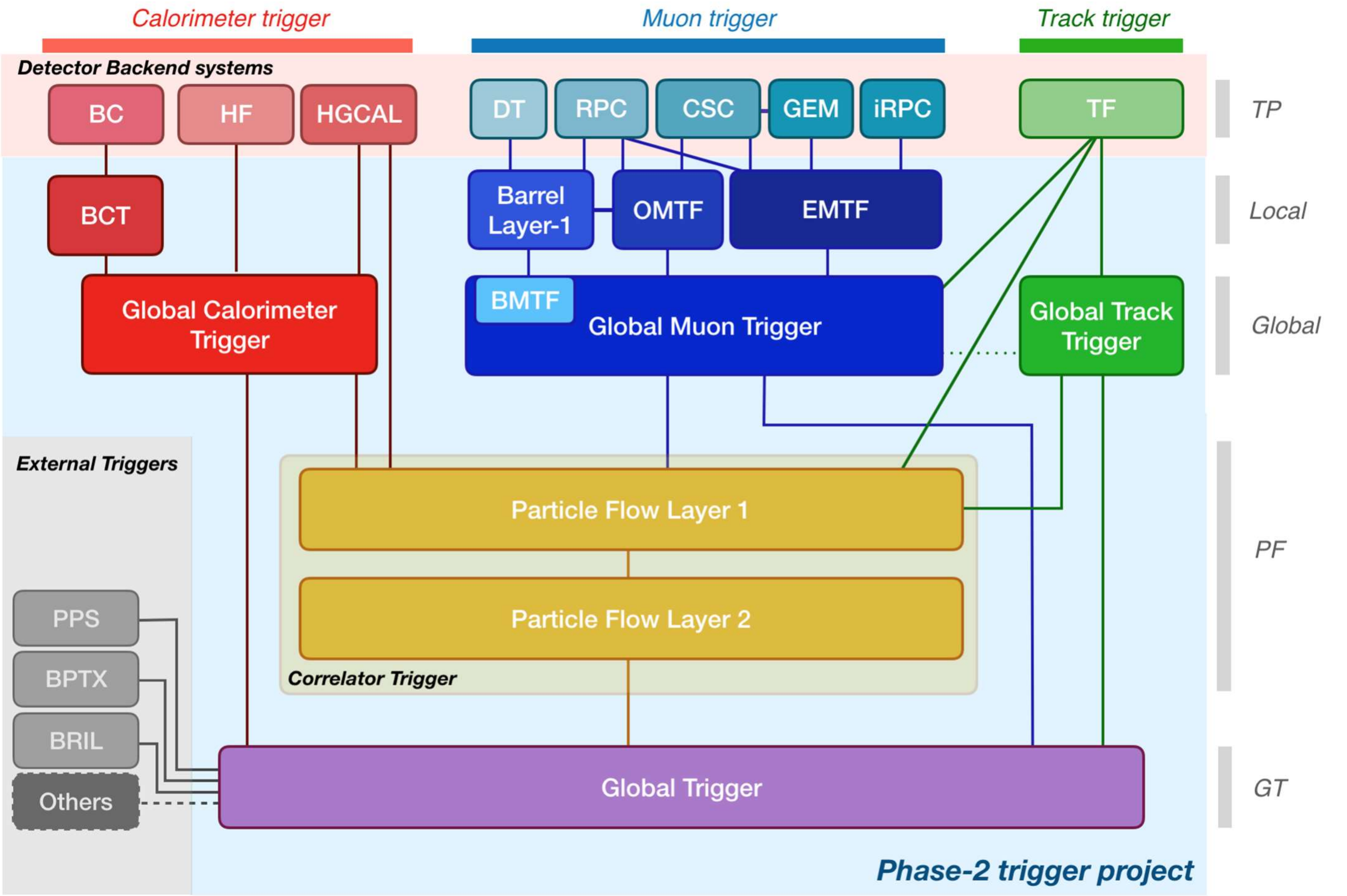

ATLAS Trigger for HL-LHC

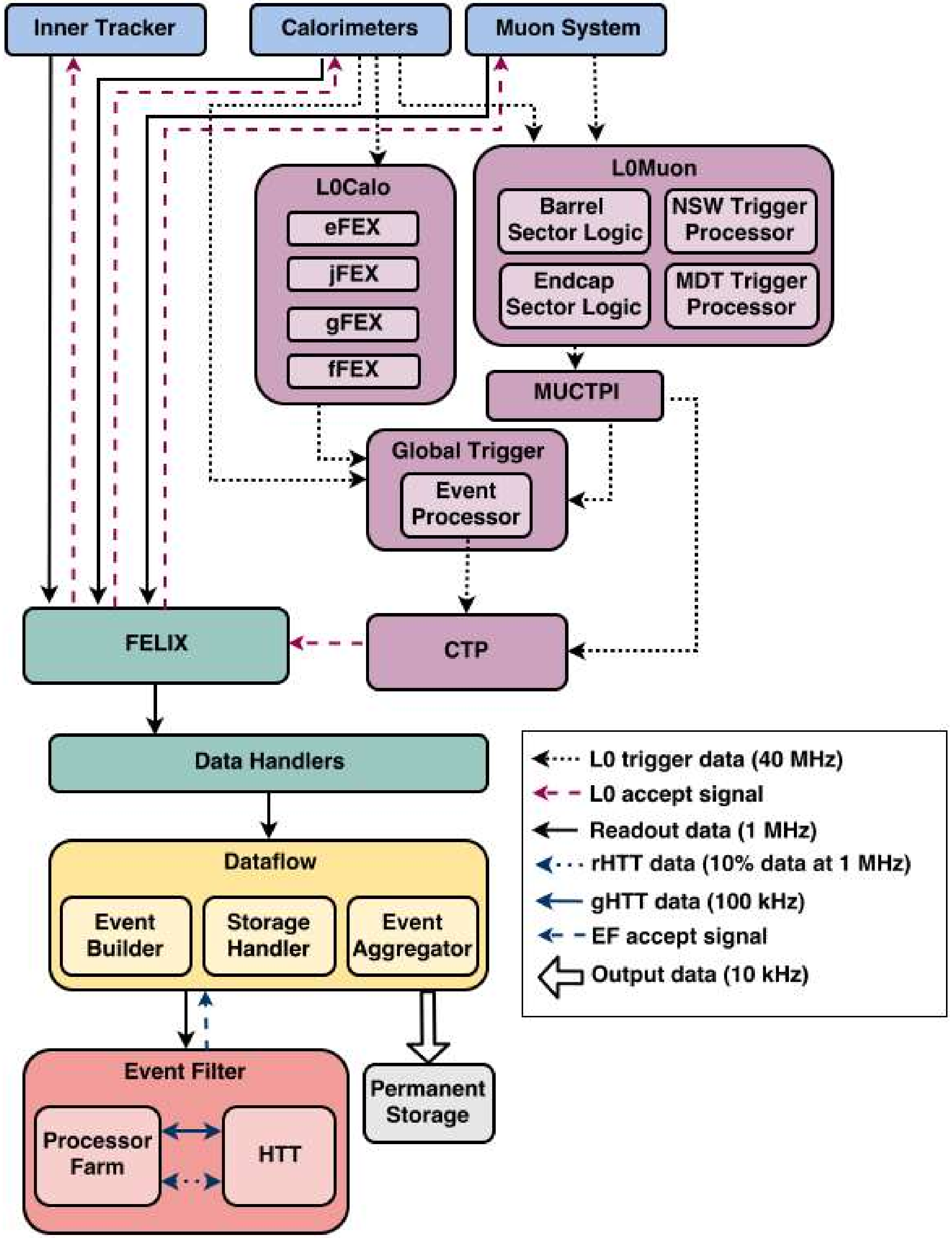

TRACKING

Istituto Nazionale di Fisica Nucleare
Sezione di Milano
UNIVERSITÀ DEGLI STUDI DI MILANO
DIPARTIMENTO DI FISICA

Silicon Detectors

For HL-LHC, two completely new full-silicon tracking systems

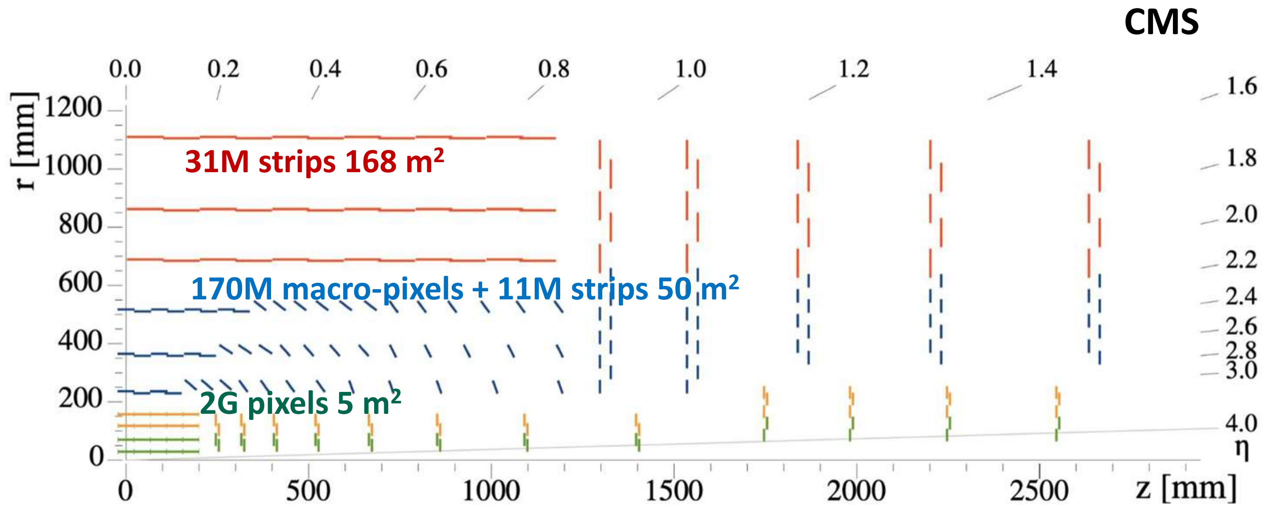

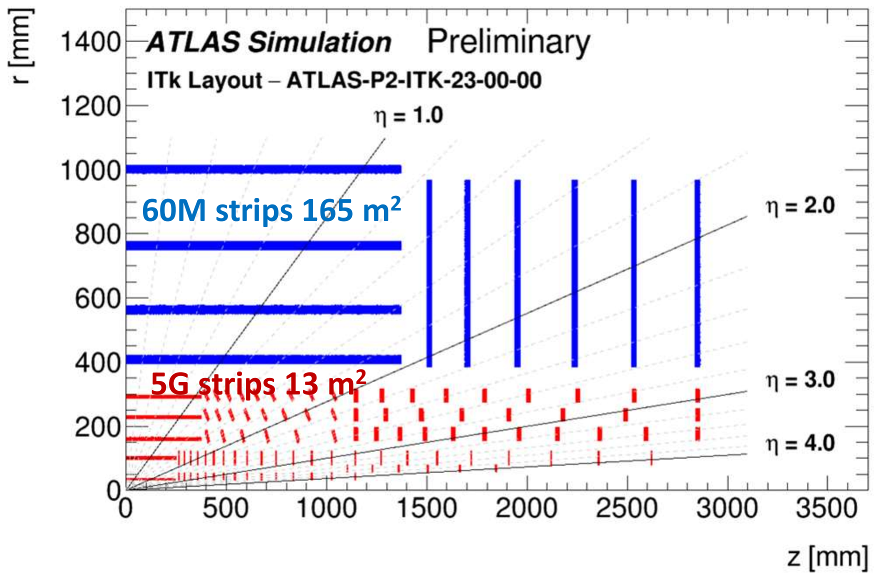

- Extend tracking to |η|=4
- n-in-p silicon sensors
- Increased particle flux+increased trigger rate: fast data transmission
- Rad-tolerant CMOS FE electronics: 65 nm pixels, 130 nm strips
- Efficient power distribution: serial power in pixel, DC-DC converters in strip
- CO_2 bi-phase cooling
- Carbon structures: stability and low mass

	CMS	ATLAS
Strip pitch [μm]	90-100	70-85
Strip length [cm]	2.5-5	2.5-8
Strip thickness [μm]	300	300
Pixel size [μm²]	25×100 25×1500 (macro)	50×50 (25×100 in L0 barrel)
Pixel thickness [μm]	<150	<150

General layout e performance

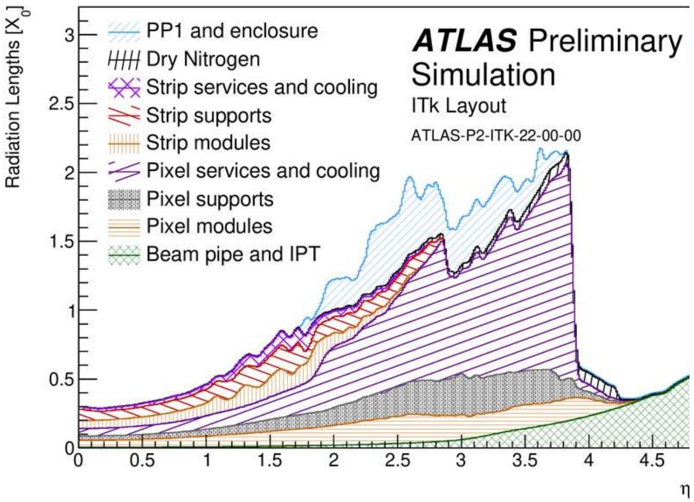

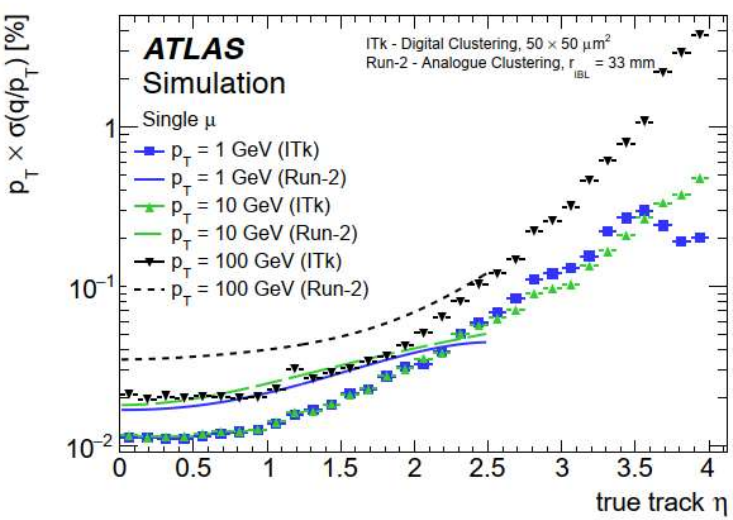

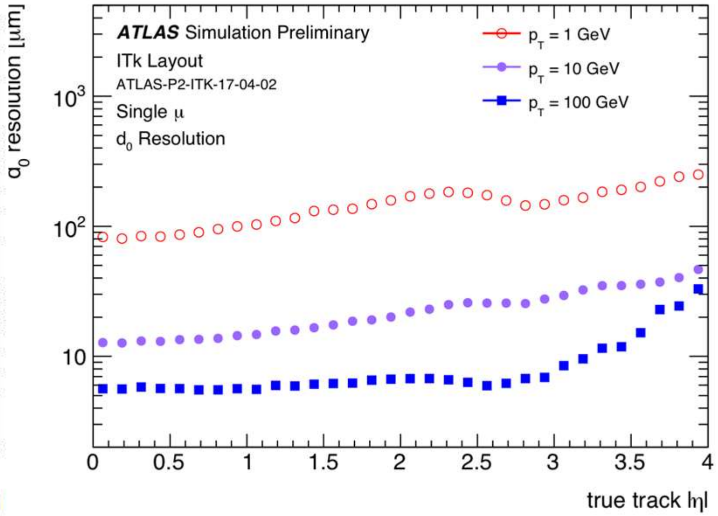

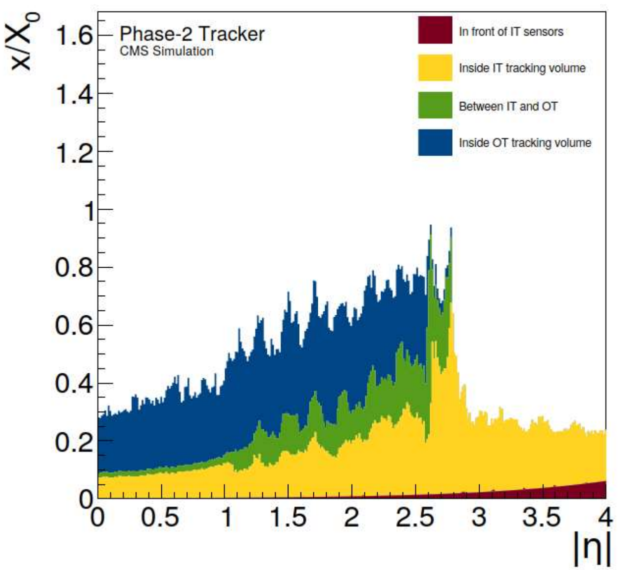

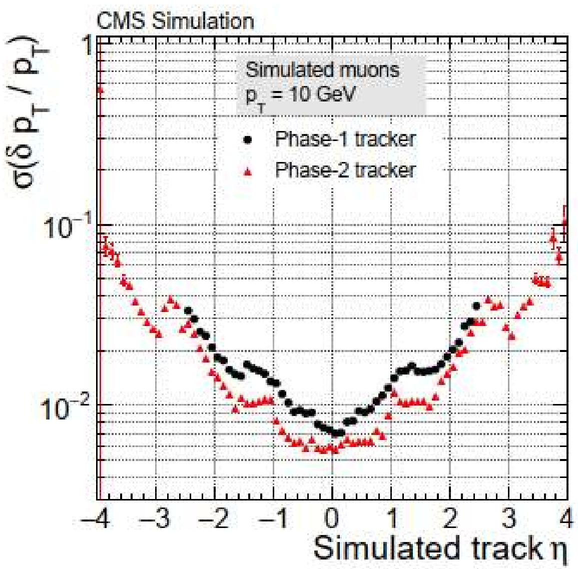

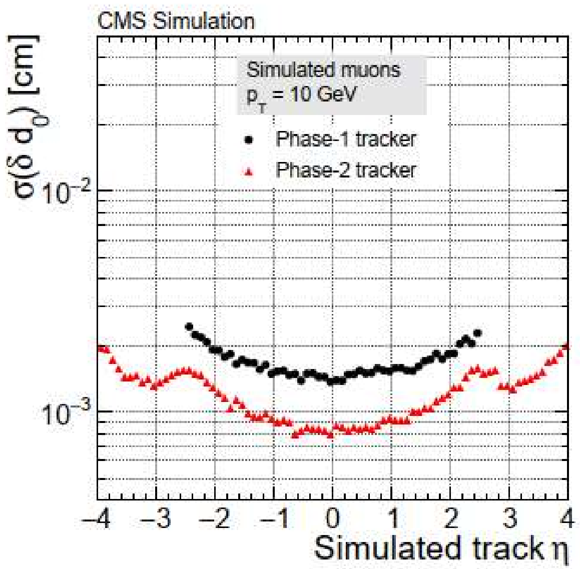

Silicon Detectors

- The simplest Silicon Detector is a reverse-biased *pn*-junction:
  - The polarization creates a field that prevents diffusion of majority carriers in a depleted region
  - **Signal** is generated by electron-hole pair production by the energy loss of charged particles
  - **Leakage current** from thermal excitation

$$I_{leak} \propto T^2 e^{-\frac{E_g}{k_B T}}$$

    - T temperature
    - E_g band gap
    - k_B Boltzmann constant
  - **A depleted region is created spontaneously also in absence of an external polarization:**

$$V_{BI} = \frac{k_B T}{e} \ln\left(N_A N_D / n_i^2 \right)$$

25 mV at room T

Dopant densities 10^{14-18} cm^{-3}

Intrinsic carriers density ~10^{13} cm^{-3}

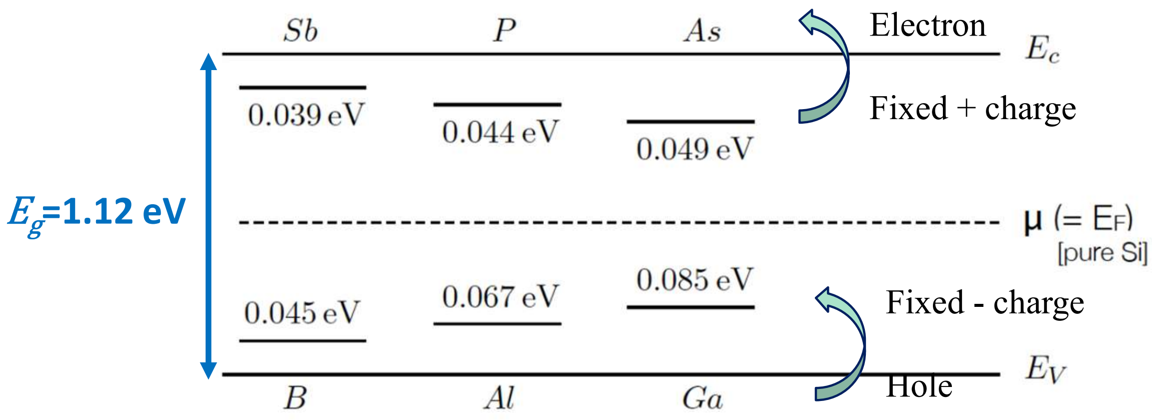

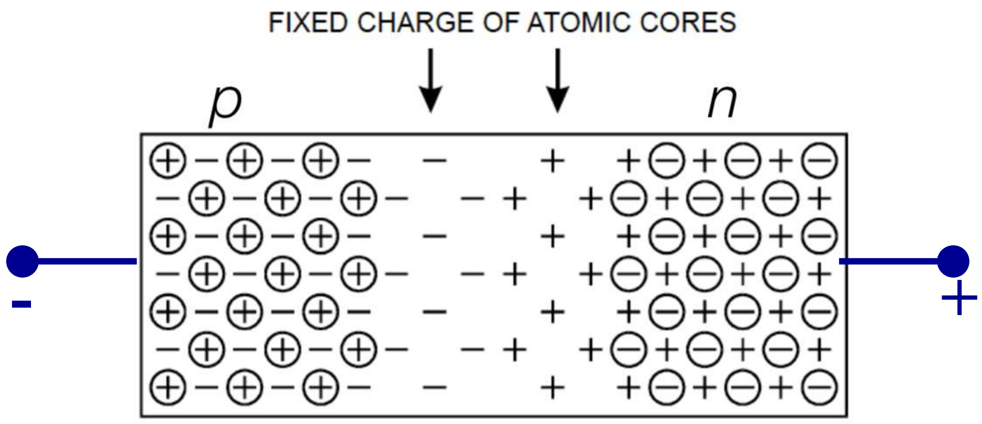

pn-junction: basic properties

- Relationships between bias voltage V_B, depletion d, electric field E, and dopant concentrations $N_{A,D}$, can be obtained solving the Poisson equation:

$$\frac{dE_x}{dx} = \frac{\rho}{\varepsilon}$$

- Property determined by the less doped material
  - assuming it is *n*-type: $N_D \ll N_A$

$$E_{\max} = -\sqrt{\frac{2eV_B N_D}{\varepsilon}}$$

$$d = x_p = \sqrt{\frac{2\varepsilon V_B}{eN_D}}$$

$$C = \varepsilon\frac{A}{d} = A\sqrt{\frac{\varepsilon e N_D}{2V_B}}$$

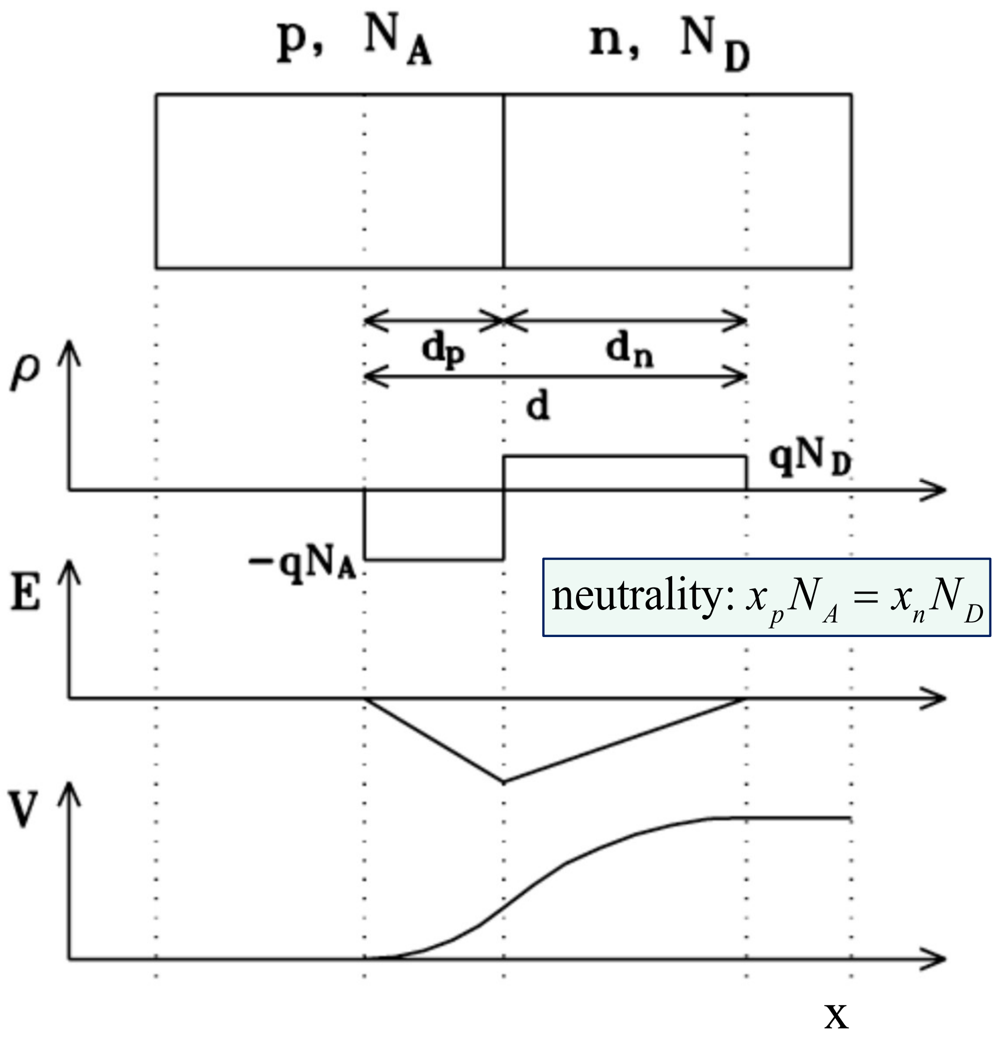

pn-junction: basic properties

- Previous formulae are valid as long as the depleted region thickness d is smaller then the actual device thickness w
- The depletion voltage V_{depl} is defined by $x = w$:

$$w = \sqrt{\frac{2\varepsilon V_{\text{depl}}}{eN_D}} \quad \Rightarrow \quad V_{\text{depl}} = \frac{w^2 e N_D}{2\varepsilon}$$

$$E(x) = -\frac{eN_D}{\varepsilon}(w - x) = -\frac{2V_{\text{depl}}}{w^2}(w - x)$$

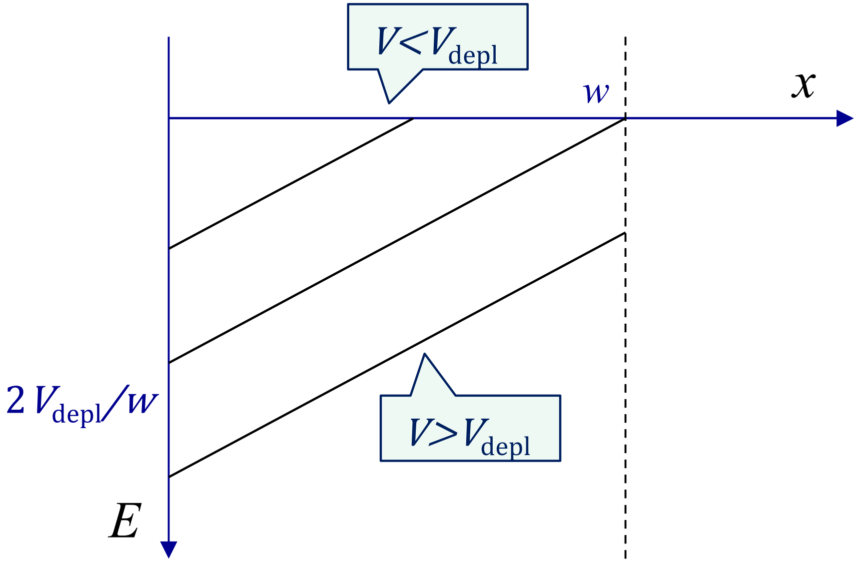

- For $V_B > V_{\text{depl}}$, E may change at most by a constant:

$$E(x) = -\frac{2V_{\text{depl}}}{w^2}(w - x) - \frac{V_B - V_{\text{depl}}}{w}$$

There is no region with null field: faster charge collection (see next slide)

Drift and diffusion of charge carriers

- If $n(\vec{x})$ and $p(\vec{x})$ are inhomogeneous concentrations of free electrons and holes, their corresponding current densities J are:
$$\vec{J}_p = qp\mu_h\vec{E} - qD_p\vec{\nabla}p$$
$$\vec{J}_n = -qn\mu_e\vec{E} + qD_n\vec{\nabla}n$$
$$\vec{J} = \vec{J}_p + \vec{J}_n$$
- The drift velocities are
$$v_{D,h} = \mu_h E$$
$$v_{D,e} = -\mu_e E$$
- Relationships are linear as far as
$$v_D \ll v_{\text{thermal}}$$
- above v_D saturates at approximately 0.8×10^7 cm/s
- In the linear region the mobility μ is related to the collision time τ_c and the effective carrier mass m^*:
$$\mu_h = \frac{q\tau_c}{m_h^*}$$
$$\mu_e = \frac{q\tau_c}{m_e^*}$$
- in this situation also holds Einstein's relation:
$$D_{p,n} = \frac{k_B T}{q}\mu_{h,e}$$
- At room temperature:
  - μ_h = 480 cm²/Vs
  - μ_n = 1350 cm²/Vs
- A useful relation is the resistivity
$$\rho = \frac{1}{q(n\mu_e + p\mu_h)}$$
  - assuming it is *n*-type, $N_D \ll N_A$: $\rho = \frac{1}{N_D\mu_e}$ which is a macroscopical measurable quantity (unlike N_D)

- Similar to gas discharges, it is possible to achieve charge multiplication when the energy gained between two collisions is larger than the excitation energy.

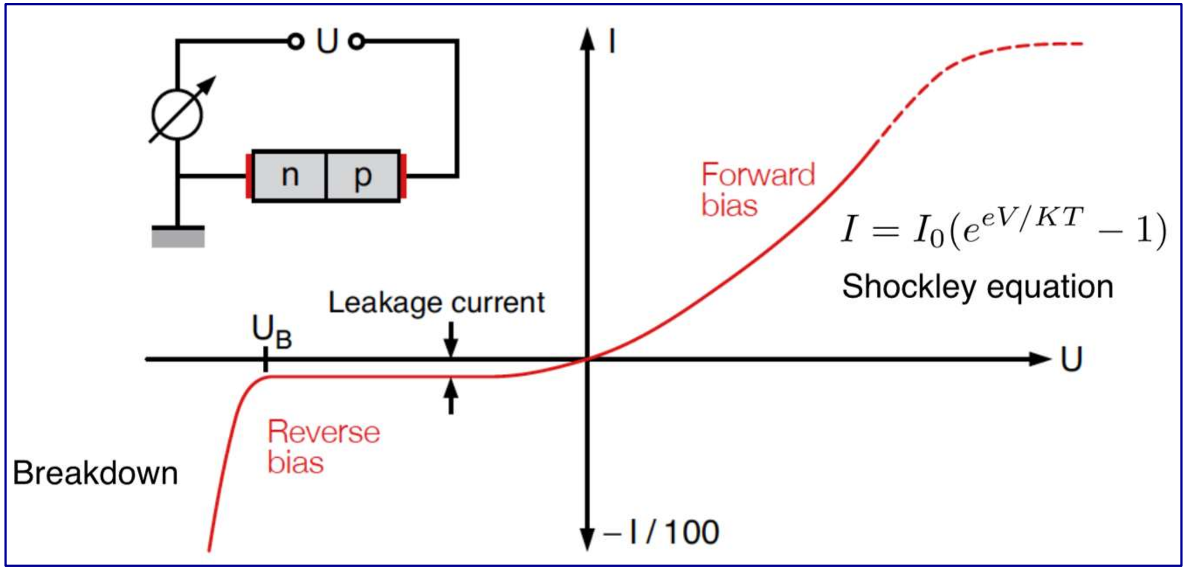

$$\Delta E_{\text{kin}} = -q\Delta V \approx qE\Delta x$$

$$= \left| qE\upsilon_{\text{drift}}\tau_c \right| = \left| q \right| E^2 \mu\tau_c \qquad \Delta E_{\text{kin}} > E_G \quad \Rightarrow \quad E_{\text{bd}} = \sqrt{\frac{E_G}{q\mu\tau_c}}$$

  – ***E***

- The maximum value of the field is at the junction:

$$E(0) = \frac{eN_D x_n}{\varepsilon} = \frac{1}{\varepsilon\rho\mu_e}\sqrt{2\varepsilon\rho\mu_e V_0} = \sqrt{\frac{2V_0}{\varepsilon\rho\mu_e}} \qquad V_{\text{bd}} = \frac{\varepsilon\rho\mu_e}{2} E_{\text{bd}}^2$$

- **In real life dominated by implantation shapes and defects.**

Radiation damage in silicon

- The most critical requirement for operation at the HL-LHC is **radiation hardness**
- Two main radiation effects:
  - **Bulk damage**: damage of the crystal lattice
    - increase of leakage current
    - change of “effective” doping concentration
    - trapping of charge carriers
    - depends on Non-Ionizing Energy Loss (NIEL)
    - measured relatively to the one induced by a fluence of 1 MeV neutrons
  - **Surface damage**: concentration of surface charge
    - affecting the electric field and breakdown voltage
    - proportional to Total Ionization Dose (TID)

Bulk damage

- Bulk damage is mainly induced by displaced atoms
- Production of several energy levels in the band gap
- Defect may diffuse: it changes with time

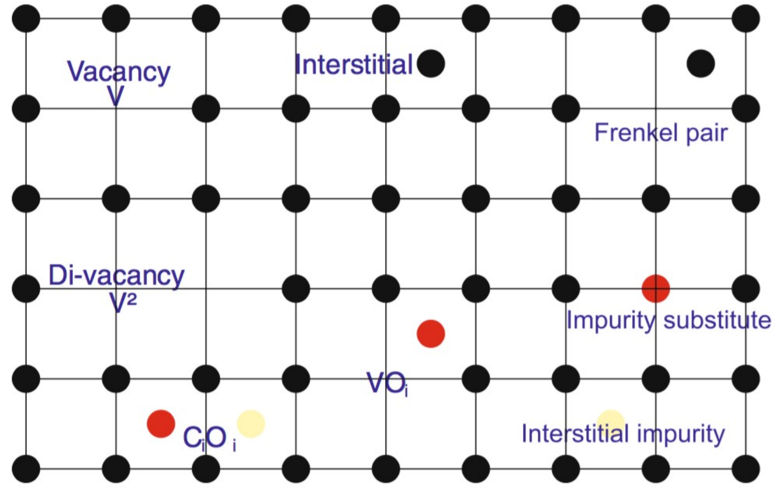

Example : Energy Levels of impurities in Si

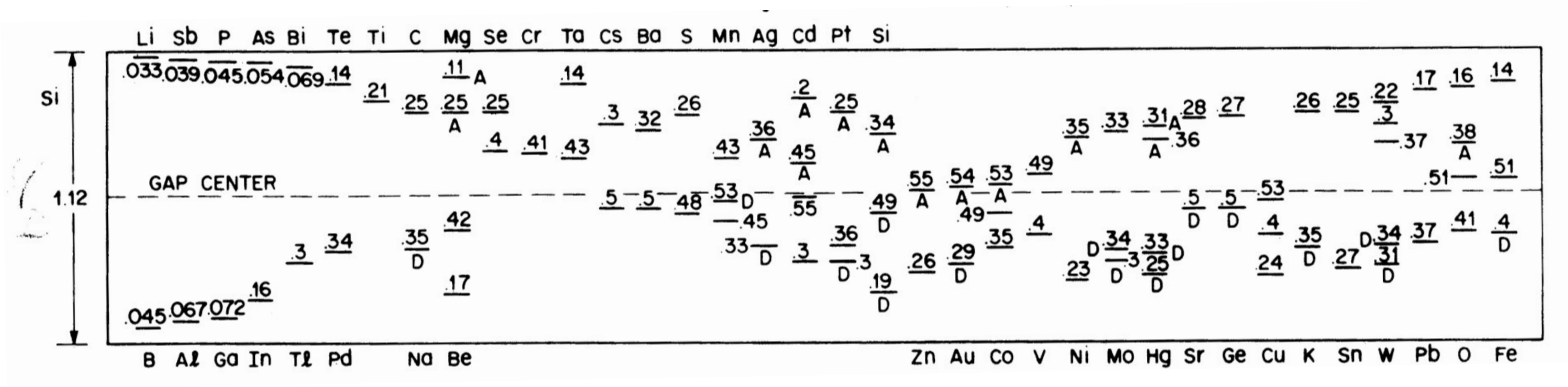

Da: S. M. Sze, Physics of Semiconducor Devices, Wyley & Sons, Singapore, 1981

Radiation effects

Leakage current

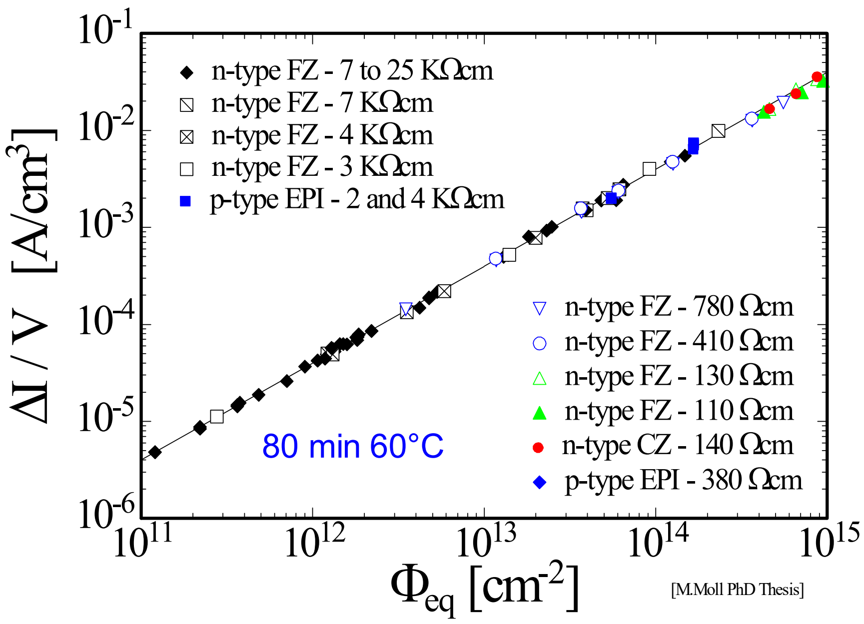

Effective doping concentration

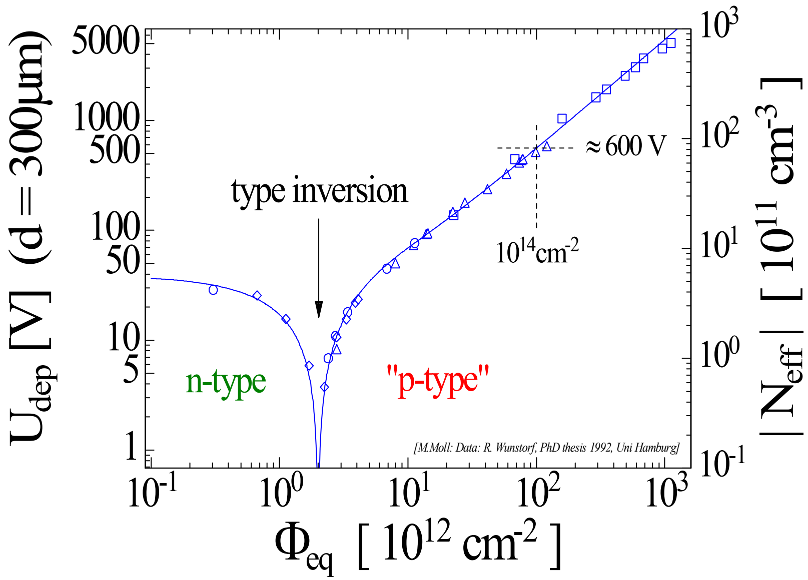

- Increasing leakage current:
  - source of noise in the readout electronics $\sqrt{I}$
  - increase power dissipation
- Reduce detector operational temperature

- Increasing the amount of defects increase the electric field needed to deplete the detector
- Smears out gradients of doping concentration:
  - higher breackdown voltage

Radiation effects

Trapping time

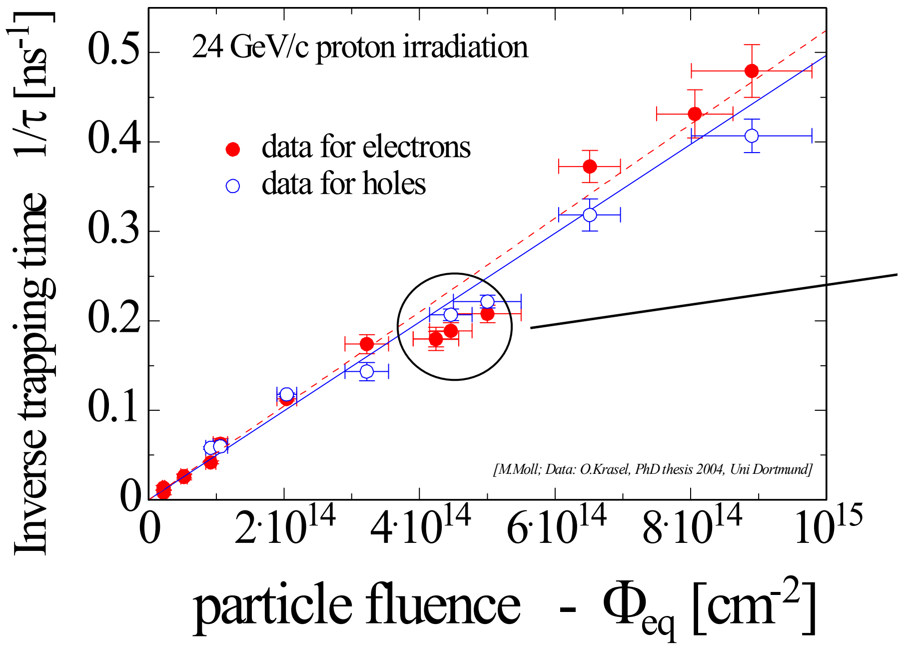

- Trapping probability per unit time:
  - The longer the collection time the more likely charge carriers are lost
- Increase applied electric field
- Thin sensors behave better

Example

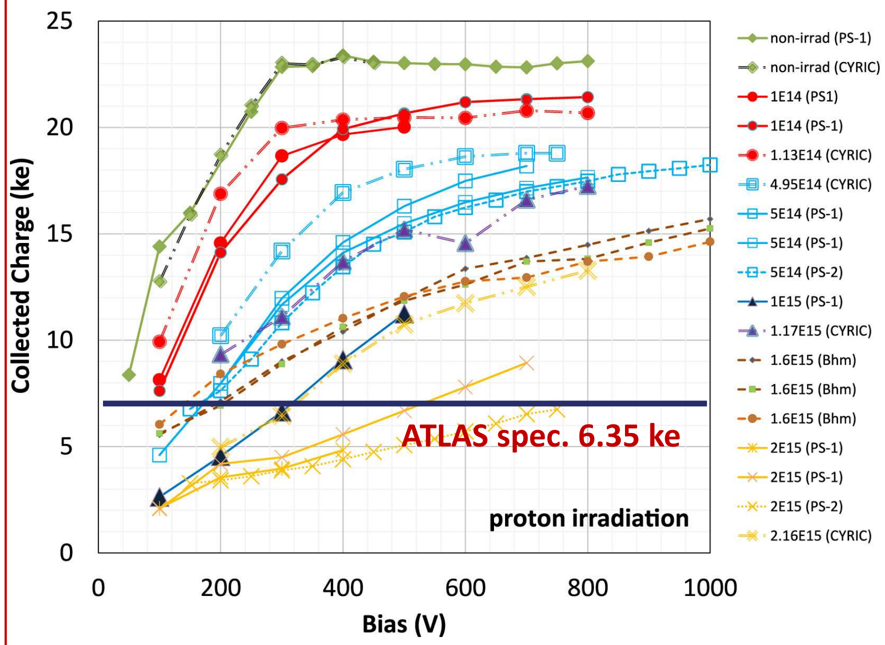

- ATLAS Strip sensor:
  - 320 μm thick silicon
  - 75.5 μm strip pitch

Planar and 3D detectors

- The radiation level is particularly severe for detectors near to the interaction region:
- 3D detectors are an option to increase radiation hardness my improving charge collection
  - larger capacitance (higher noise)
  - more complex fabrication steps
  - preferred choice for innermost layers

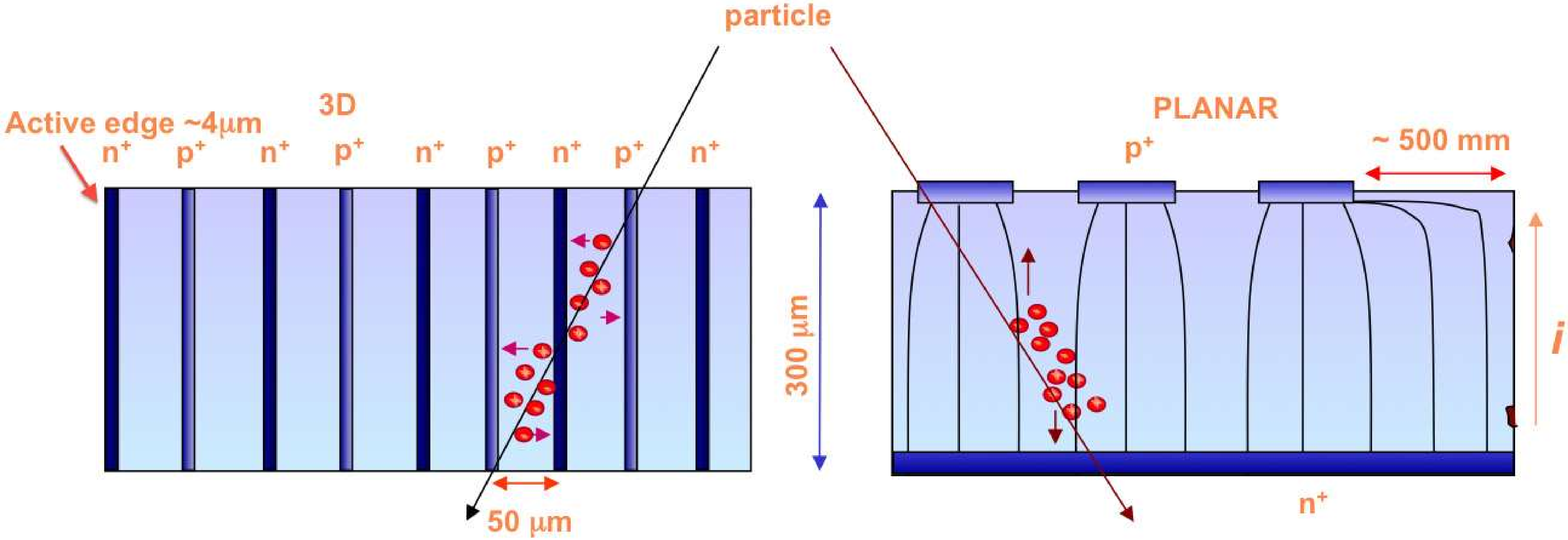

FBK 3D Sensors

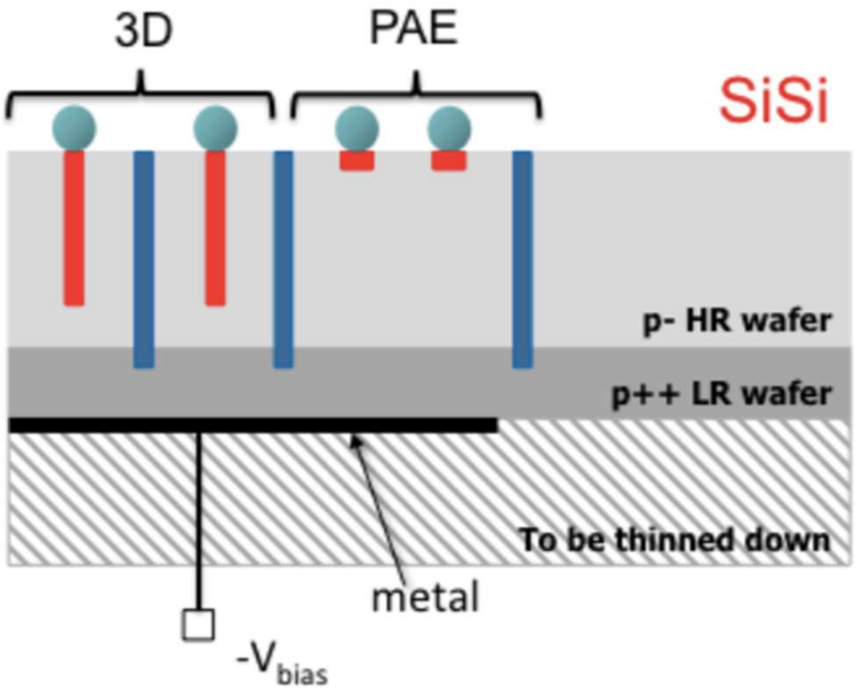

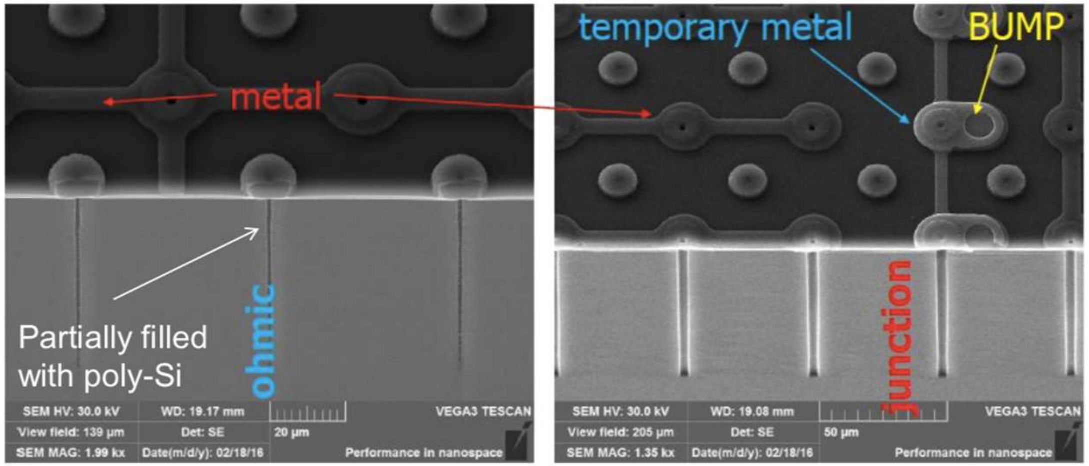

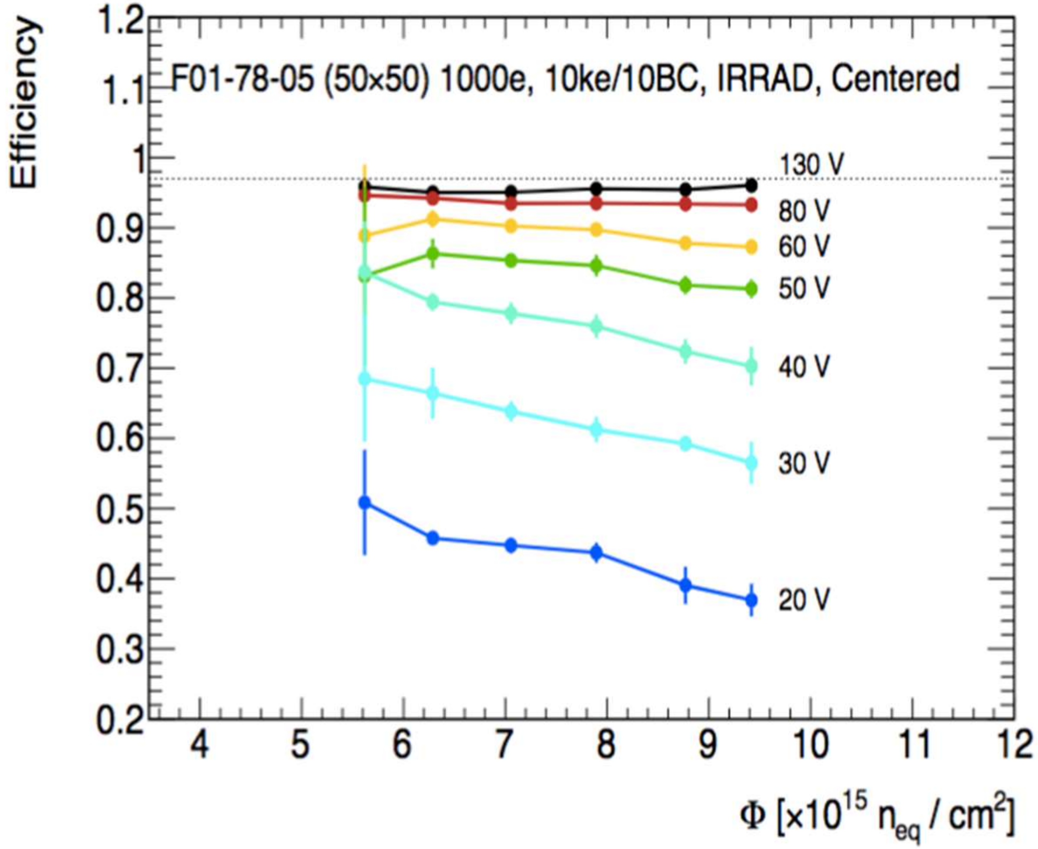

How real modules looks like

CMS Pixels

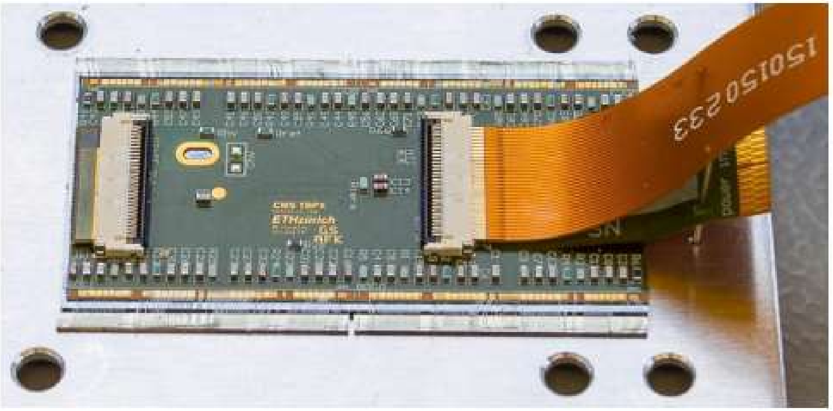

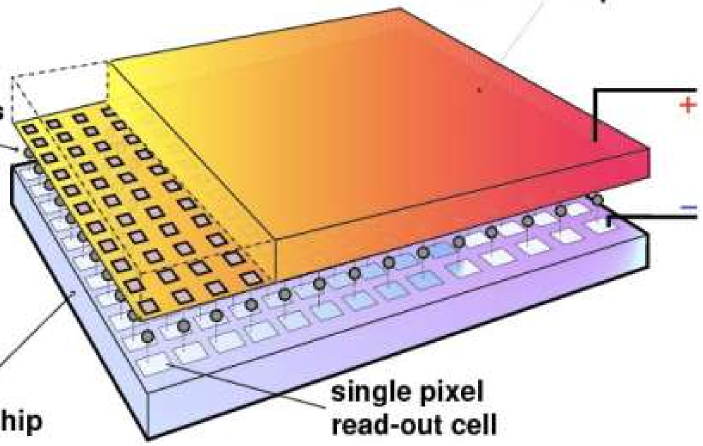

ATLAS Strips

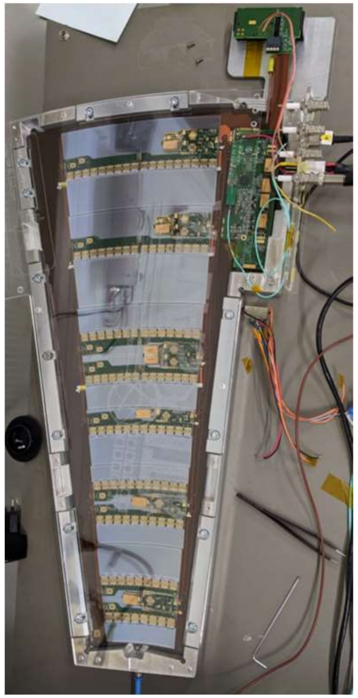

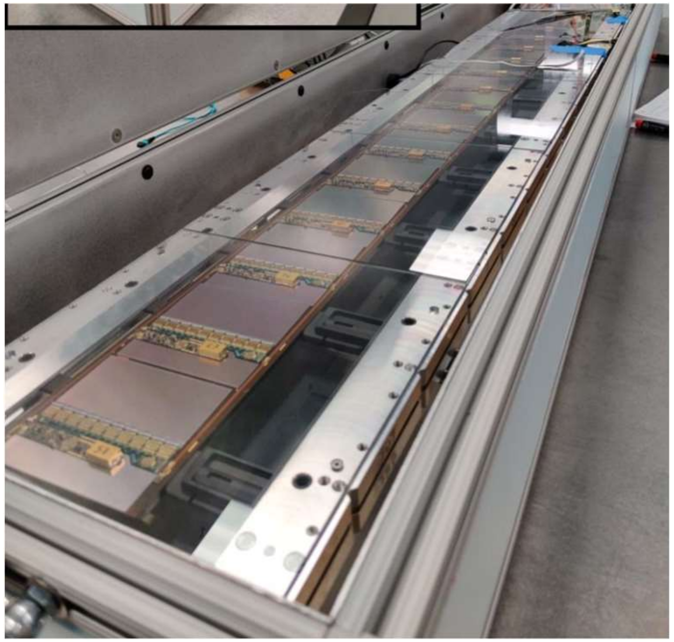

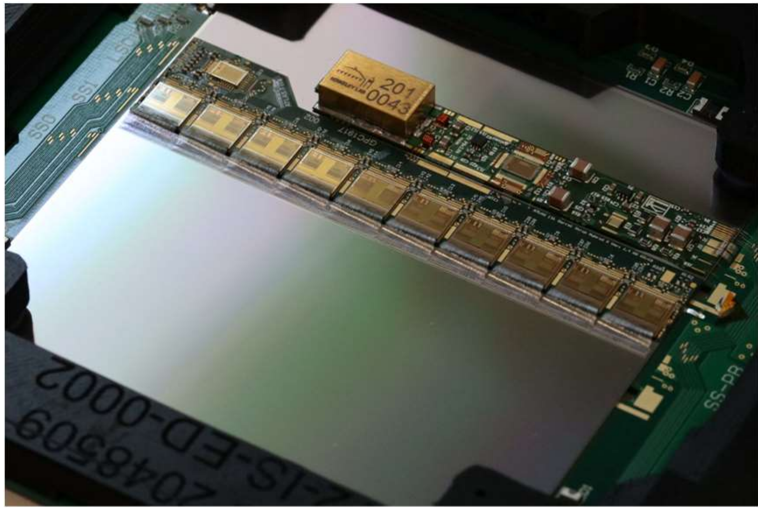

Tracking at trigger level

CMS p_T module concept

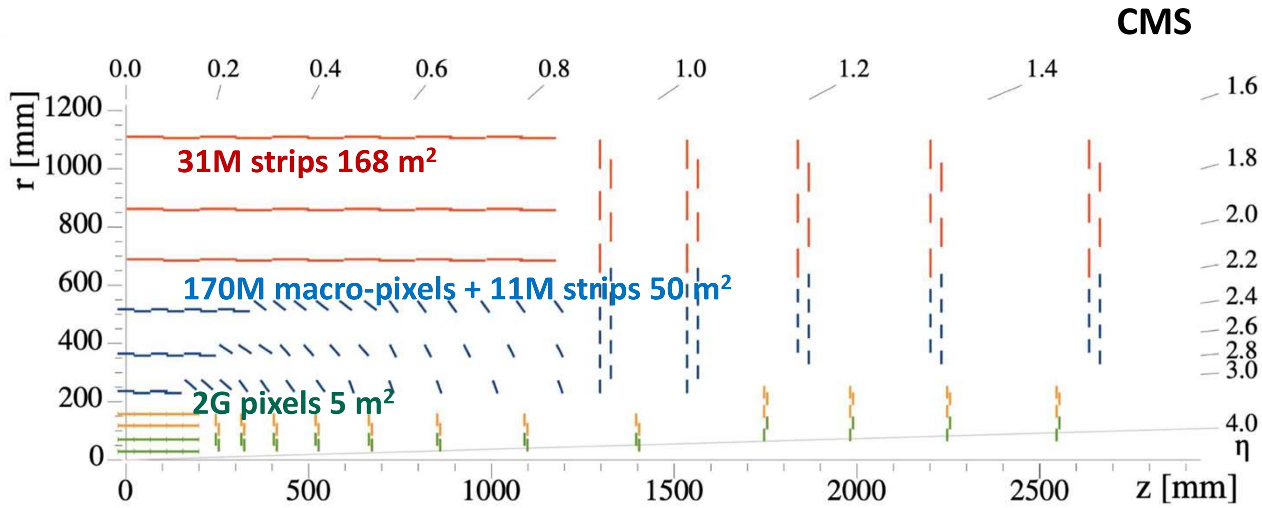

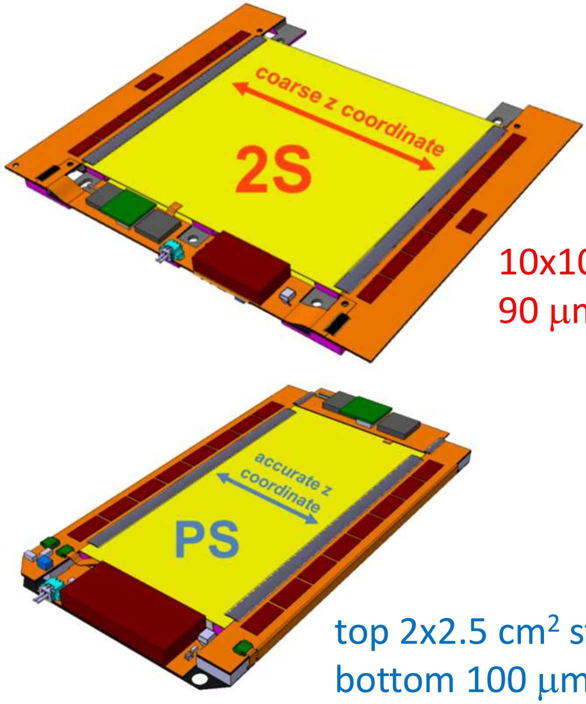

10x10 cm² strip doublet
90 μm pitch

top 2x2.5 cm² strips 100 μm pitch
bottom 100 μm x 1.5 mm pixels

- p_T discrimination in FE electronics by providing correlations between closely space doublet of sensors.
- Send to trigger only "stubs" (hit pairs) compatible with particle of p_T >2 GeV/c
- Data reduction by factor 10-20:
  - at HL-LHC expect 7000 tracks/BX, but only 200 with p_T >2 GeV/c
  - still data rate of 30 TB/s, and 15k stubs to start pattern recognition
- Highly parallel processing + full FPGA based system

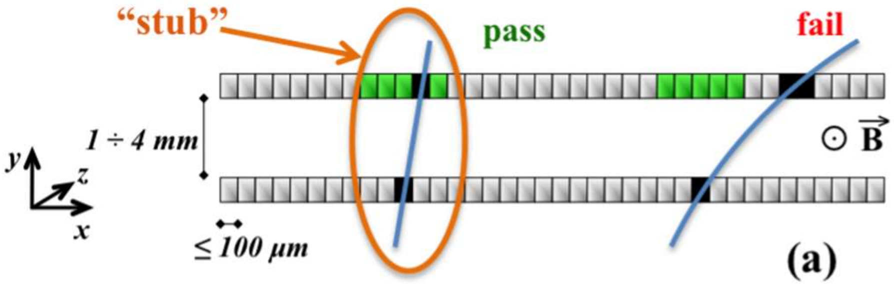

CMS Track Trigger performance

Track Reconstruction

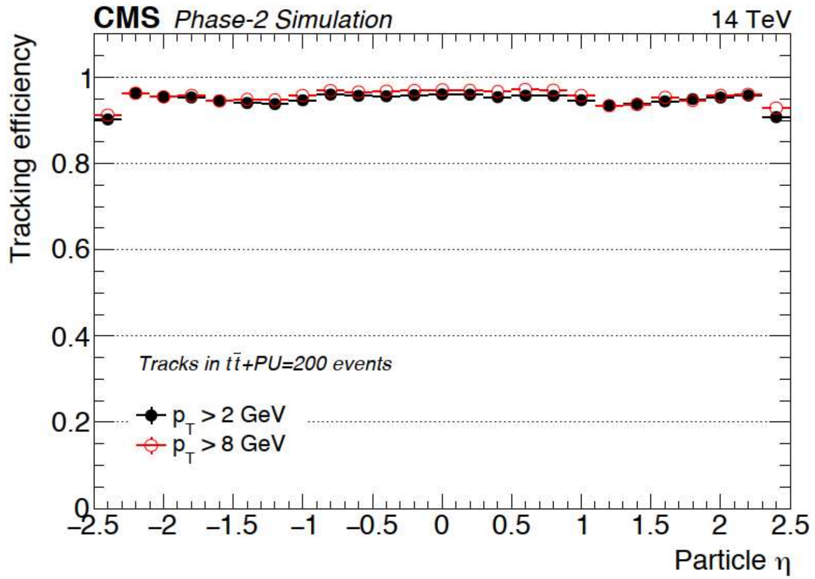

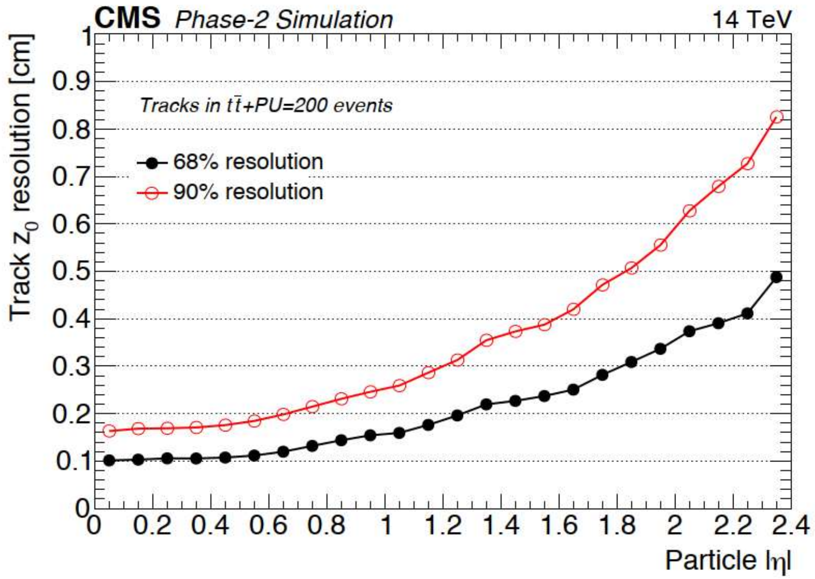

Application to HH→bbττ

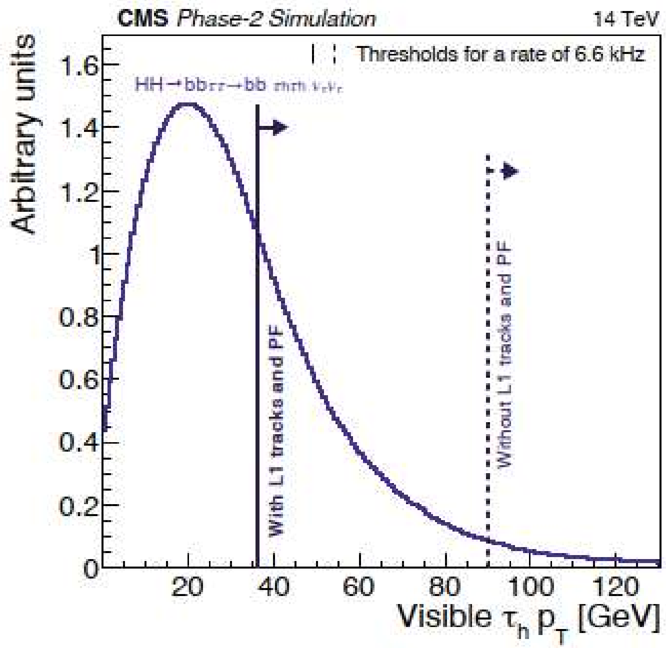

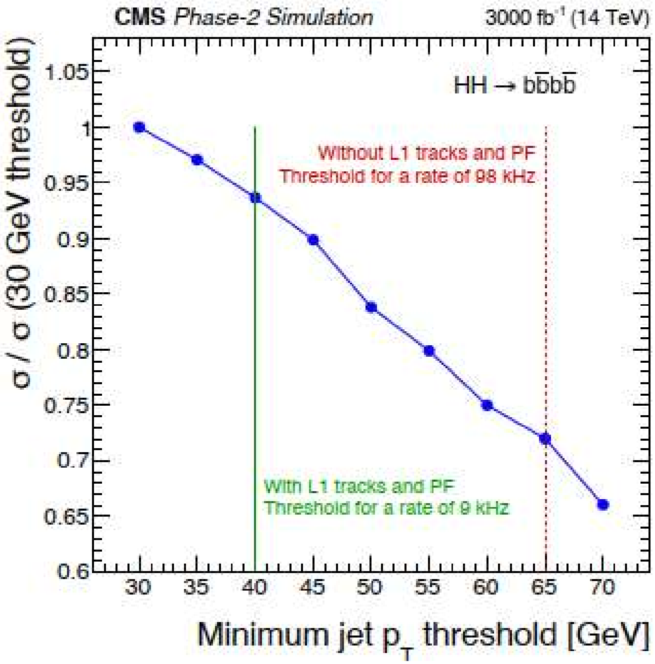

TIMING MEASUREMENTS

Timing motivations

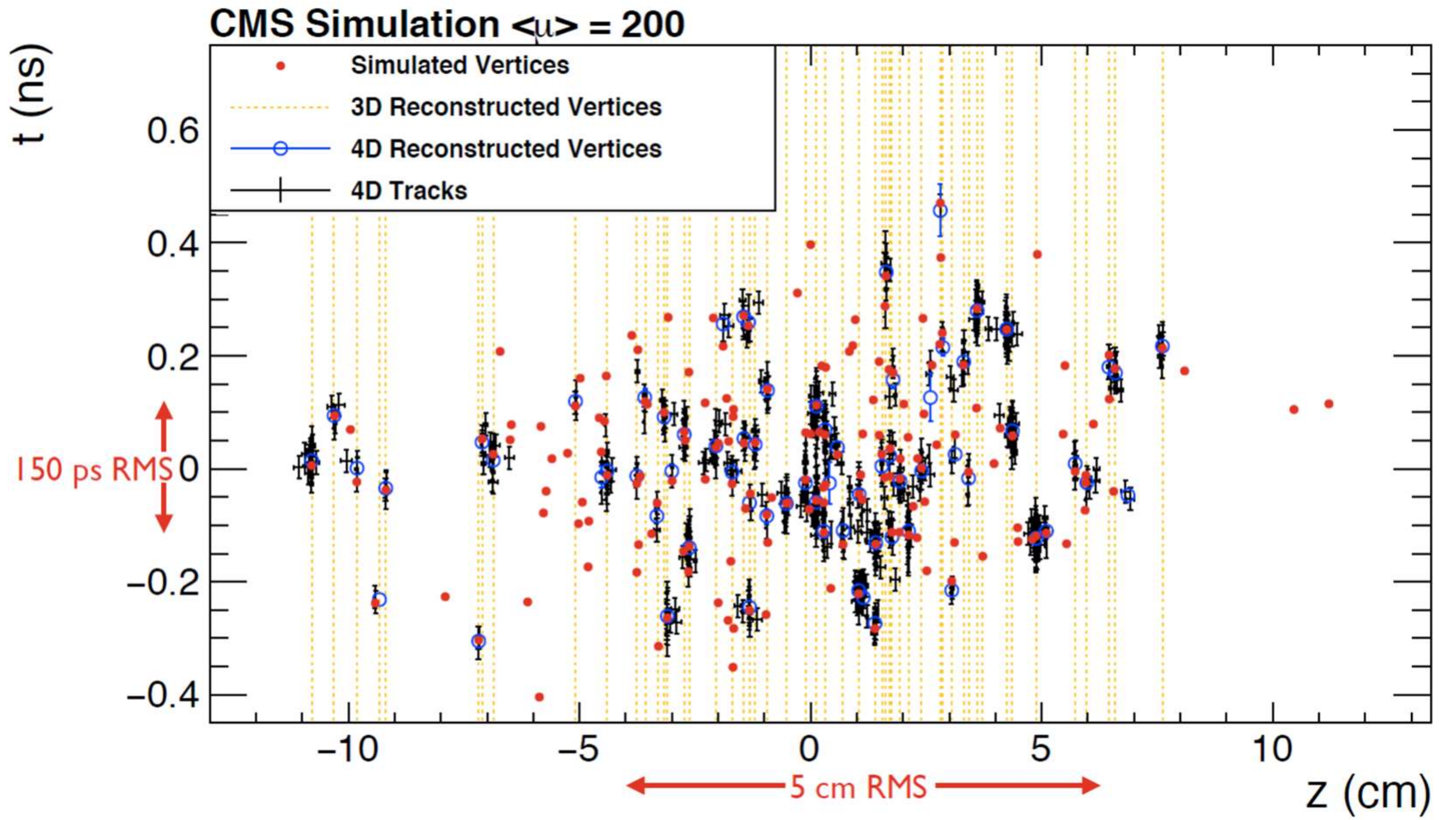

- Vertex density at HL-LHC does not allow to reconstruct primary vertices by spatial information alone.
- Due to the finite size of the bunch, interactions do not happen all at the same time but have a distribution with standard deviation

$$\sigma_t = \frac{\sigma_z}{c} \approx \frac{5\ \text{cm}}{c} \approx 180\ \text{ps}$$

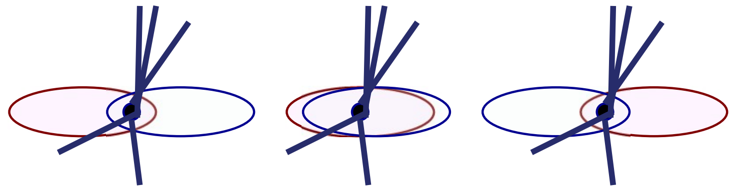

- Timing information helps in separating random geometrical overlaps if $\sigma_t < 30$ ps

Timing motivations

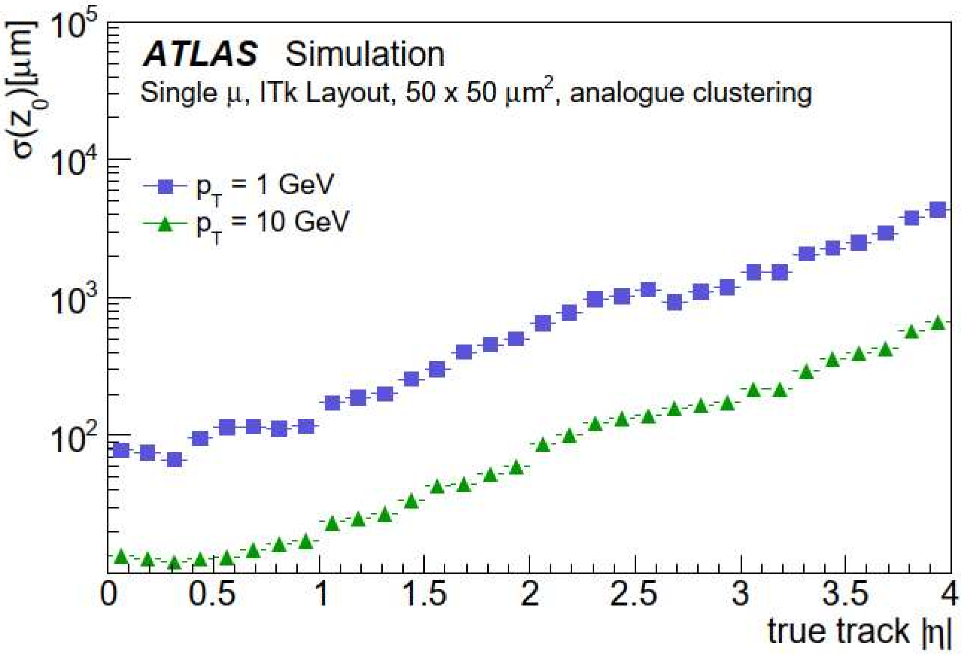

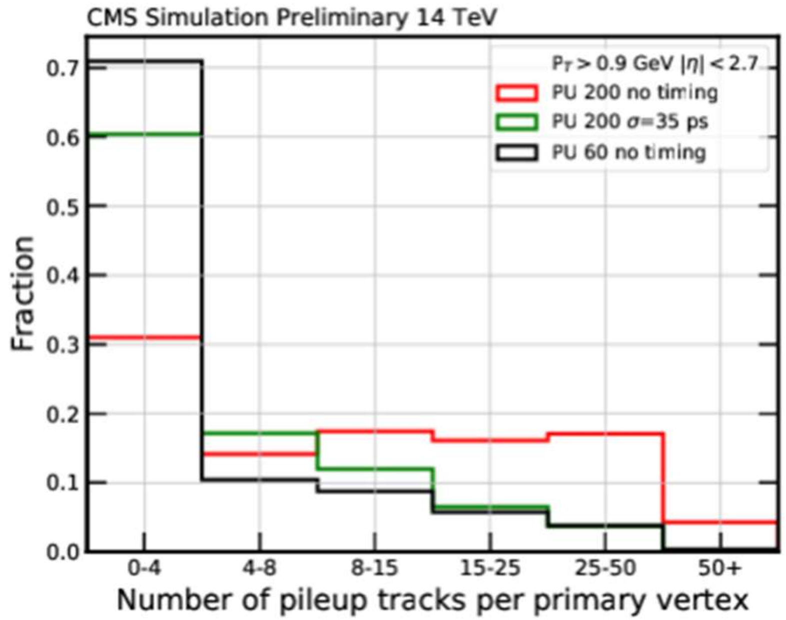

- At large |η| tracker resolution is worse than primary vertices separation
- Large contamination of tracks from pileup events: wrong computation of missing energy
- Timing separation allows to reduce contaminations at the same level as during Run-2
- CMS also explored impact on particle identification during heavy ion runs and detection of long-lived particles.

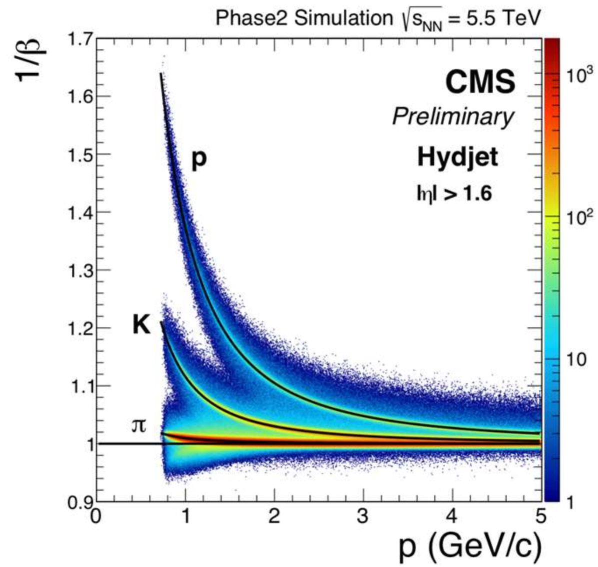

- Associate timing measurement to each reconstrunced track.

- ATLAS: High Granularity Timing Detector (HGTD)
  - based on LGAD detectors
  - covering the region $2.4<|\eta|<4$

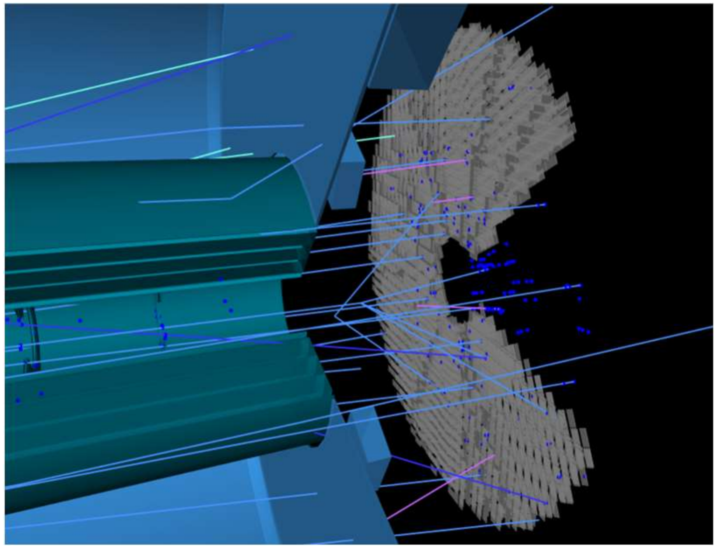

- CMS: MIP Timing Detector (MTD)
  - LGAD detectors in the forward region $1.6<|\eta|<3$
  - Scintillators (LYSO+SiPM) layer in the barrel $|\eta|<1.45$

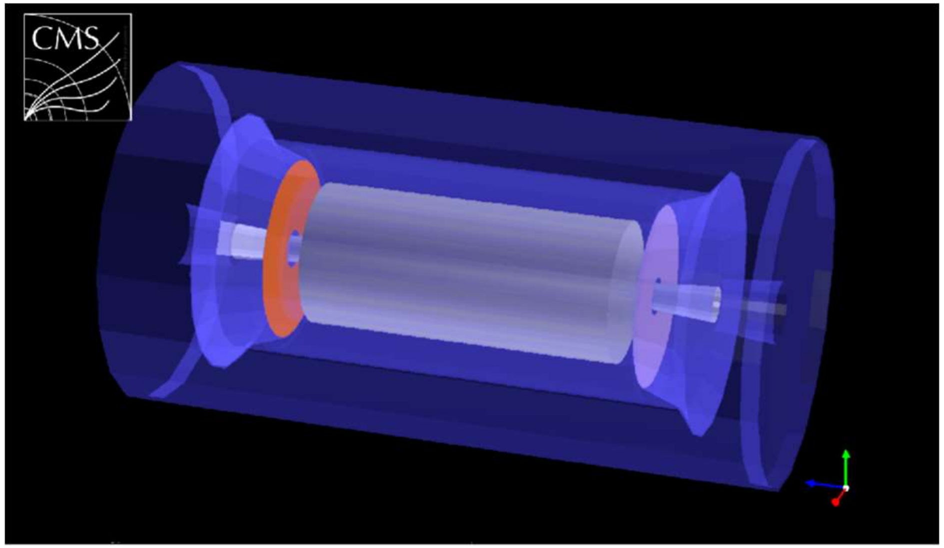

Low Gain Avalanche Diodes

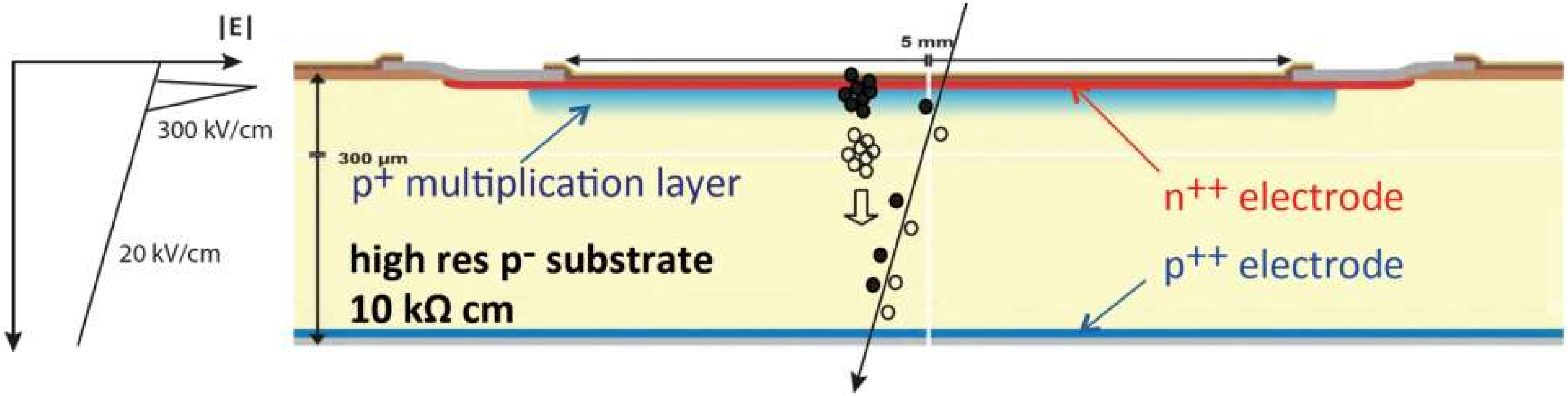

- Silicon detector with internal gain
- Arrival time defined as the time of crossing a predefined threshold
- Planar geometry to reduce arrival time fluctuatios and distorted electric field
- granularity limited by cross-talk between nearby electrodes

$$\sigma_t^2 = \underbrace{\left(\frac{V_{th}}{dV/dt}\bigg|_{rms}\right)^2}_{\sigma^2_{\text{time walk}}} + \underbrace{\left(\frac{\text{Noise}}{dV/dt}\right)^2}_{\sigma^2_{\text{noise}}} + \underbrace{\sigma^2_{\text{arrival}}}_{\text{arrival fluct.}} + \underbrace{\sigma^2_{\text{dist}}}_{\text{distortion low w-field}} + \sigma^2_{\text{TDC}}$$

$$\frac{dV}{dt} \sim \frac{V_{\text{picco}}}{\tau_r}$$

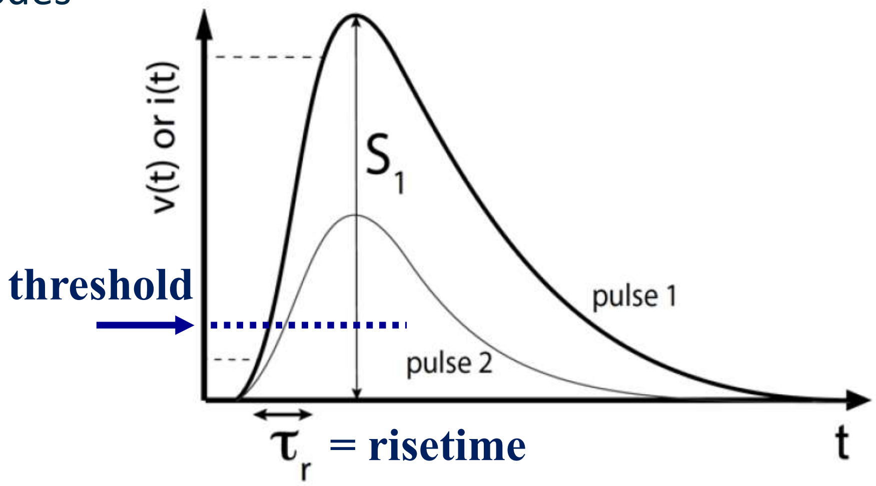

LGAD Radiation Hardness

- Radiation damage may cause loss of signal:
  - trapping of primary ionization
  - smearing of the highly doped multiplication region
- In the current prototyping phase detectors seem to maintain adequate timing resolution.
- Possible mitigation is replacement of most irradiated sensors (HGTD) and multiple measurements to reduce uncertainties

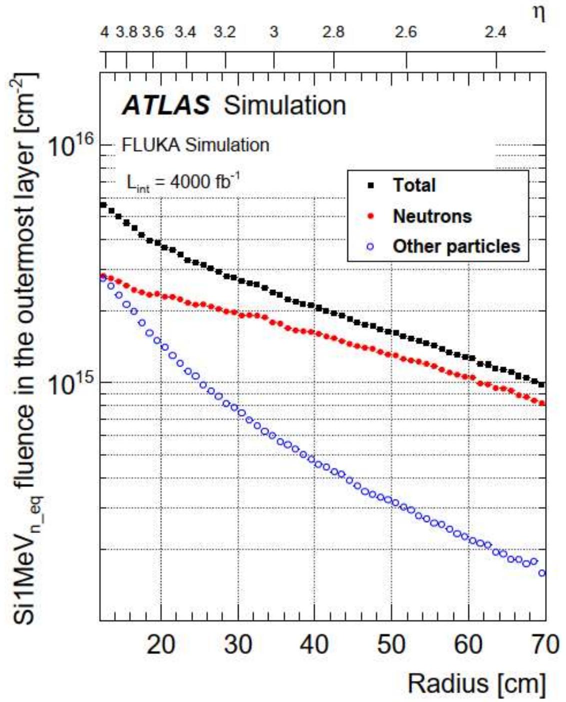

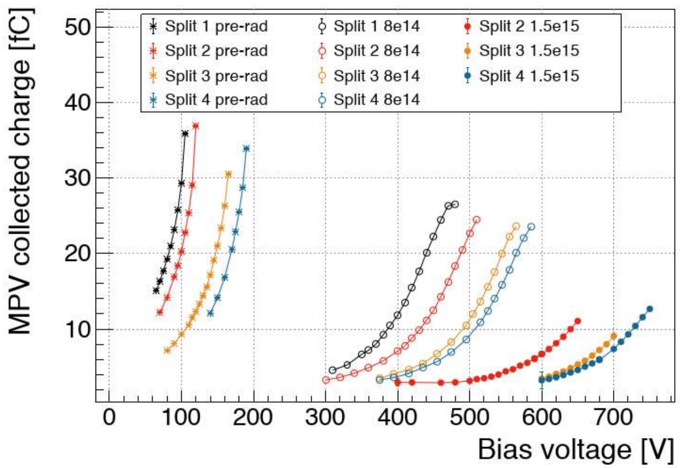

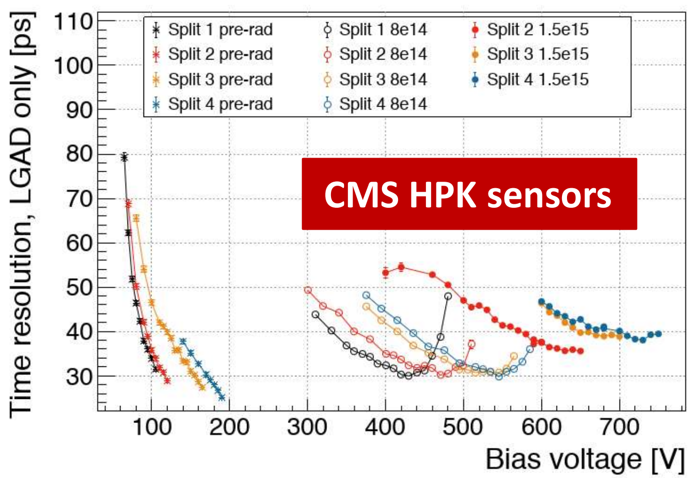

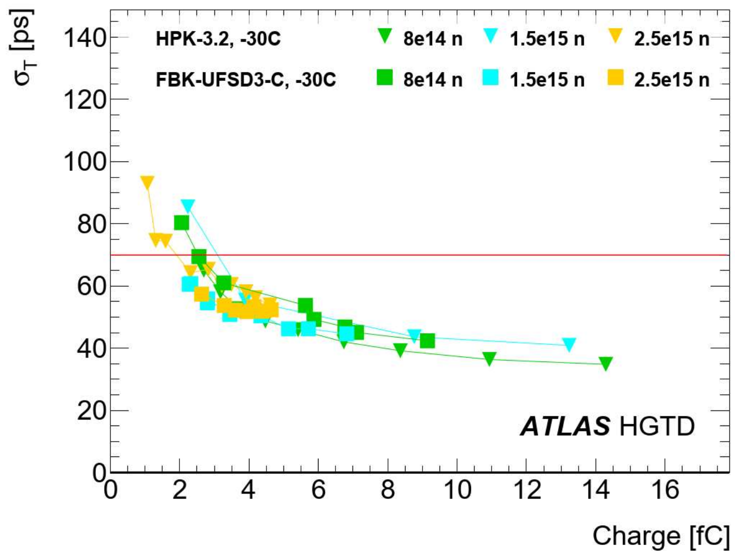

LGAD perspectives

- Main limitation of current LGADs is the segmentation:
  - 1.3 mm x 1.3 mm for both HGTD and MTD:
  - dead regions to avoid afterpulsing in nearby channels
  - different ideas being working outin in order to go towards a full 4D-sensor

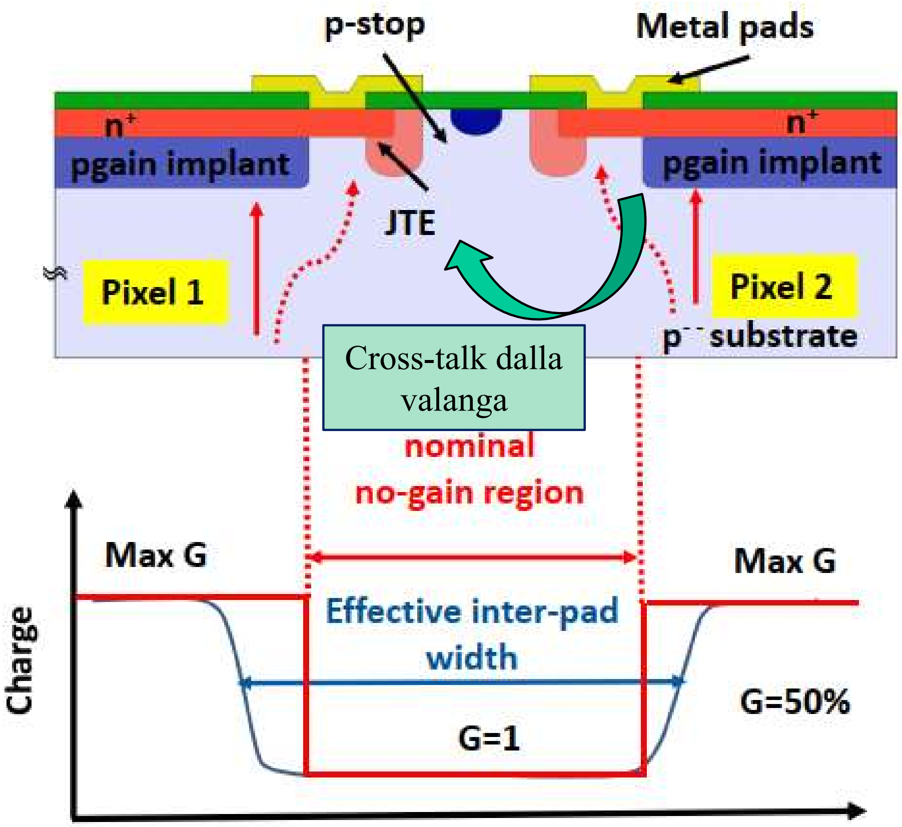

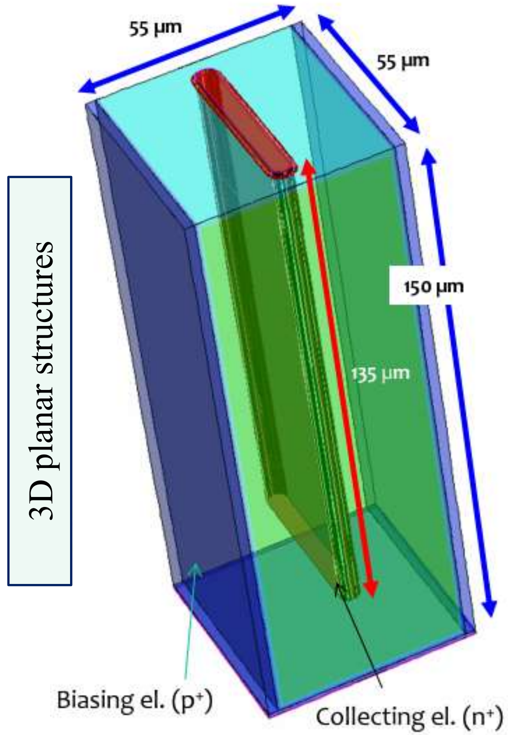

MTD: Barrel Timing Layer

- Main constraint for the barrel layer is to fit in the 40 mm gap between the CMS tracker and ECAL
- LYSO crystal bars 3x3x57 mm
- read at both ends by SiPM
- Radiation effect in the Dark Count Rate of the SiPM
- Important thermal management to keep the detector at low temperature / noise suppression in the front-end chip

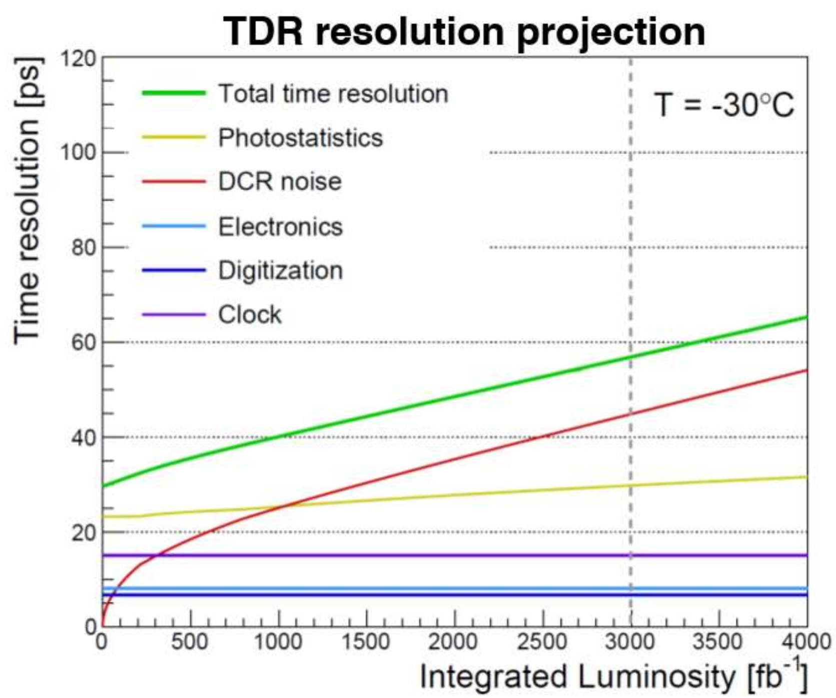

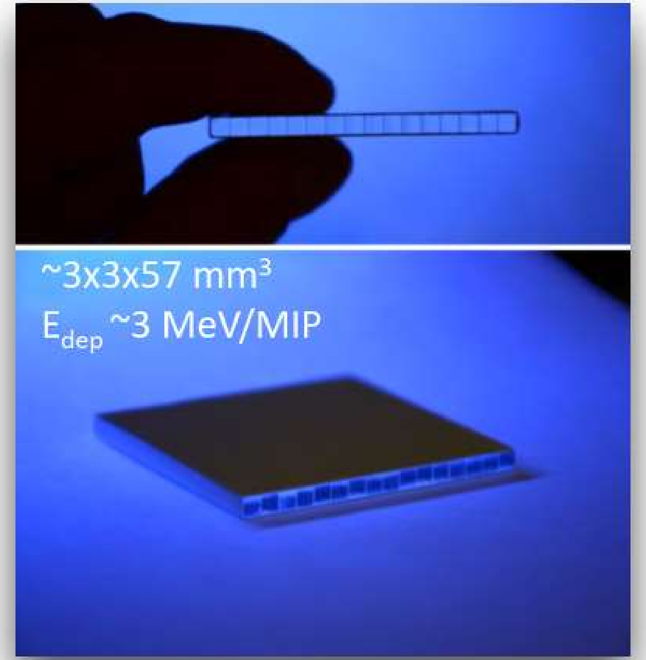

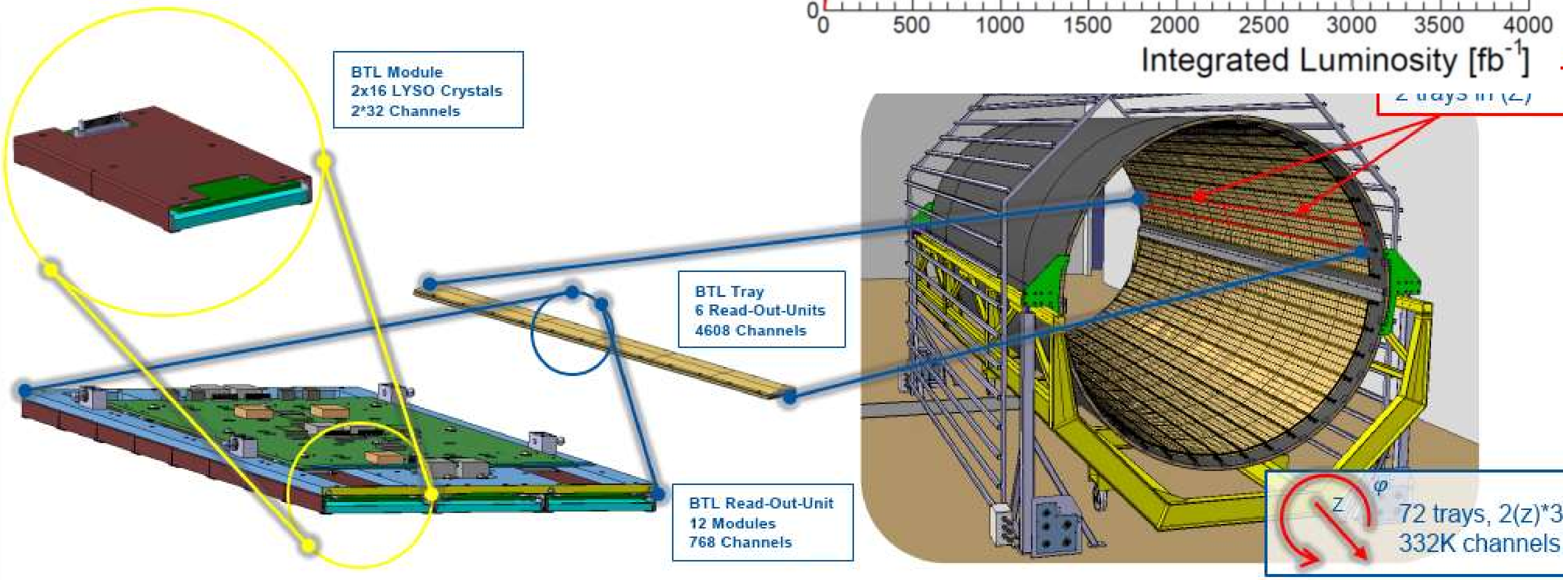

- Recent test beam results

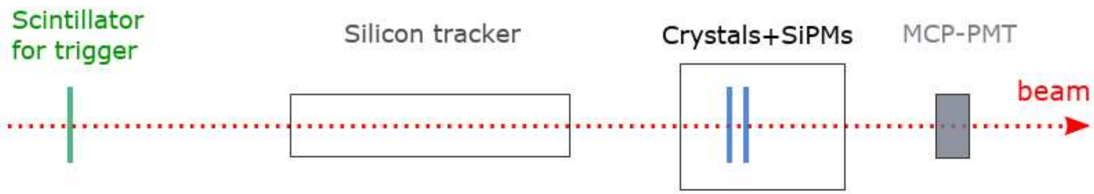

  - Time resolution from average of both ends SiPM 25 ns
  - spatial resolution along the bar, from time difference, 3 mm

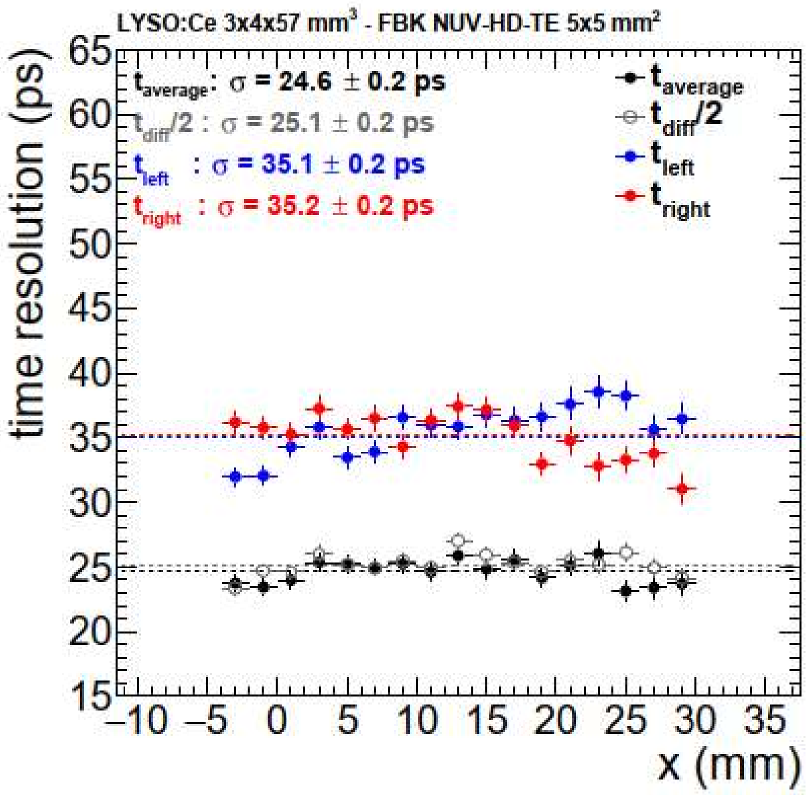

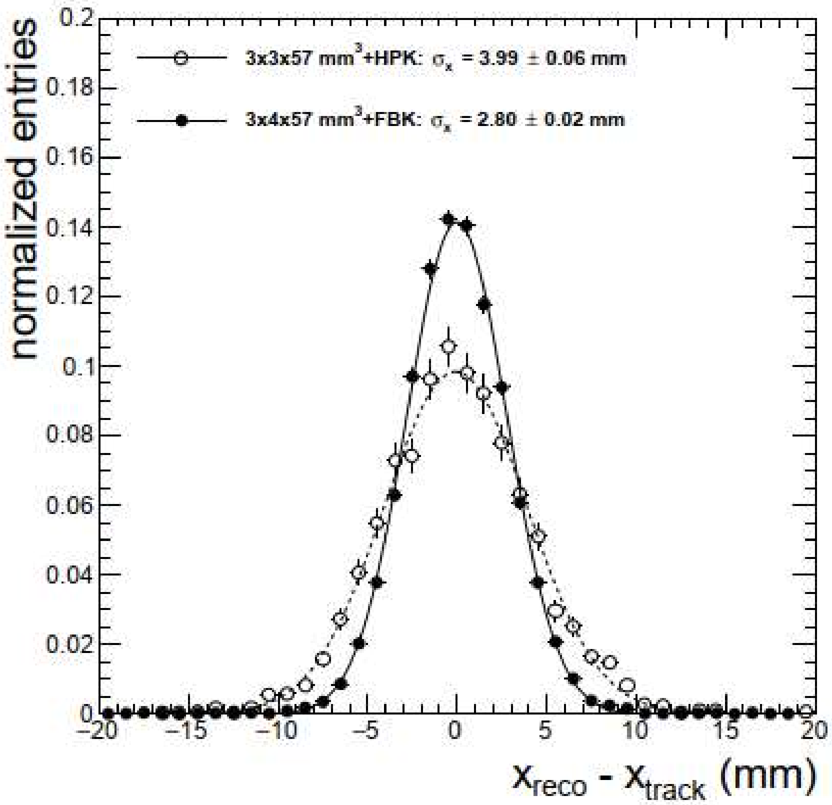

CALORIMETRY

Istituto Nazionale di Fisica Nucleare
Sezione di Milano

UNIVERSITÀ DEGLI STUDI DI MILANO
DIPARTIMENTO DI FISICA

CMS Barrel EM Calorimeter

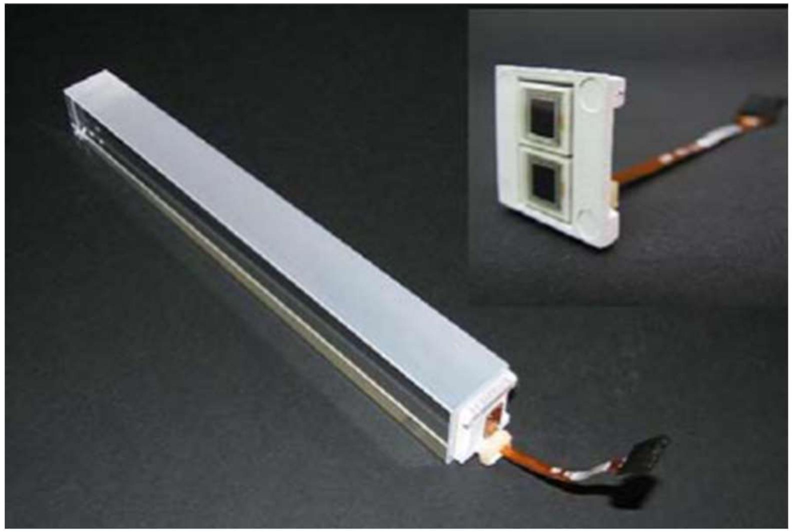

Parameter:	ρ	MP	X_0^*	R_M^*	dE/dx^*	λ_I^*	τ_{decay}	λ_{max}	$n^\dagger$	Relative output‡	Hygro-scopic?	$d(LY)/dT$
Units:	g/cm^3	°C	cm	cm	MeV/cm	cm	ns	nm				%/°C§
NaI(Tl)	3.67	651	2.59	4.13	4.8	42.9	245	410	1.85	100	yes	−0.2
BGO	7.13	1050	1.12	2.23	9.0	22.8	300	480	2.15	21	no	−0.9
BaF_2	4.89	1280	2.03	3.10	6.5	30.7	650^s $<0.6^f$	300^s 220^f	1.50	36^s 4.1^f	no	-1.9^s 0.1^f
CsI(Tl)	4.51	621	1.86	3.57	5.6	39.3	1220	550	1.79	165	slight	0.4
CsI(Na)	4.51	621	1.86	3.57	5.6	39.3	690	420	1.84	88	yes	0.4
CsI(pure)	4.51	621	1.86	3.57	5.6	39.3	30^s 6^f	310	1.95	3.6^s 1.1^f	slight	−1.4
$PbWO_4$	8.30	1123	0.89	2.00	10.1	20.7	30^s 10^f	425^s 420^f	2.20	0.3^s 0.077^f	no	−2.5
LSO(Ce)	7.40	2050	1.14	2.07	9.6	20.9	40	402	1.82	85	no	−0.2
PbF_2	7.77	824	0.93	2.21	9.4	21.0	-	-	-	Cherenkov	no	-
CeF_3	6.16	1460	1.70	2.41	8.42	23.2	30	340	1.62	7.3	no	0
$LaBr_3$(Ce)	5.29	783	1.88	2.85	6.90	30.4	20	356	1.9	180	yes	0.2
$CeBr_3$	5.23	722	1.96	2.97	6.65	31.5	17	371	1.9	165	yes	−0.1

- **PbWO4 crystals**
  - 23 cm (26 X_0) x 2.2 cm (~1 ρ_M)
  - isolated em shower contained in 3x3 crystals
  - 4.5 photons / MeV
- **APD** (Avalanche PhotoDiode) **readout**
  - 6 μm eff. thickness
  - 50x gain
- **Front-end electronics**
  - 250 nm CMOS
  - CR-RC shaping
  - τ = 40 ns
  - ENC = 8 ke

Testbeam results

$$\left(\frac{\sigma}{E}\right)^2 = \left(\frac{2.8\%}{\sqrt{E}}\right)^2 + \left(\frac{0.12}{E}\right)^2 + (0.30\%)^2$$

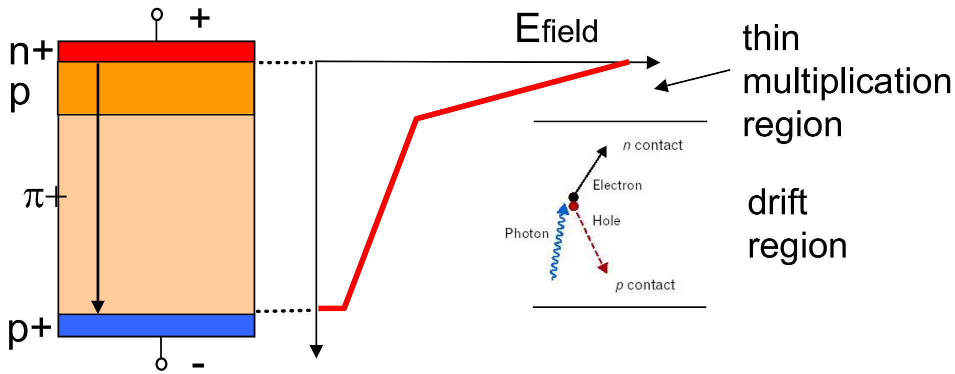

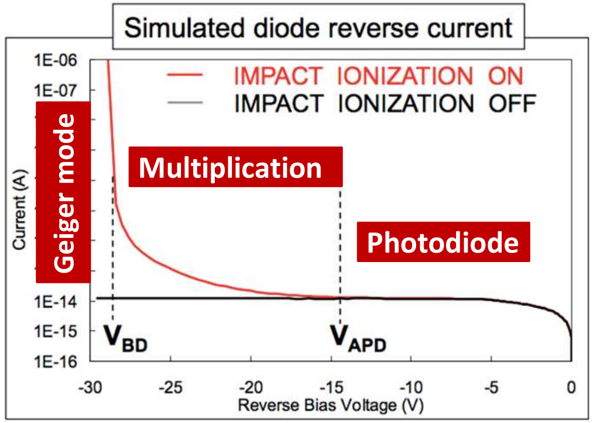

CMS EB: Radiation Effects

- **PbWO4 crystals**
  - Creation of color centers due to atomic displacement in the crystal
  - Shift of the absorption edge, overlapping with the peak of photon emission spectrum
  - Reduced transmission in the material
  - Light output at and of Phase2 reduced to 25—40%, depending on η
- **APD**
  - Main effect is the displacement damage in the silicon bulk
  - Causing increase in dark current I_{Dark}
  - Noise term if proportional to $\sqrt{I_{Dark}}$
  - A factor 10 increase on noise term (~1 GeV at 3000 fb^{-1})
- **Mitigation**
  - Operation at lower temperature
  - I_{Dark} reduces by about a factor 2 every 8 °C

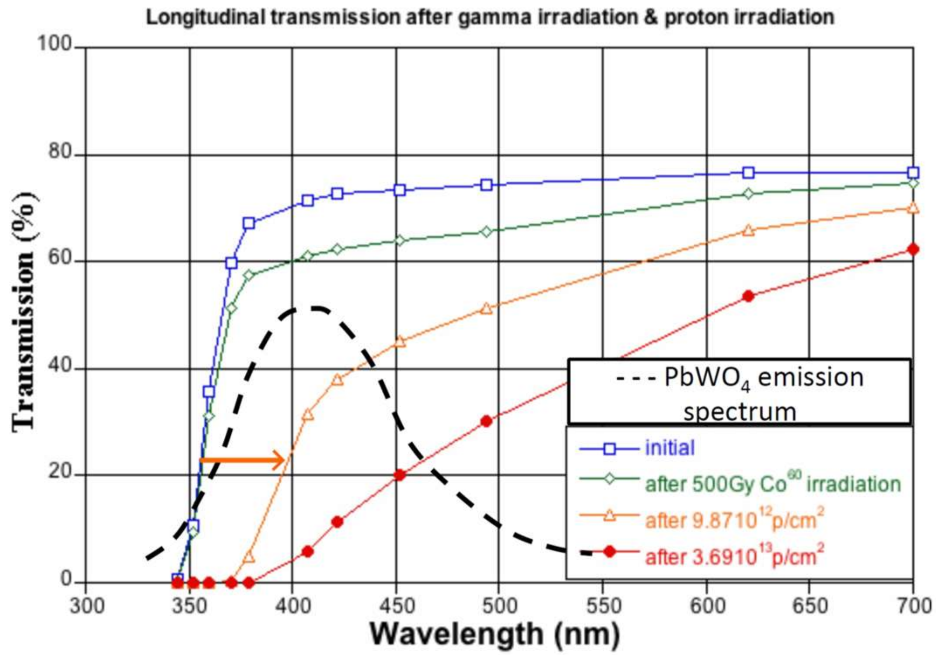

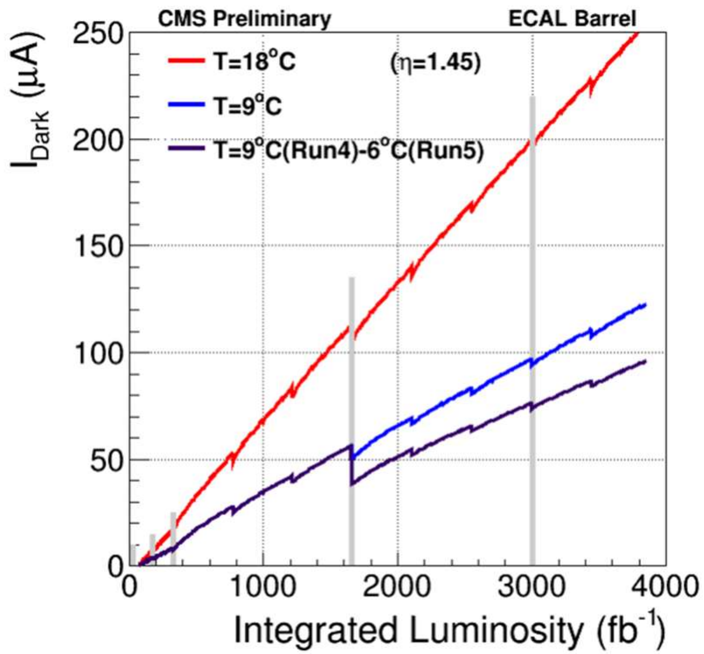

UNIVERSITÀ DEGLI STUDI DI MILANO

CMS EB: Pileup Mitigation

- **Cannot change the detector, so upgrade the readout electonics**
- **Front-end**
  - Effect of pileup signals from nearby bunches
  - Increase in dark current I_{Dark} due to radiation damage
  - Both contribution reduced by fast shaping time
  - **Trans Impedence Amplifier**
  - **Sampling at 160 MHz**
- **L1 Trigger signal**
  - Current detector integrates the signals of a 5x5 crystals towers
    - cannot apply isolation cuts
  - Includes an on chip suppression of spikes
    - large signals in individual APD
    - due to hadronic interactions in the sensor
  - **move full data of each crystal off-detector**
  - **perform pulse shape analysis and trigger algorithm** (isolation, spike rejection) **on FPGA**

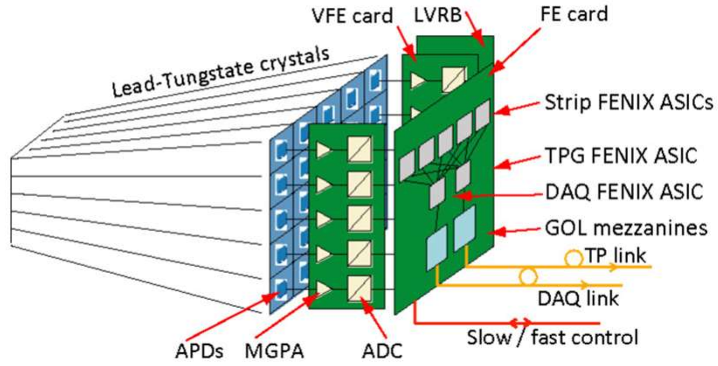

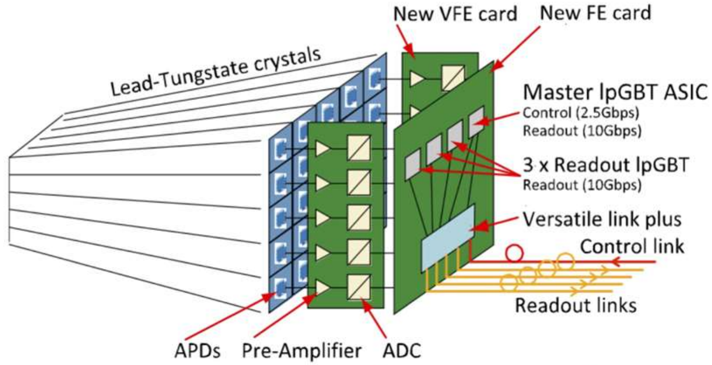

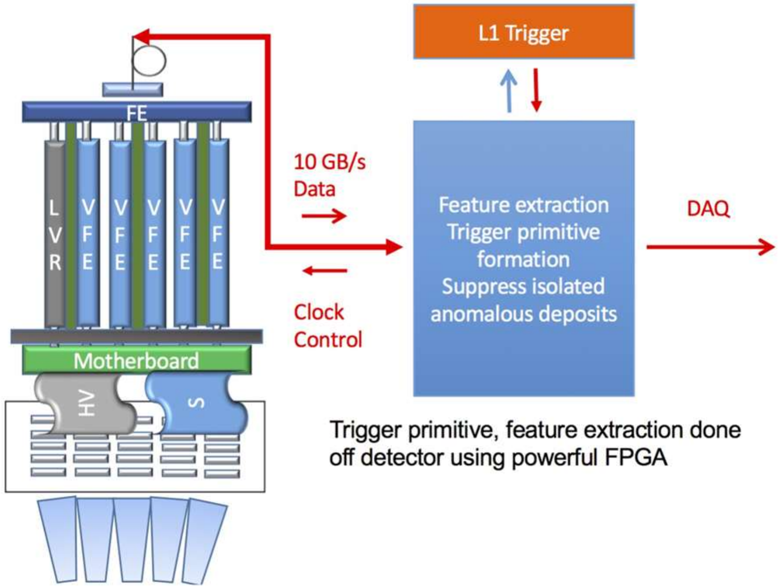

Trigger primitive, feature extraction done off detector using powerful FPGA

CMS EB: Pileup Mitigation

- **Cannot change the detector, so upgrade the readout electonics**
- **Front-end**
  - Effect of pileup signals from nearby bunches
  - Increase in dark current I_{Dark} due to radiation damage
  - Both contribution reduced by fast shagping time
  - **Trans Impedence Amplifier**
  - **Sampling at 160 MHz**
- **L1 Trigger signal**
  - Current detector integrates the signals of a 5x5 crystals towers
    - cannot apply isolation cuts
  - Includes an on chip suppression of spikes
    - large signals in individual APD
    - due to hadronic interactions in the sensor
  - **move full data of each crystal off-detector**
  - **perform pulse shape analysis and trigger algorithm** (isolation, spike rejection) **on FPGA**

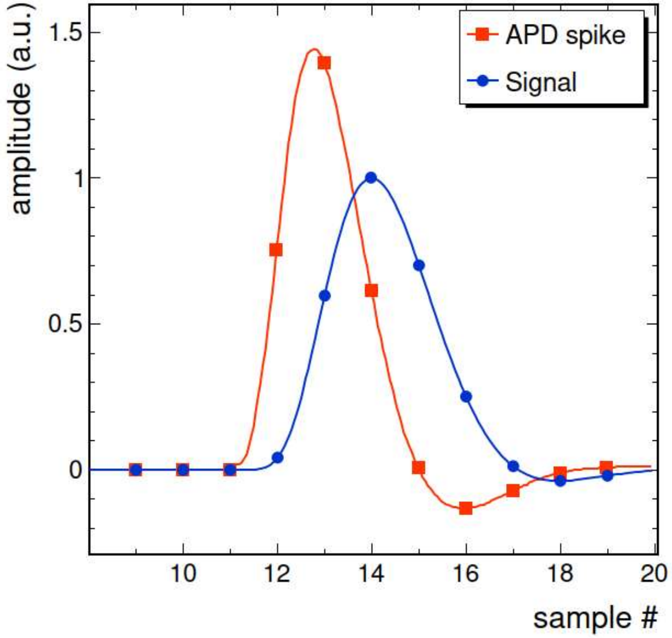

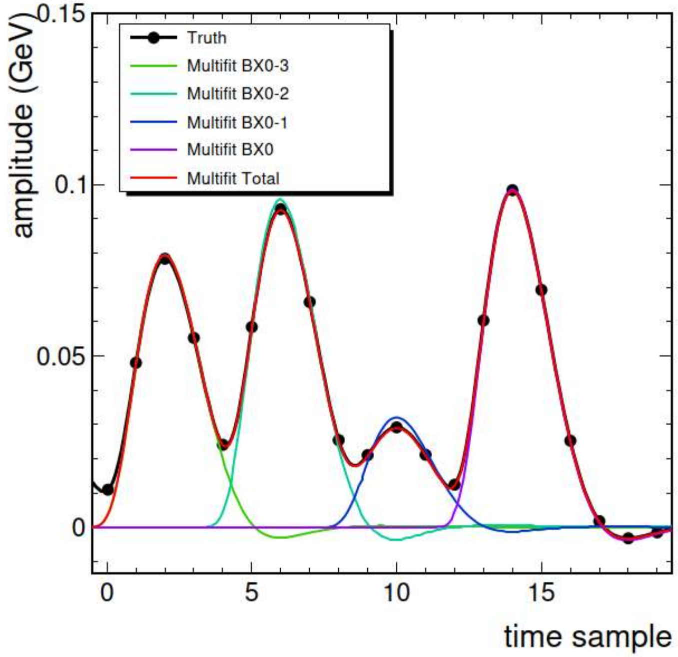

ATLAS Liquid Argon Calorimeter

- **Sampling calorimeter**
  - **Pb absorber**
  - **LAr active ~2 mm gap**
  - Segmented Cu electrode
  - Reduced sensitivity to irradiation
- Lateral and **longitudinal** segmentation
  - π^0 identification by γ separation at the beginning of the shower
  - direction measurement
  - leakage corrections
- **Readout electronics**
  - CR-(RC)^2 bipolar shaping to reduce pileup effects
  - Optimal performance at τ_{shaper} = 13 ns
  - 40 MHz sampling
  - Optimal filtering for energy measurement
  - **Update FE and readout system and L1 trigger improvements**

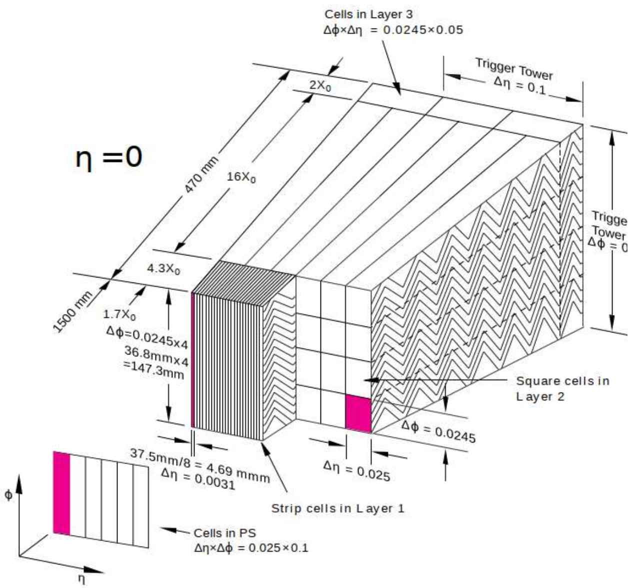

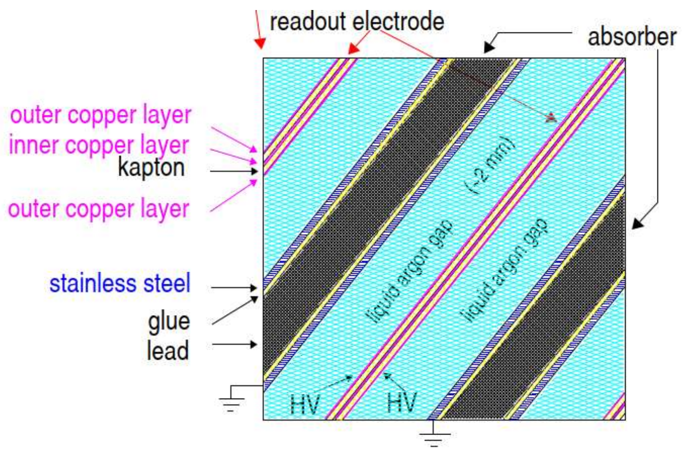

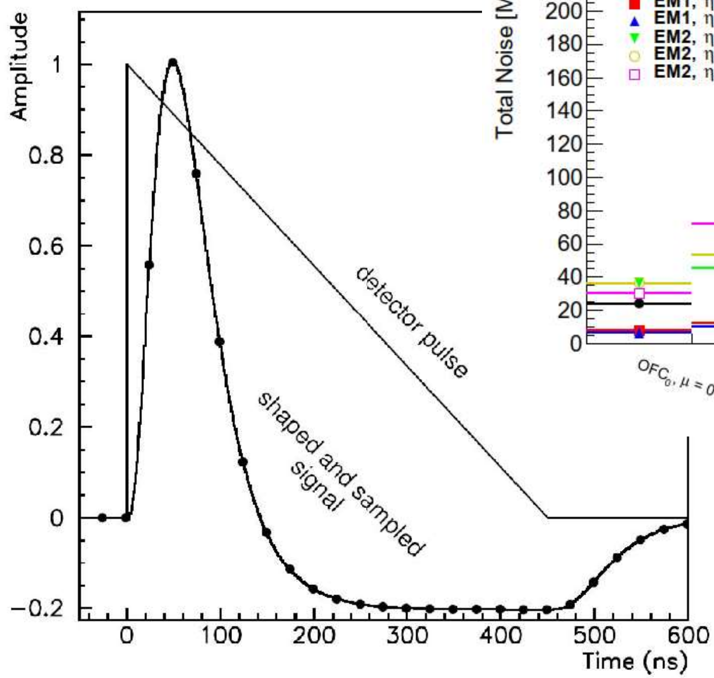

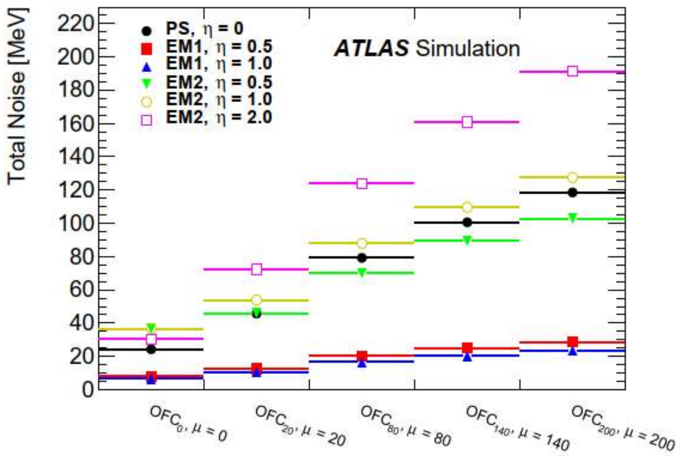

ATLAS LAr upgrades

- **L1 Trigger**
  - L1 trigger had access only to total energy in a tower $\Delta\eta \times \Delta\phi = 0.1 \times 0.1$
  - During LS2 upgraded to provide more granular Super Cell output
  - improved energy determination and shower shape pe variables

	Layer	Elementary Cell	Trigger Tower		Super Cell	
		$\Delta\eta \times \Delta\phi$	$n_\eta \times n_\phi$	$\Delta\eta \times \Delta\phi$	$n_\eta \times n_\phi$	$\Delta\eta \times \Delta\phi$
0	Presampler	0.025×0.1	4×1		4×1	0.1×0.1
1	Front	0.003125×0.1	32×1	0.1×0.1	8×1	0.025×0.1
2	Middle	0.025×0.025	4×4		1×4	0.025×0.1
3	Back	0.05×0.025	2×4		2×4	0.1×0.1

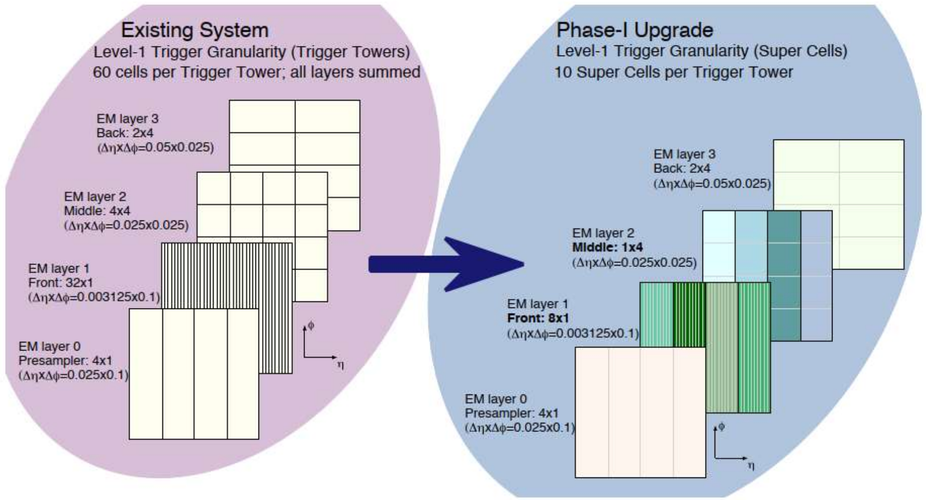

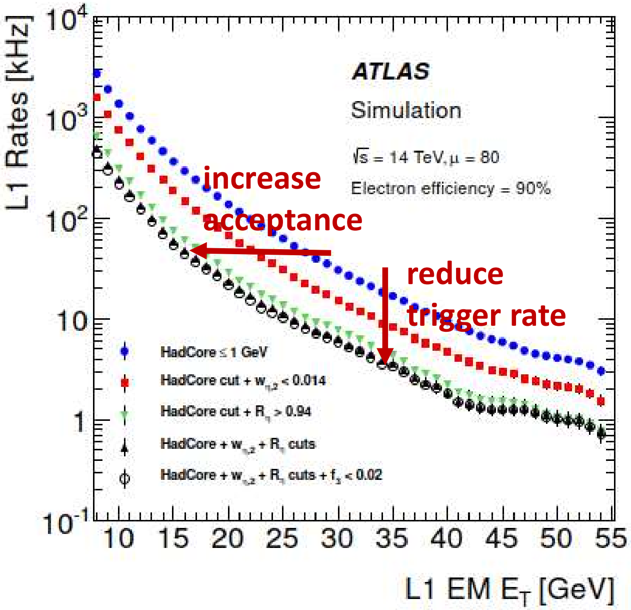

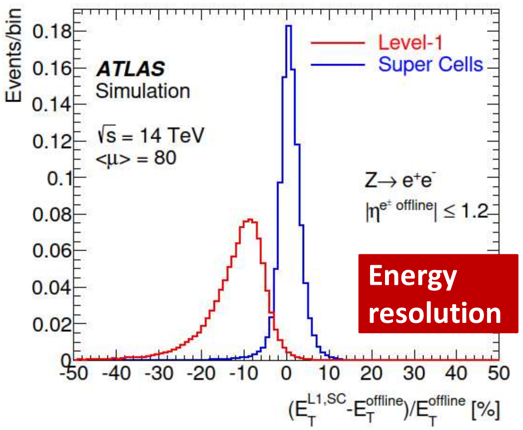

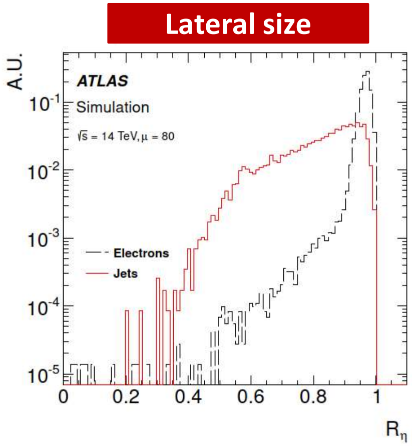

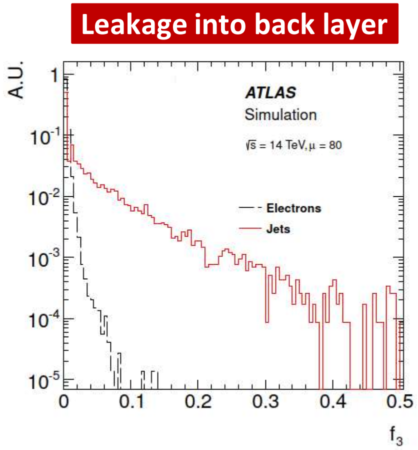

CMS High Granularity Calorimeter

- Radiation damage in the forward calorimeter region much higher than in barrel
  - Same values as in the tracker region

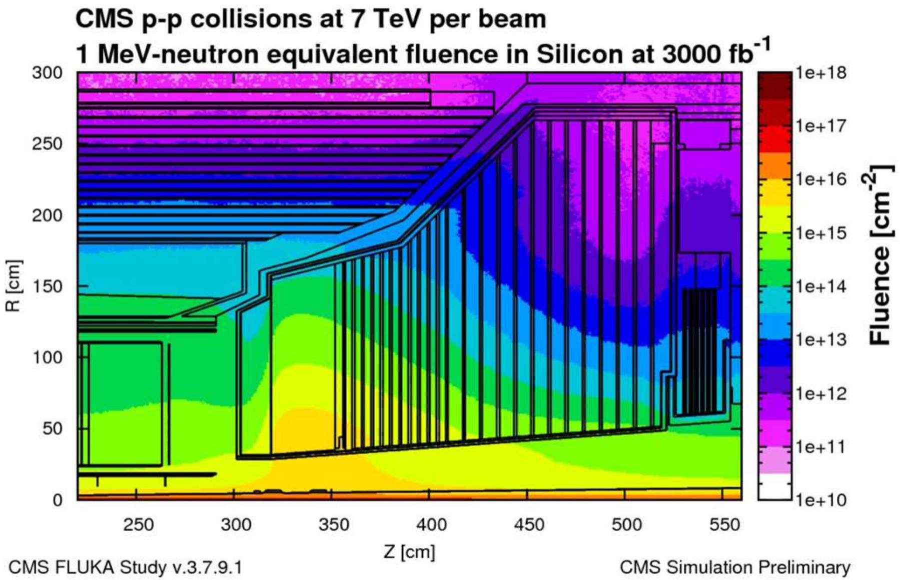

- $PbWO_4$ crystals will degrade excessively after 500 pb^{-1}
- Complete replacement of endcap calorimetry:

> - Electromagnetic section CE-E
>   - **Silicon** + Cu, CuW, Pb, 26 layers, 28 X_0, ~1.5 λ
> - Hadronic section CE-E
>   - **Scintillators** and **Silicon** + Steel, 7+14 layers, ~8.5 λ
> - Polytilene shield to reduce albedo neutrons into the tracker

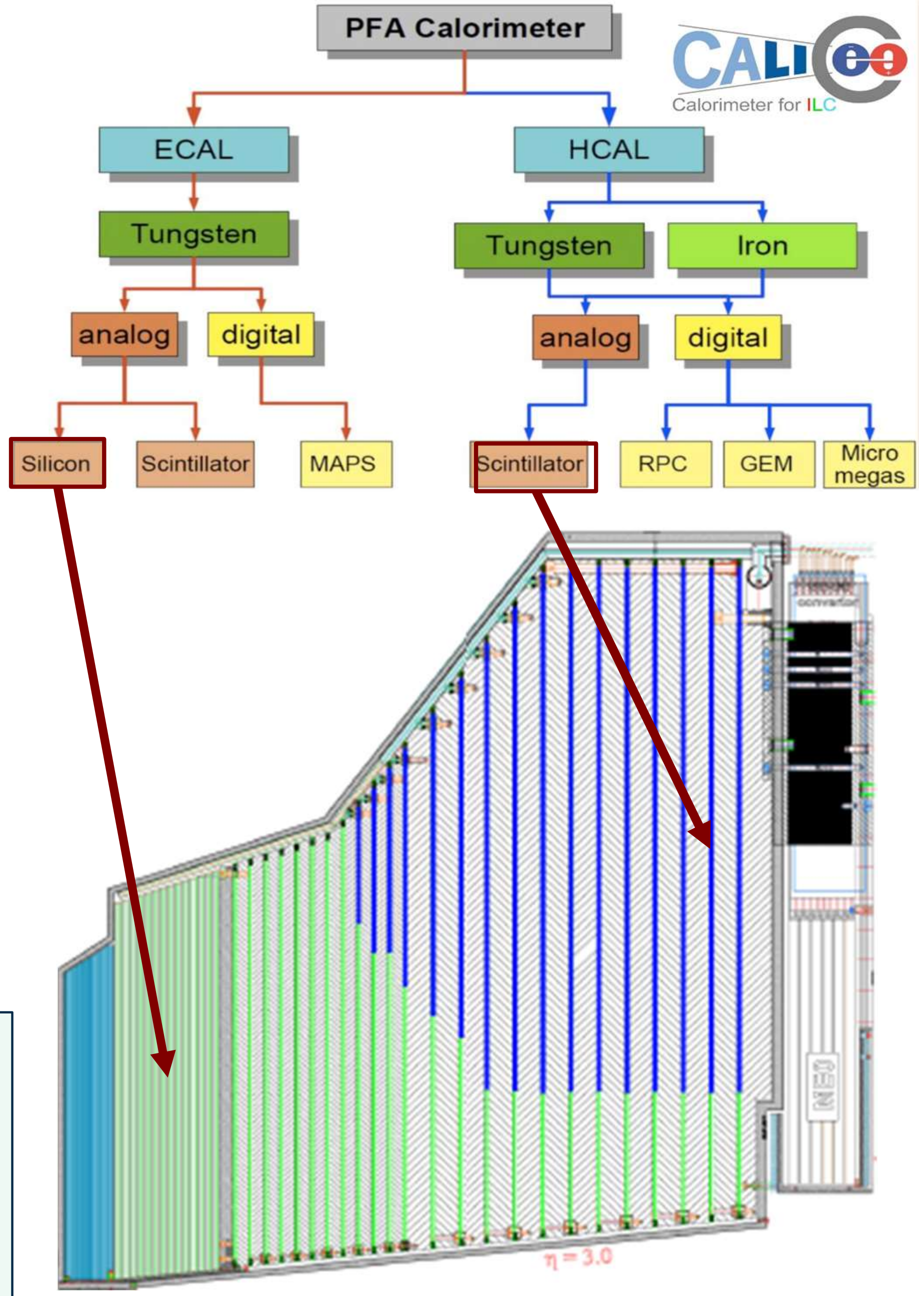

The Silicon Module

- Total of 620 m^2 of silicon sensors
- Hexagonal tiles from 8"wafer
- Different sensors depending on radiation level:
  - 1.18 cm^2 cell on 300 μm substrate
  - 1.18 cm^2 cell on 200 μm substrate
  - 0.52 cm^2 cell on 120 μm substrate

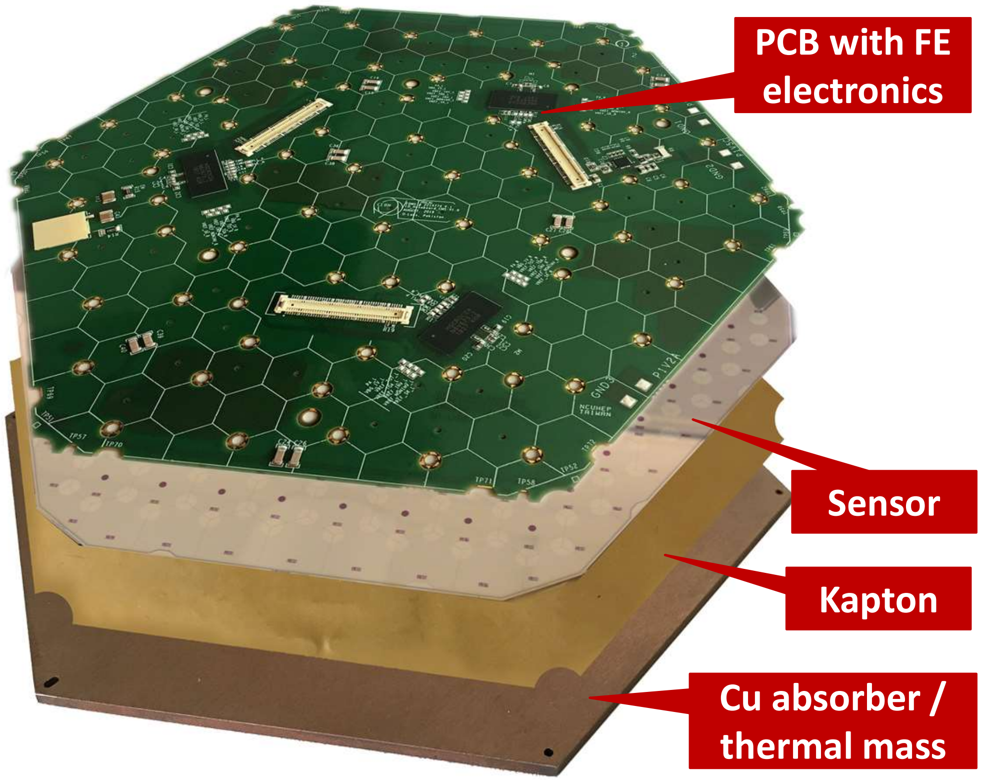

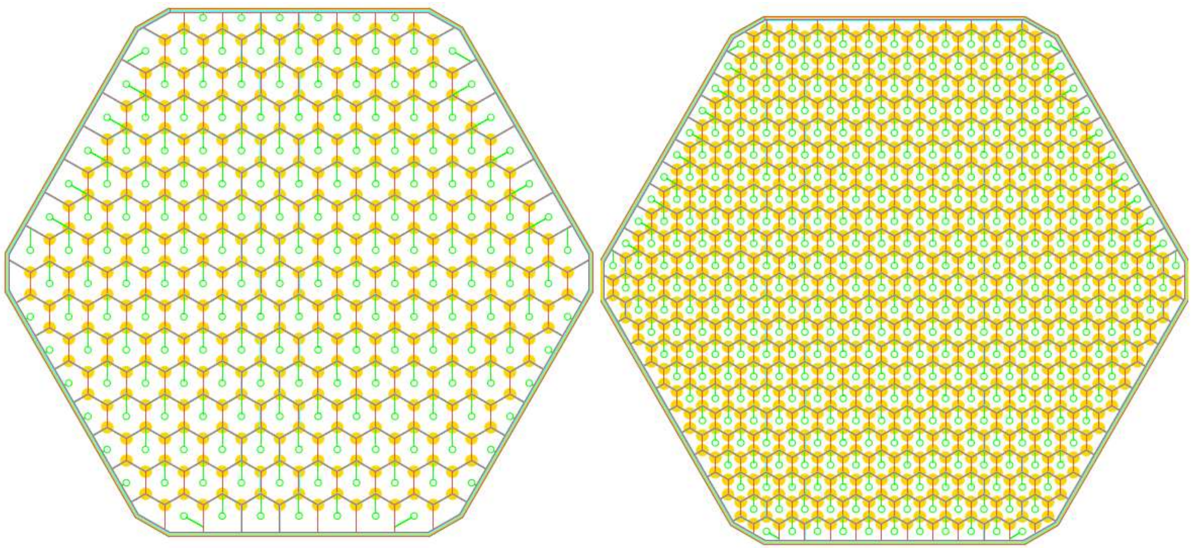

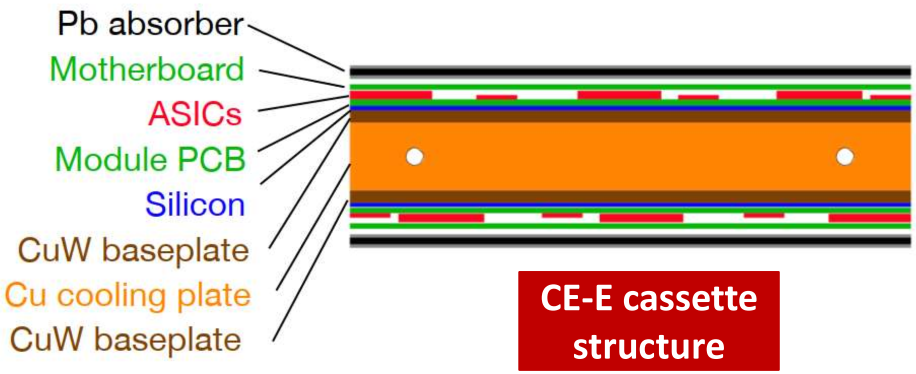

Sensor radiation hardness

- Radiation level comparable with silicon tracker
- Thin sensors provides required radiation hardness
- Cell size adapted to maintain sufficiently low sensor capacitance (<65 pF)
- Operation at -30 °C to reduce leakage current

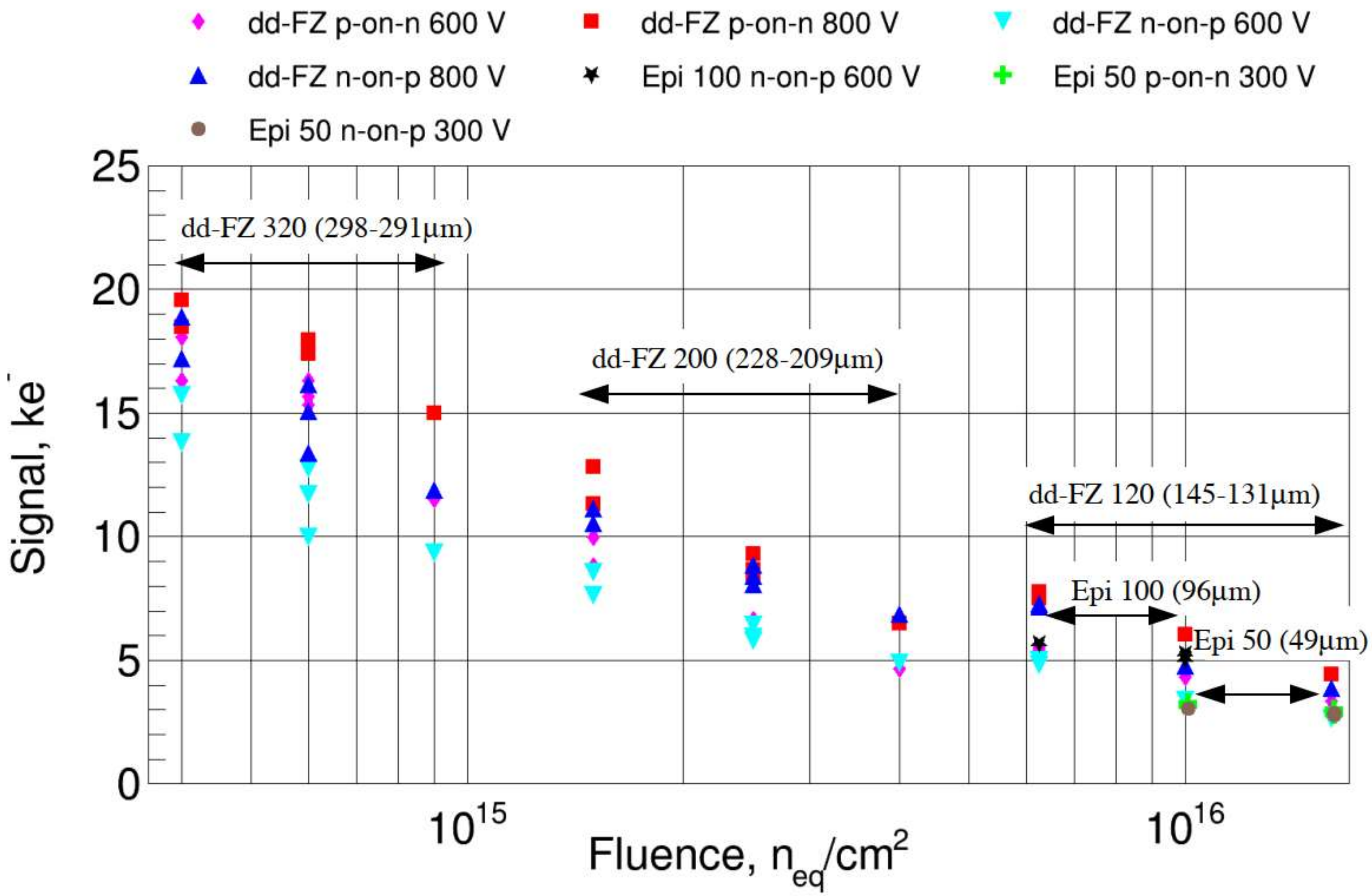

Scintillator modules

- Total of 320 m^2 of silicon sensors
- 3 mm thick scintillator tiles ranging from 2×2 cm^2 to 5.5×5.5 cm^2 area
- 2 mm^2 SiPM-on-tile readout
- Cooling at -30 °C helps in keeing low dark rate even after radiation damage
- MIP's S/N>5 for the whole detector lifetime

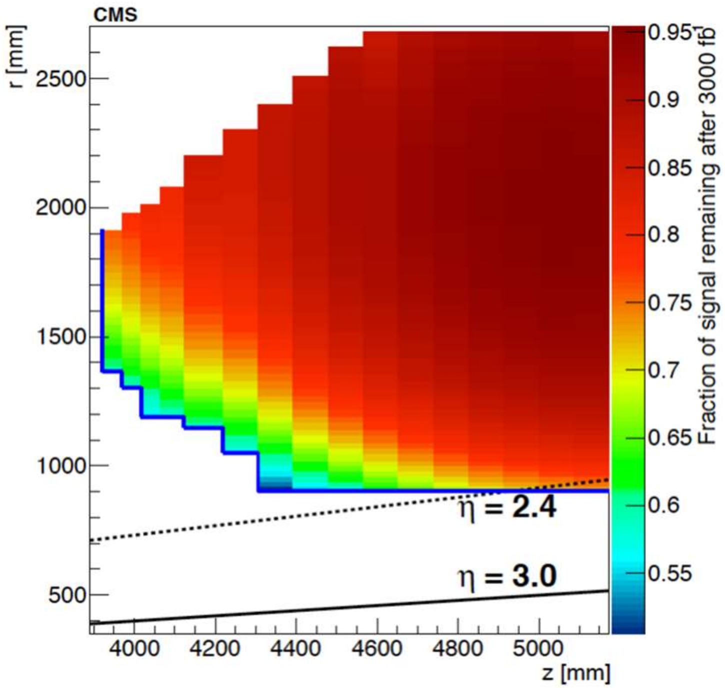

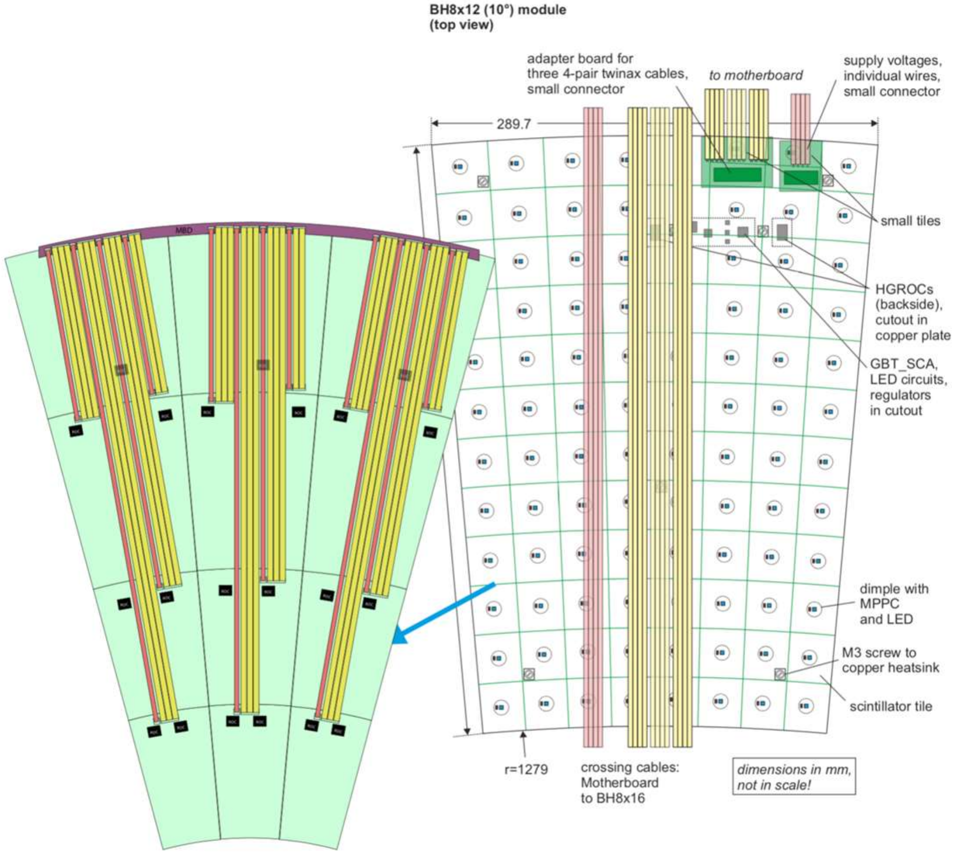

HGCAL: HGROC FE

HGROC3 characteristics

- Same readout chip for Si and SiPM readout
- 72 channels
- <20 mW power
- Radiation tolerant: 2 MGy and 1×10^{16} n_{eq}/cm^2
- ENC<2500 e with 65 pF load
- Timing resolution of 10s ps

- On chip zero suppression
- Fixed latency path for sum of trigger cells

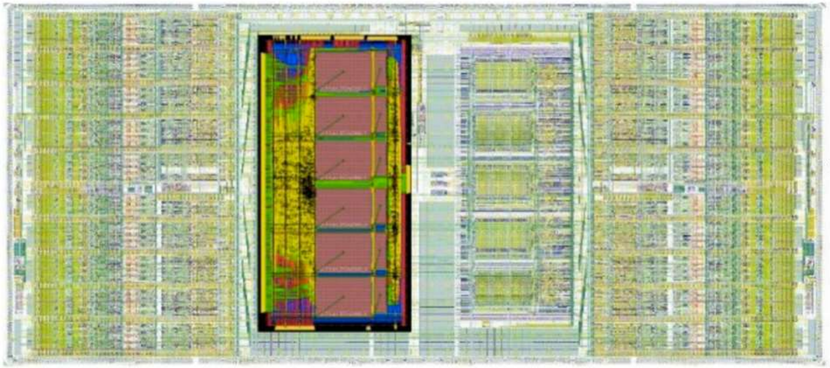

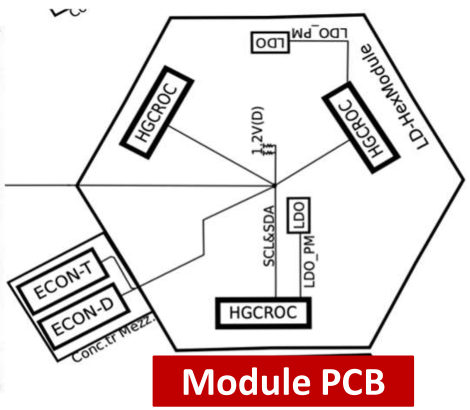

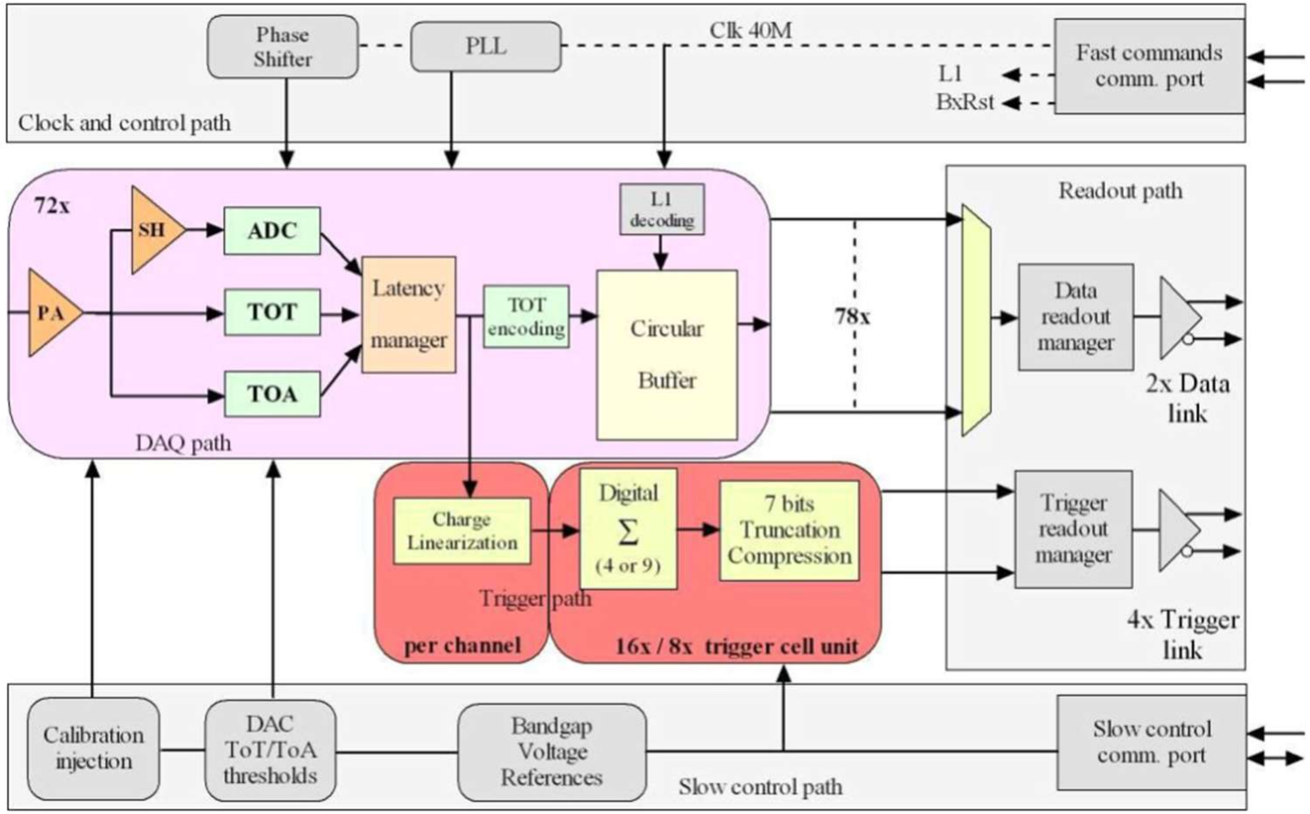

HGCAL: Trigger signal

On detector

- zero suppression
- analog sum
- Latency 1.5 μs

Off detector

- 3D clustering
- η-ϕ energy map
- Latency 3.5 μs

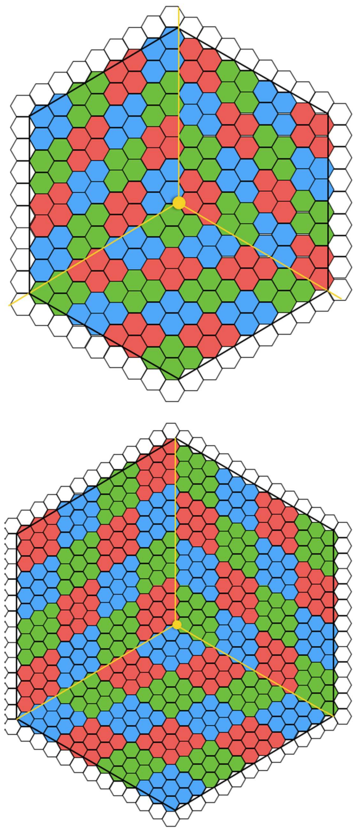

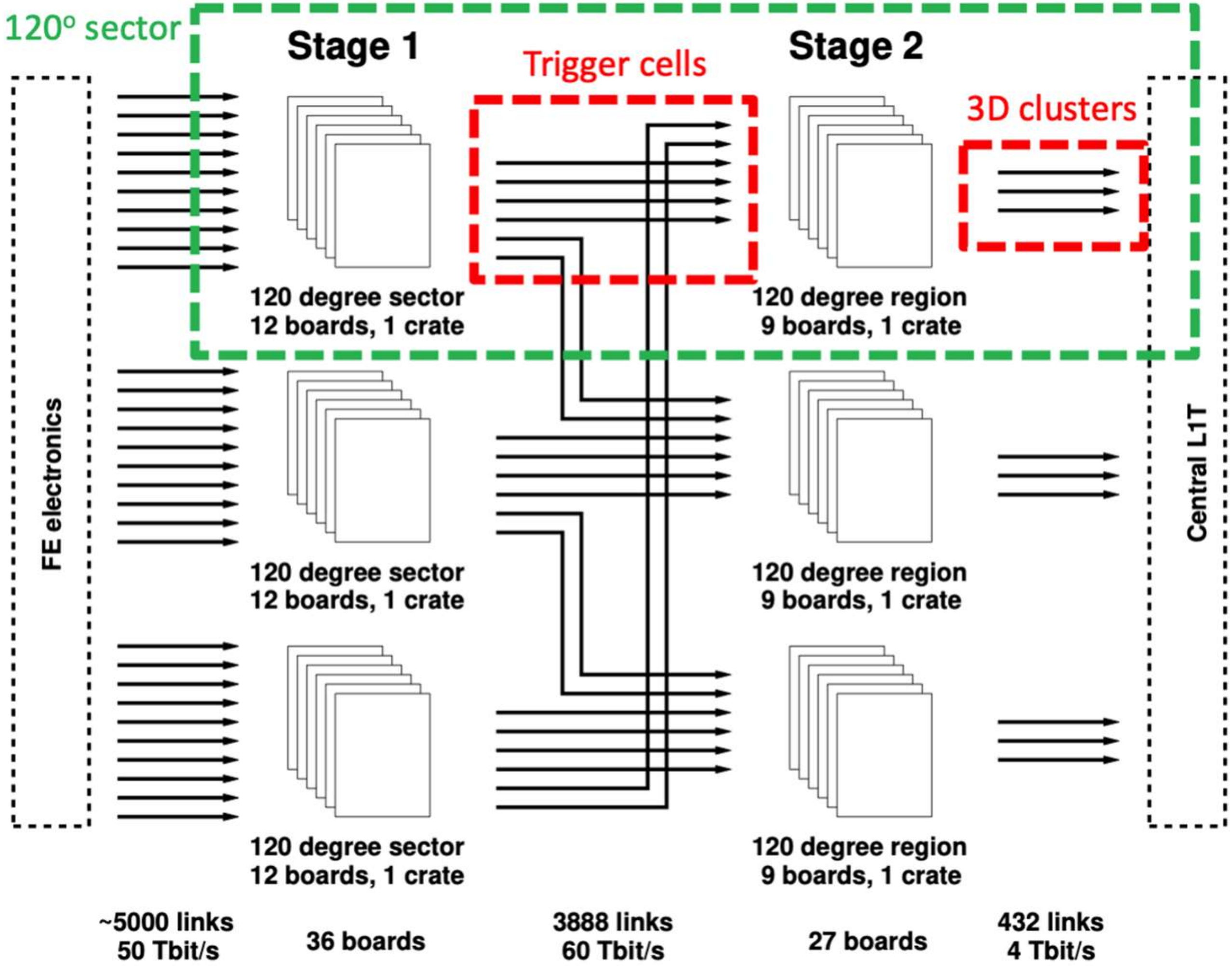

HGCAL: Test beam images

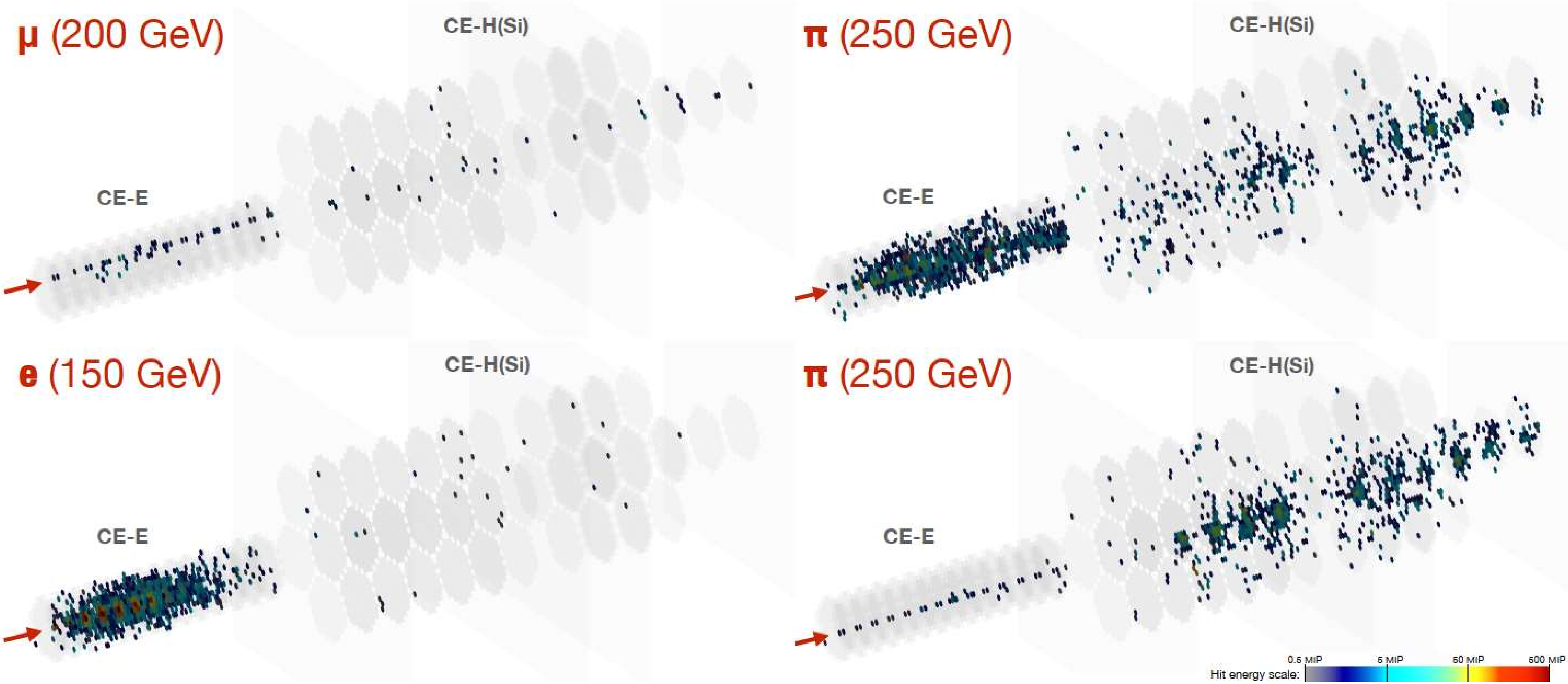

MUON SYSTEM

INFN Sezione di Milano
Istituto Nazionale di Fisica Nucleare
UNIVERSITÀ DEGLI STUDI DI MILANO
DIPARTIMENTO DI FISICA

ATLAS Muon System

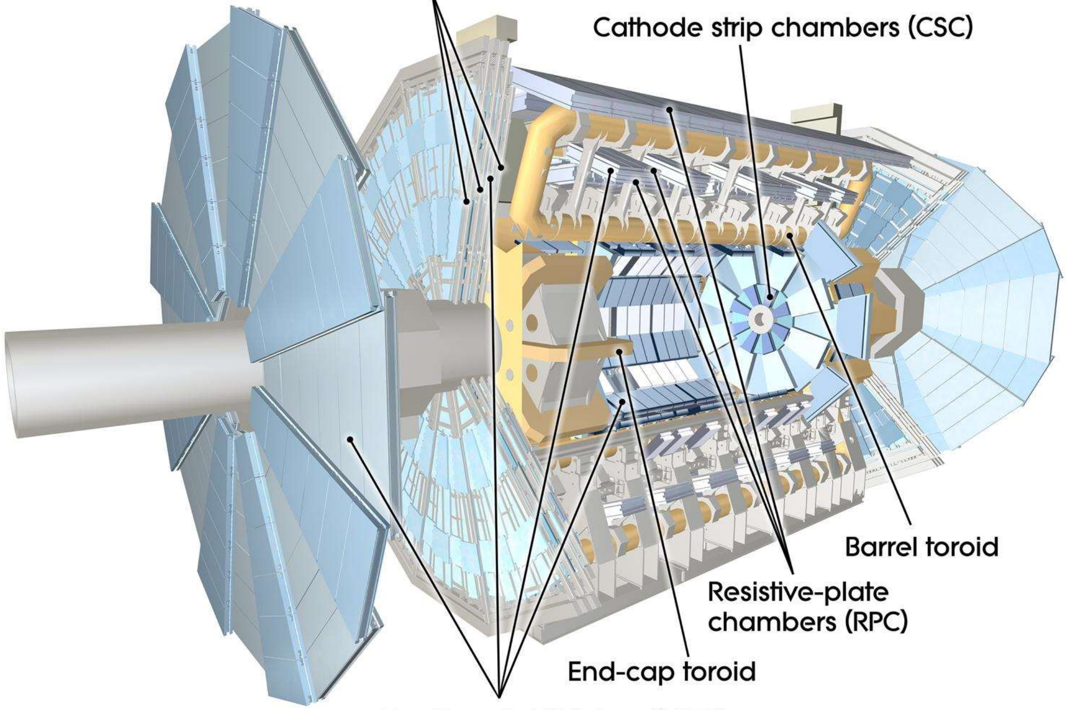

The Muon System has two functions:

- different detector technologies

Precision Tracking

- MDT (Monitored Drift Tubes)
- CSC (Cathode Strip Chambers)
- Precision measurements on the bending plance for momentum determination
- Measurement of drift time

Trigger

- RPC (Resistive Plate Chambers)
- TGC (Thin gap chambers)
- Fast signal (short drift distance)
- Measurement on the perpendicular coordinate.

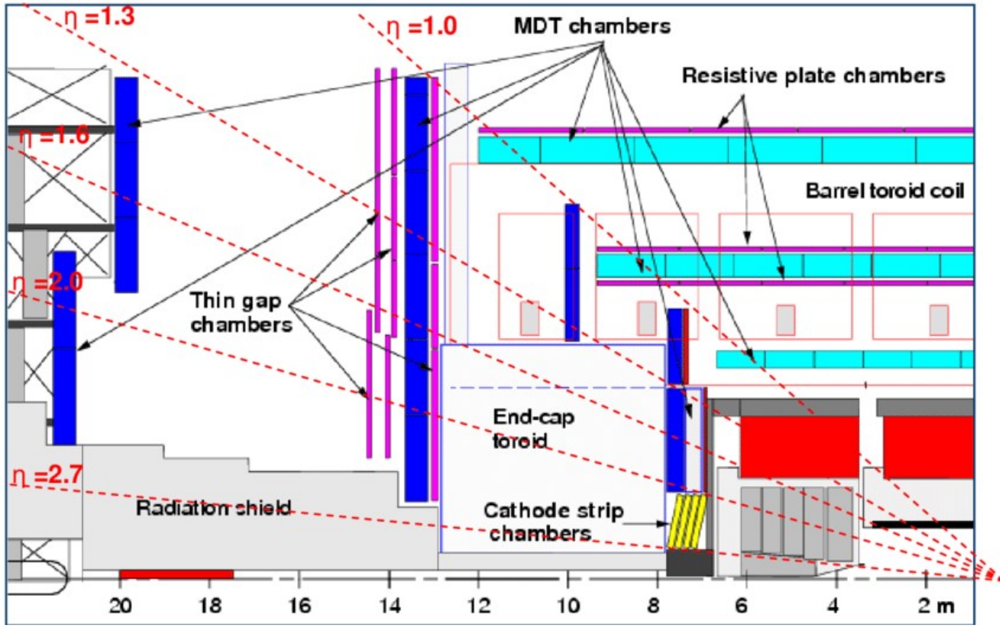

Gas detector basics

Keywords to remember

- Primary ionization tens of e-/cm
- Electron drift velocity O(cm/µs)
- Moltiplication in high electric field near the collecting electrode
- Space charge of positive ions distorts the electric field

Gas	Density, $\mathrm{mg\,cm^{-3}}$	E_x eV	E_I eV	W_I eV	$dE/dx\|_{min}$ $\mathrm{keV\,cm^{-1}}$	N_P $\mathrm{cm^{-1}}$	N_T $\mathrm{cm^{-1}}$
Ne	0.839	16.7	21.6	30	1.45	13	50
Ar	1.66	11.6	15.7	25	2.53	25	106
Xe	5.495	8.4	12.1	22	6.87	41	312
CH_4	0.667	8.8	12.6	30	1.61	37	54
C_2H_6	1.26	8.2	11.5	26	2.91	48	112
iC_4H_{10}	2.49	6.5	10.6	26	5.67	90	220
CO_2	1.84	7.0	13.8	34	3.35	35	100
CF_4	3.78	10.0	16.0	54	6.38	63	120

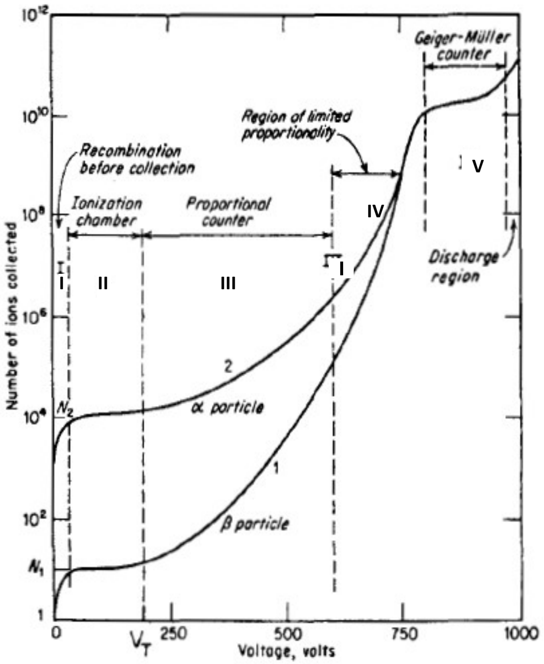

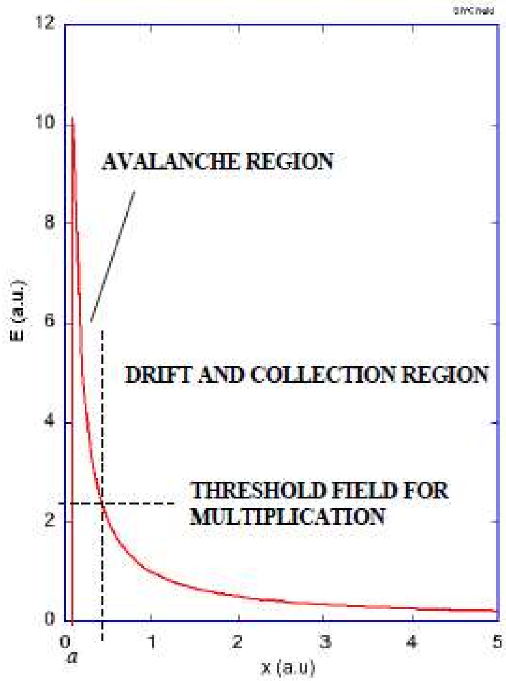

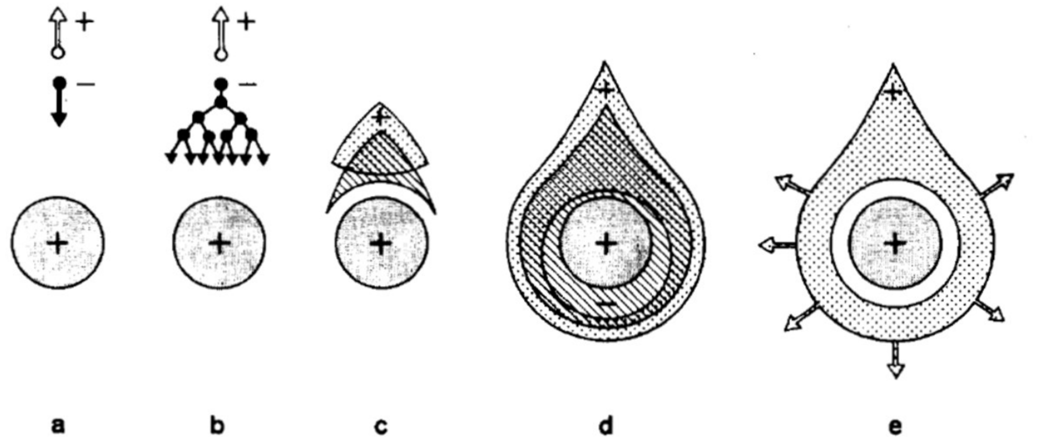

49 Time development of an avalanche in a proportional counter[30]. A single primary electron proceeds towards the anode, in regions of increasingly high fields, experiencing ionizing collisions; due to the lateral diffusion, a drop-like avalanche, surrounding the wire, develops. Electrons are collected in a very short time (1 nsec or so) and a cloud of positive ions is left, slowly migrating towards the cathode.

ATLAS Muon Drift tubes

- 30 mm diameter
- 50 μm wire diameter
- Ar/CO_2+H_2O gas mixture
- 20000 gain at 3080 V
- 700 ns max drift time
- Point resolution ~100 μm

$$\sigma_r = v_d\left(E(r)\right)\sigma_t \oplus \sqrt{2Dt}$$

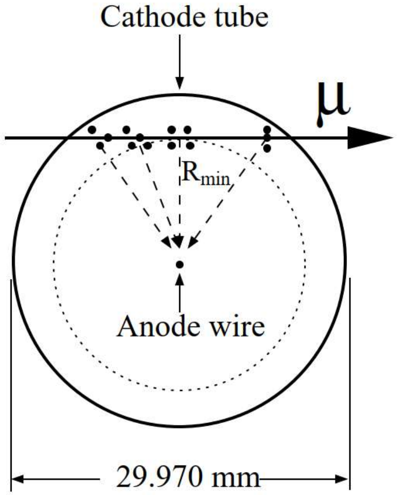

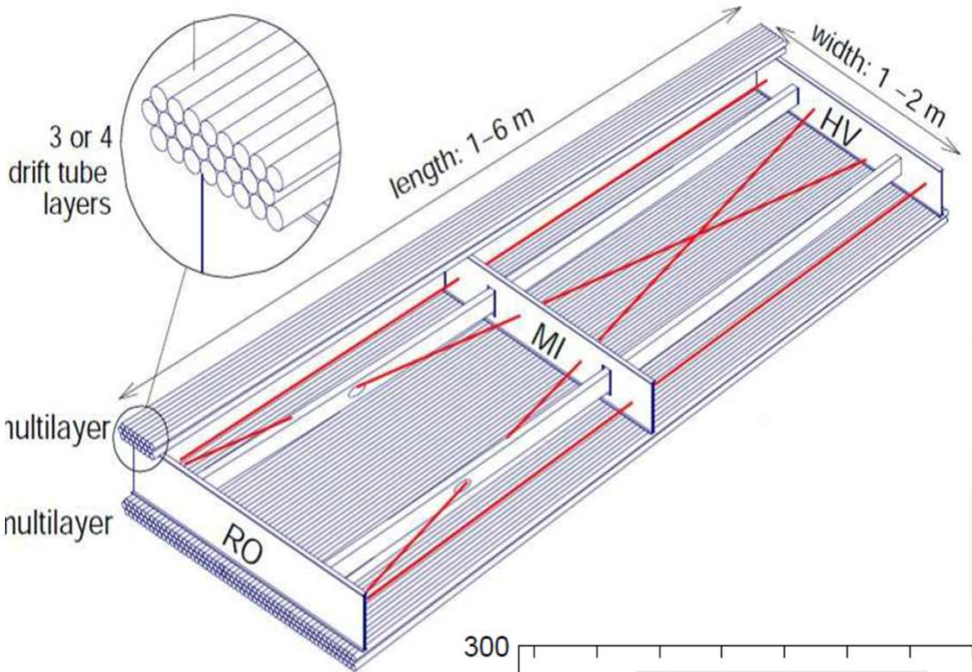

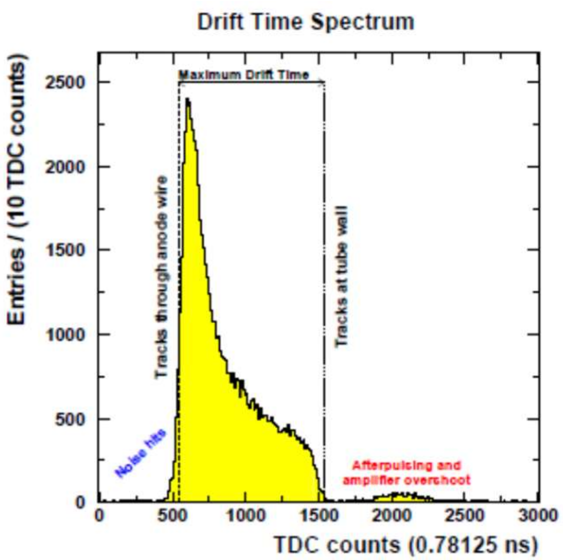

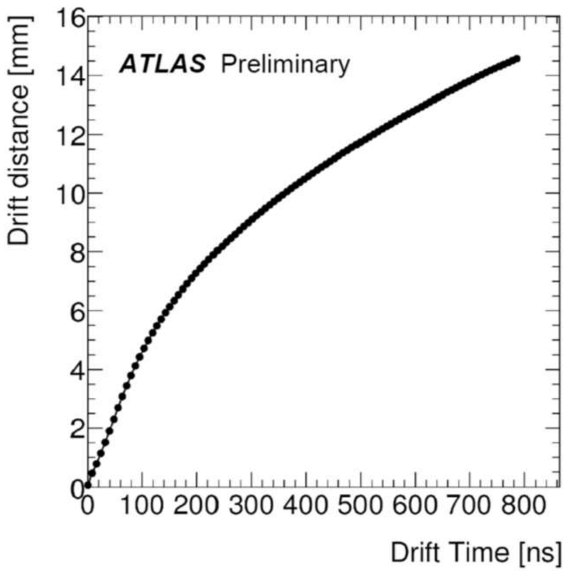

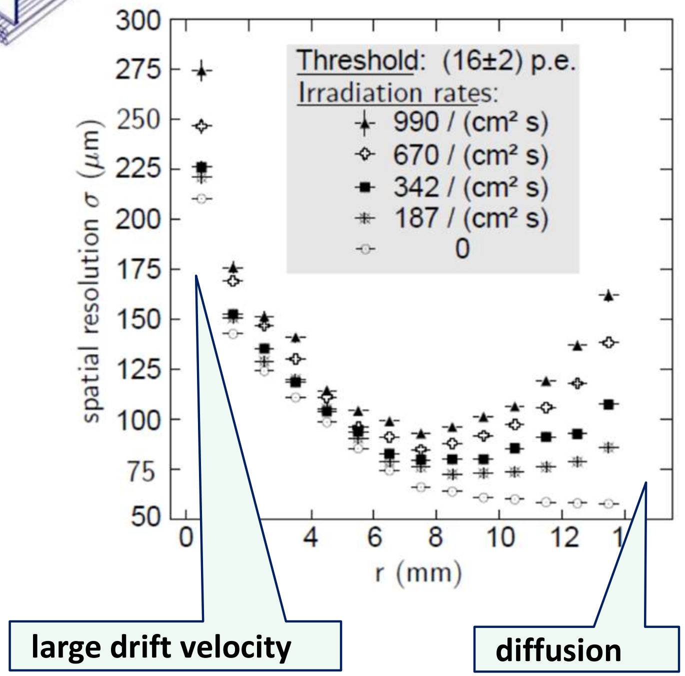

ATLAS Muon Trigger Detectors

RPC

- Parallel plate capacitors with high electric field
- E = 4.8 kV/mm, gain 10^7
- Time resolution 1.9 ns

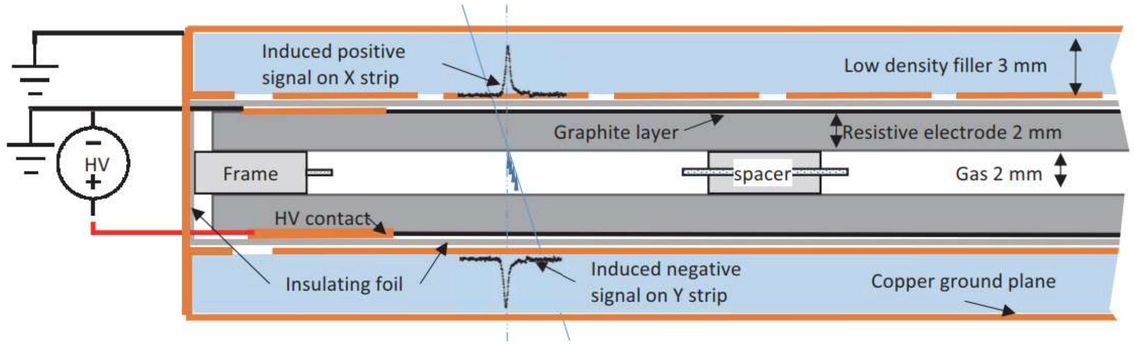

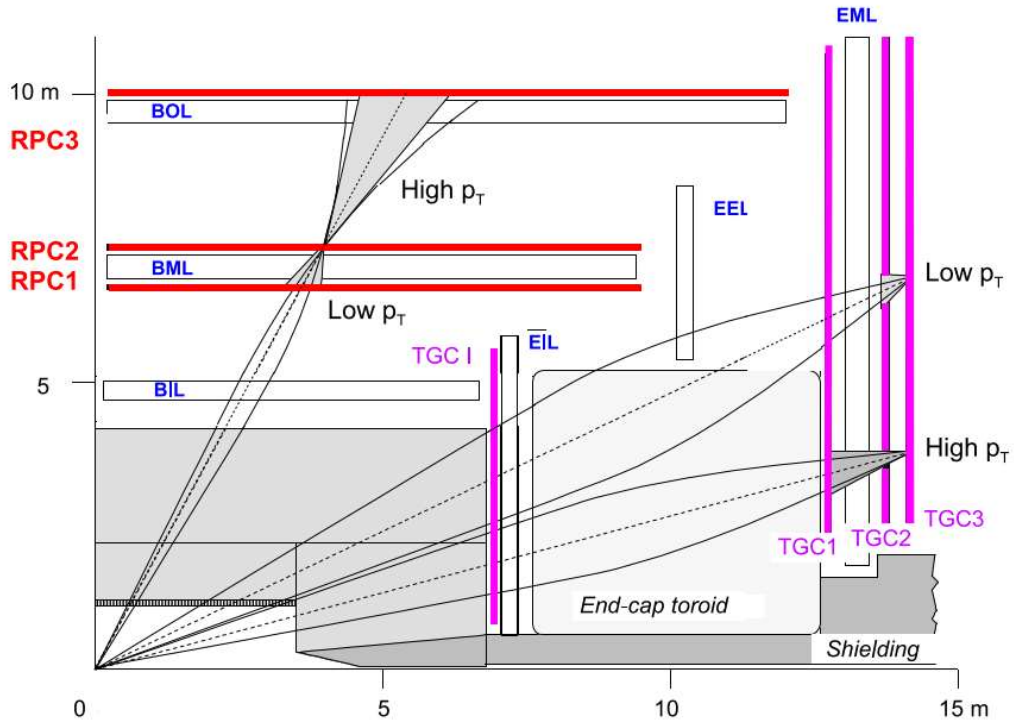

TGC

- Proportional chamber with small gas gaps
- 50 μm anode wire
- Gain 3×10^5 at 2.9 kV
- Response time <25 ns with 99% probability

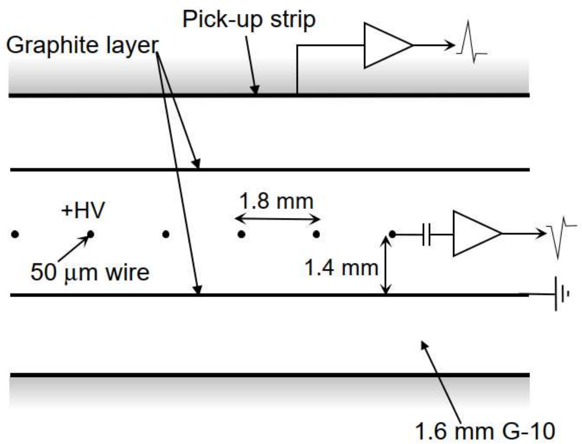

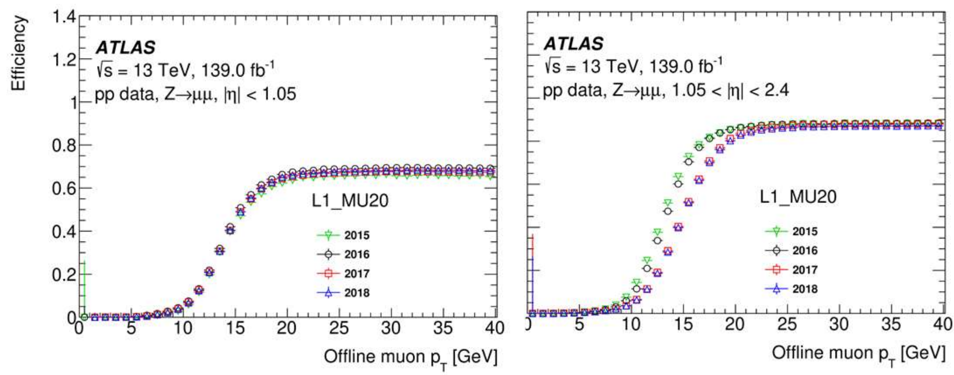

CMS Muon System

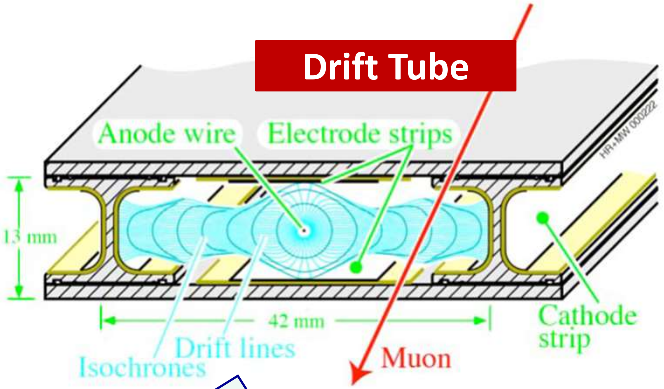

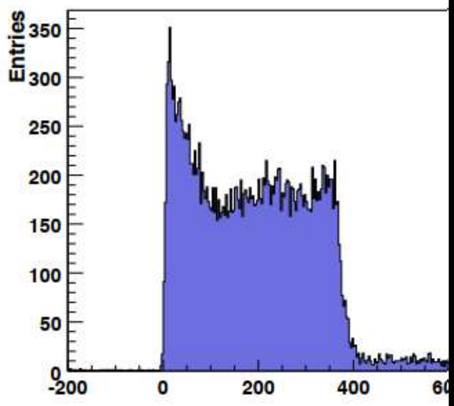

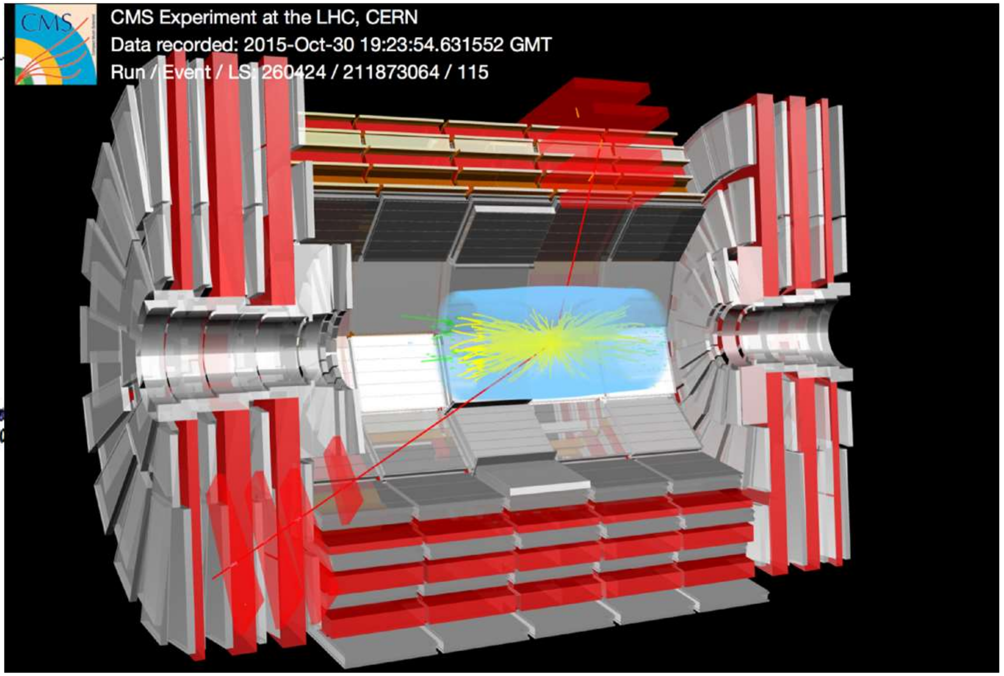

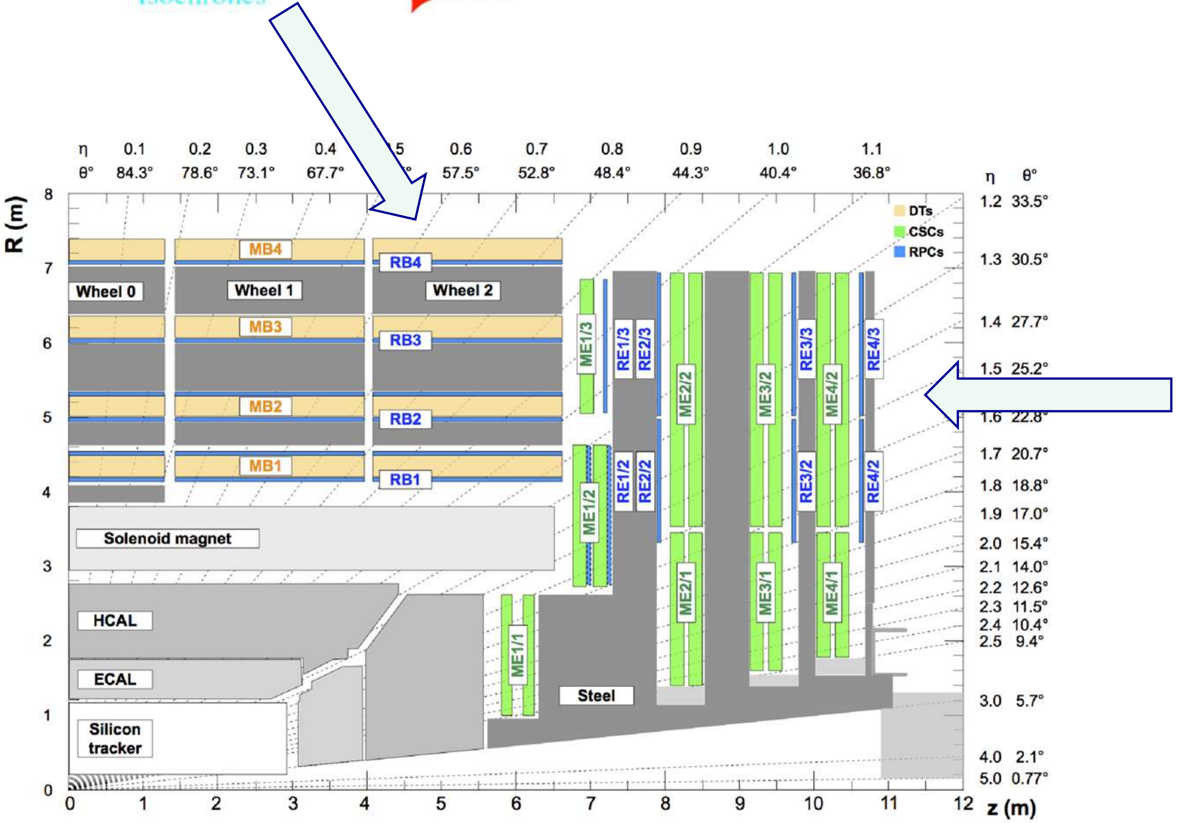

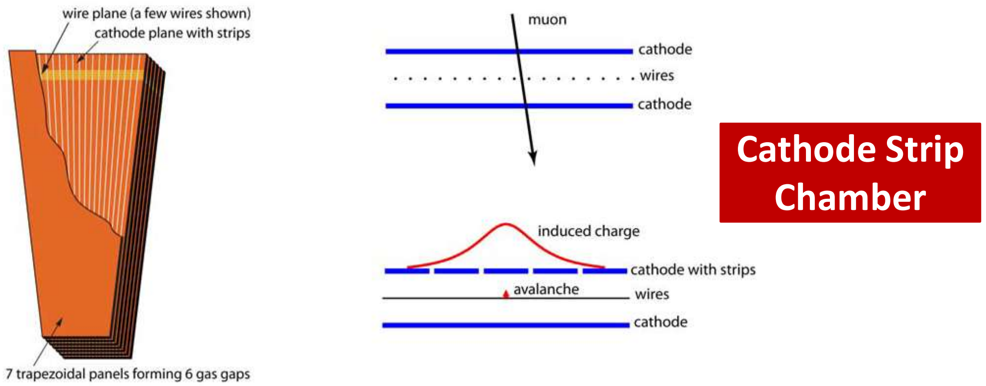

- **Drift Tubes** (barrel) and **Cathode Strip Chambers** (endcap) for trigger+tracking
- **RPC** for trigger with 1 ns time resolution

Muons System for HL-LHC

- Detector for the muon systems where initially designed for:
  - the nominal LHC rate corresponding to 1034 cm-2s-1
  - radiation damage corresponding to a total integrated luminosity of 500 fb-1
- Many different interventions are needed to cope with the higher particle rate (in particular electronics improvement)
- Radiation damage ~released charge per unit area/length
  - can be tuned by reducing gain at the cost of performance
- I'll shortly discuss only two upgrades:
  - addressing the most critical **forward region** deploing large areas fo **micropattern gas detectors**

ATLAS New Small Wheels

- Most L1 muon trigger in the forward regions are fake.
  - They need to be rejected more efficiently to stay within the HL-LHC trigger rate budget
- Match between track segments before and after the forward toroid
- The current detector has not the efficiency and accuracy needed
- **Replace the detectors in front of the toroid with New Small Wheels** (NSW)

- Detector requirements:
  - contribute to L1 trigger
  - reconstruct online track segments with >95% efficiency
  - position resolution <50 μm
  - angular resolution <1 mrad
  - sustain rate and radiation levels at HL-LHC
- Replace CSC+MDT with **Micromegas** detectors for precision tracking
- Replace TCGs for **sTGC** for trigger

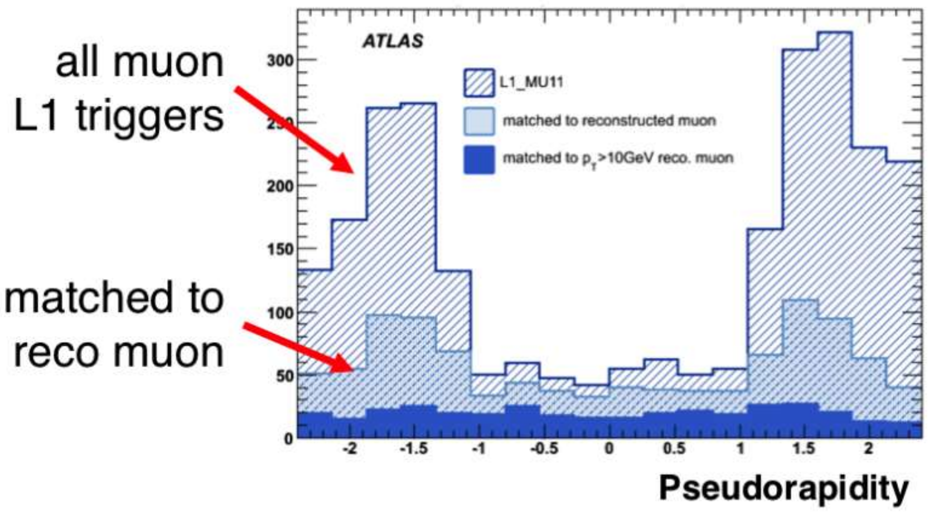

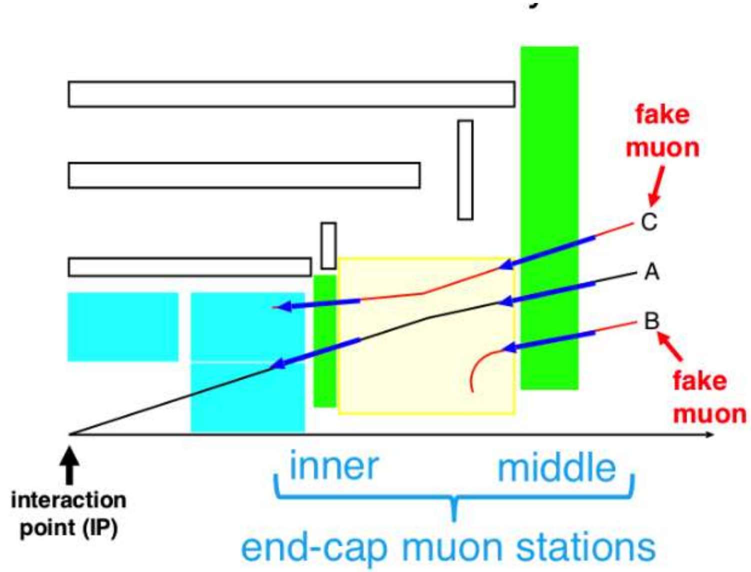

ATLAS New Small Wheels

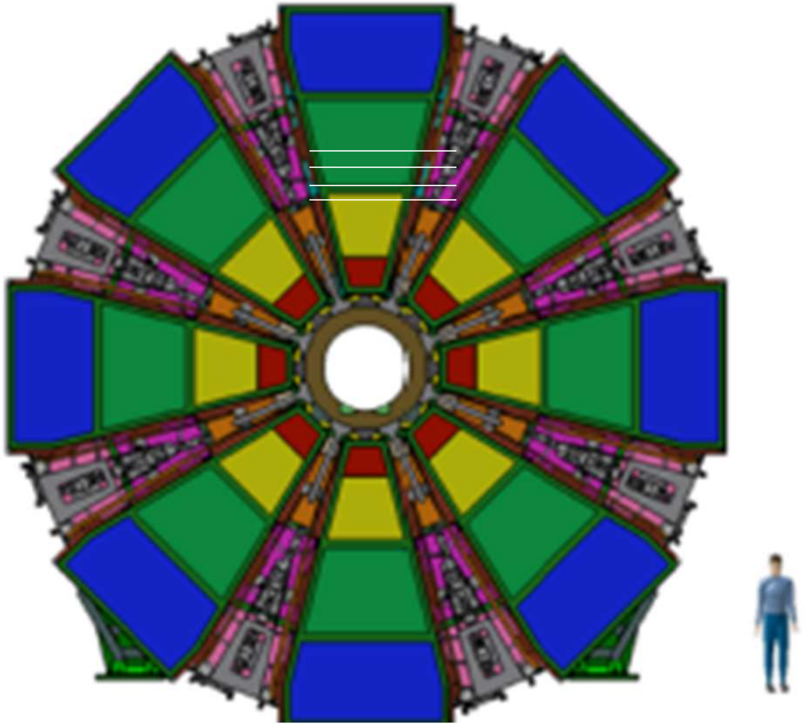

- Micromegas detector
  - micromesh transparent to electrons
  - separate the drift and charge multiplication region
  - finely segmented readout pitch

- NSW parameters
  - Ar/CO2 93%/7%
  - Short drift time: 100 ns
  - Spatial resolution <50 μm

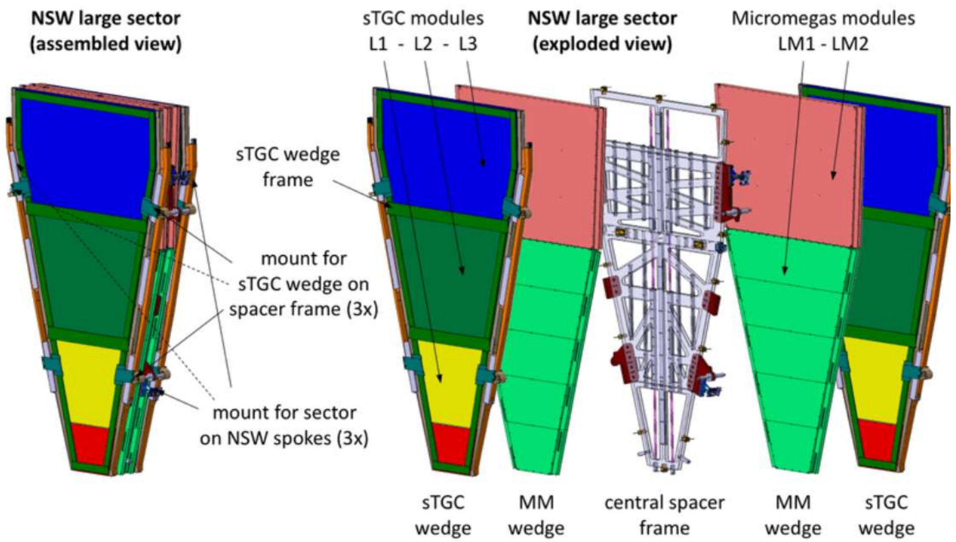

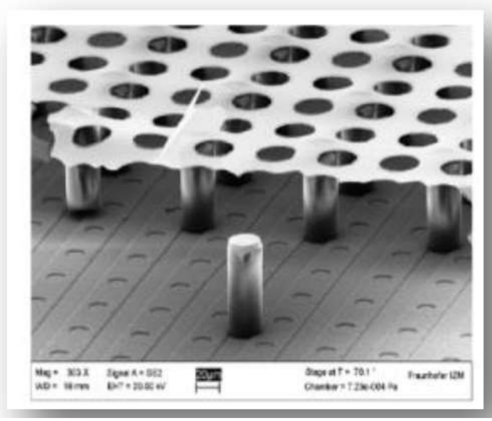

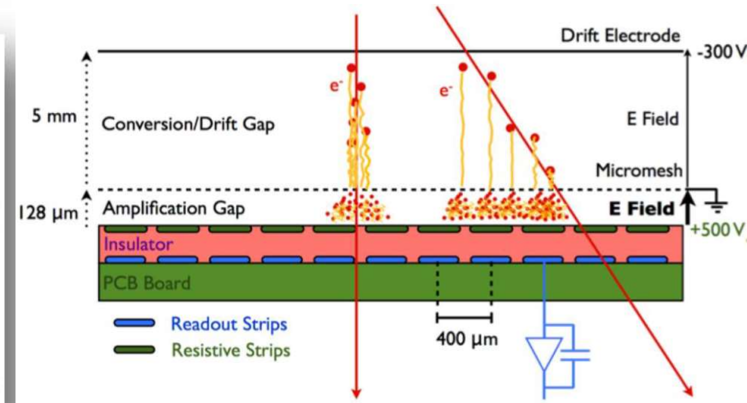

CMS Forward region updgrade

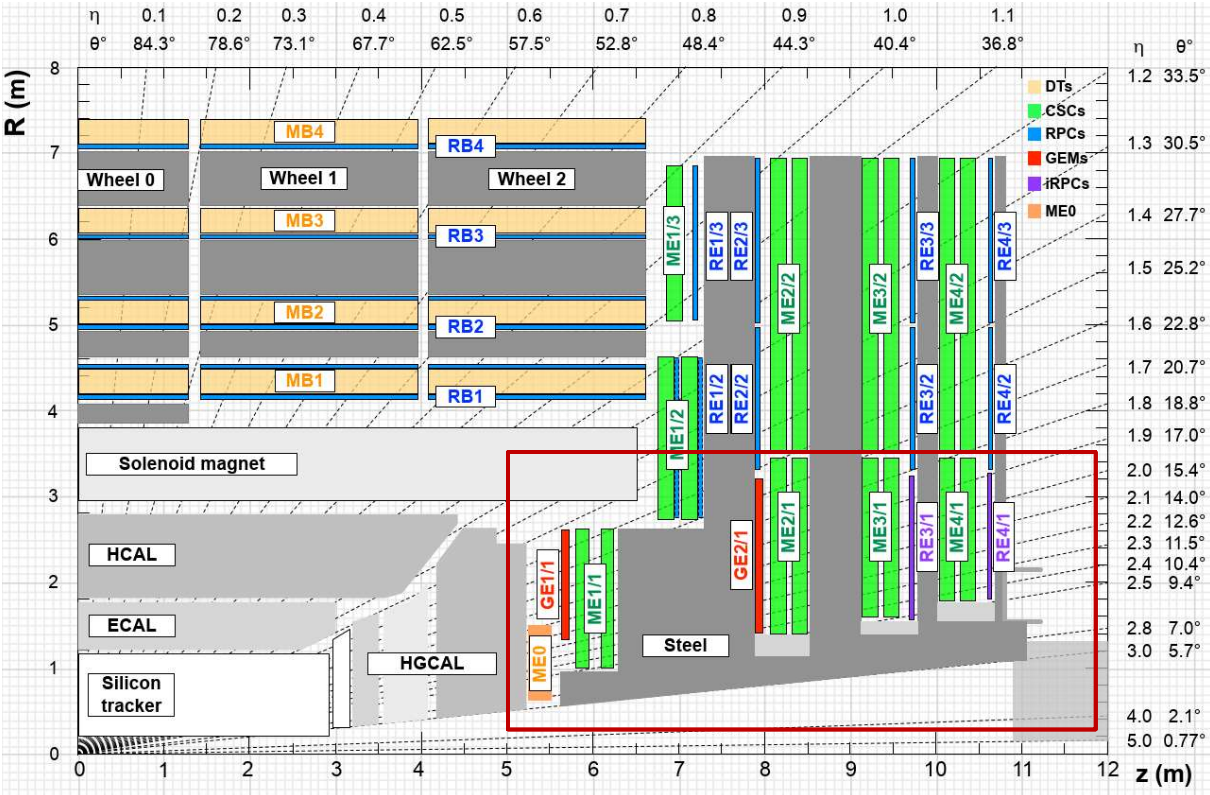

To cope with the high rate of particles in the high-η region, redundancy need to be added.

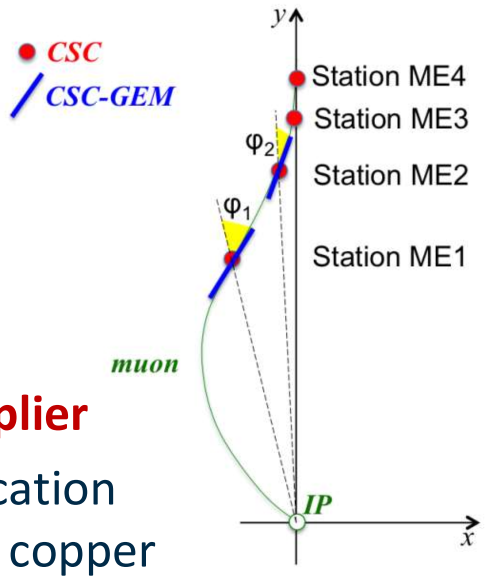

Gas Electron Multiplier

- charge multiplication inside gaps of a copper coated kapton foil
- most ions collected in the foil
- stacked to improve performance

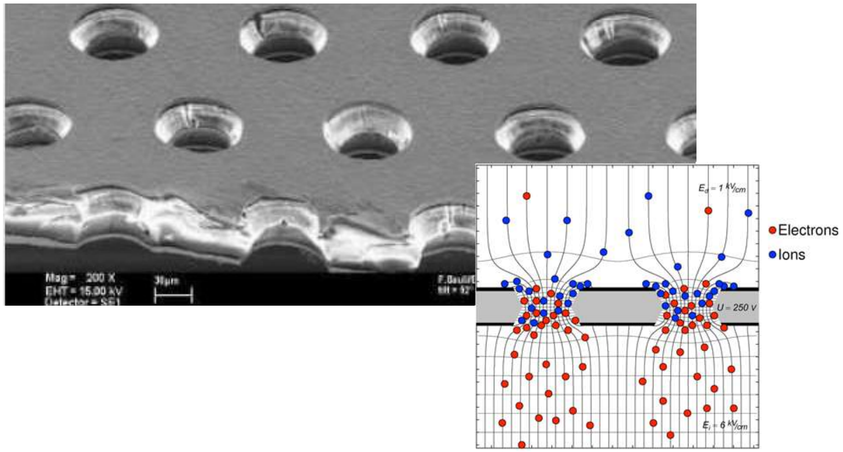

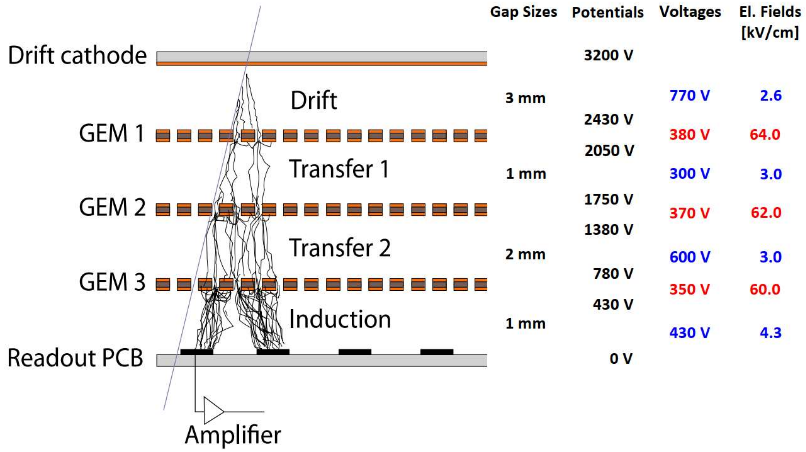

CONCLUSIONS

Istituto Nazionale di Fisica Nucleare

Sezione di Milano

UNIVERSITÀ DEGLI STUDI DI MILANO
DIPARTIMENTO DI FISICA

Conclusions

- LHC has exceeded the design expectation
  - the machine is already running at twice its design luminosity
  - detectors are behaving greatly, despite the harsher conditions
  - ...and you will see physics analysis are doing even better
  - I hope to have shown you the key techniques and choice that made that possible
- The HL-LHC upgrade is not a free lunch
  - an enormous amount of time and ingenuity has been spent to prepare the detector upgrades
  - that sometimes required to find innovative solutions to old problems
  - hope to meet you again in seven years and celebrate success
  - for the time being....

Thanks for giving me the opportunity to share my enthusiasm with you